LATERAL LOAD DISTRIBUTION ON TRANSVERSE FLOOR BEAMS IN STEEL PLATE GIRDER BRIDGES

by

K. R. Pennings, K. H. Frank,
S. L. Wood, J. A. Yura, and J. O. Jirsa

Research Report 1746-3

Research Project 0-1746

EFFECTS OF OVERLOADS
ON EXISTING STRUCTURES

conducted for the

Texas Department of Transportation

in cooperation with the

U.S. Department of Transportation
Federal Highway Administration

by the

CENTER FOR TRANSPORTATION RESEARCH
BUREAU OF ENGINEERING RESEARCH
THE UNIVERSITY OF TEXAS AT AUSTIN

August 2000

Research performed in cooperation with the Texas Department of Transportation and the U.S. Department of Transportation, Federal Highway Administration.

ACKNOWLEDGEMENTS

We greatly appreciate the financial support from the Texas Department of Transportation that made this project possible. The support of the project director, John Holt (DES), and program coordinator, Ronald Medlock (CST), is also very much appreciated. We thank Project Monitoring Committee members, Keith Ramsey (DES), Curtis Wagner (MCD), Charles Walker (DES), and Don Harley (FHWA).

DISCLAIMER

The contents of this report reflect the views of the authors, who are responsible for the facts and the accuracy of the data presented herein. The contents do not necessarily reflect the view of the Federal Highway Administration or the Texas Department of Transportation. This report does not constitute a standard, specification, or regulation.

NOT INTENDED FOR CONSTRUCTION,

PERMIT, OR BIDDING PURPOSES

K. H. Frank, Texas P.E. #48953

S. L. Wood, Texas P.E. #83804

J. A. Yura, Texas P.E. #29859

J. O. Jirsa, Texas P.E. #31360

Research Supervisors

TABLE OF CONTENTS

LIST OF FIGURES

LIST OF TABLES

SUMMARY

Many twin plate girder bridges have been recently rated inadequate for their current design loads. The controlling members that determine the bridge rating is often the transverse floor beams. The current provisions assume no lateral load distribution on the floor beams. This research focused on determining how the load is actually distributed. Using the SAP2000 finite element program, different floor system models were studied. The floor beam moments found by finite element modeling were 5-20% lower than the moments predicted by the current provisions due to load distribution and the moment carried by the concrete slab. An experimental test was also run on a similar floor system and the moments on the floor beam for this test were even lower than the moments predicted using finite element modeling showing that the finite element results are conservative as well. Recommended load distribution methods for the design and rating of floor beams are presented.

CHAPTER 1

INTRODUCTION

1.1 PURPOSE OF RESEARCH

Many twin plate girder bridges have been recently rated inadequate for their current design loads. The controlling members that determine the bridge rating for this bridge type are often the transverse floor beams. One option to deal with this problem would be to demolish these bridges and build replacements. A second option would involve retrofitting the floor beams to increase their capacity. However, neither may be the most cost-effective way to deal with the problem. Rather than removing from service or retrofitting bridges that might be functioning satisfactorily, it was deemed appropriate to the study the transverse floor beams in a bit more detail. The purpose of this investigation is to develop a better estimate of the actual forces on a transverse floor beam caused by truck loads on the floor system and to compare these forces with the current method for predicting the forces on the floor beams. The goal is to come up with a method that would allow one to more accurately predict the expected moment in these floor beams.

1.2 FLOOR SYSTEM GEOMETRY

The floor system in consideration is a floor beam-stringer system supported by twin plate girders. The plate girders, running the length of the bridge on the outside support the transverse floor beams, which in turn support the stringers. All bridges studied have a 6.5-inch concrete slab resting on the stringers. Figure 1.1 shows the basic floor system geometry and terminology that will be used in this report. Only floor systems containing two stringers and two design lanes were considered. A survey of TxDOT bridges revealed that this was the common system used in early long-span steel girder bridges. The main interest of this research is the maximum moment in the transverse floor beams, simply referred to as floor beams in this report.

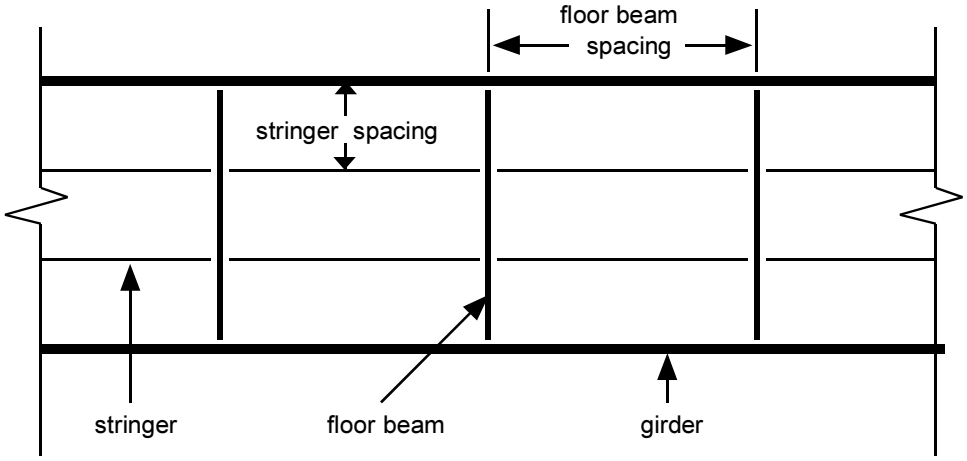

Figure 1.1 Plan View of Bridge Floor System

1.3 LOAD PATH

An understanding of the load path of the system is necessary to understanding the moment in the floor beam. The two different possible basic load paths for this floor system geometry are shown in Figure 1.2. The only difference in the two load paths is that in the first example there is no load going directly from the concrete slab to the floor beam. The entire load is transferred from the slab to the floor beam through the stringer connections. That is because there is no contact between the slab and the floor beam. The only link is through the stringers. However, when the slab is in contact with the floor beam, it is possible for some of the load to go directly from the slab to the floor beam. This is an important difference because it can significantly affect the shape of the moment diagram of the floor beam.

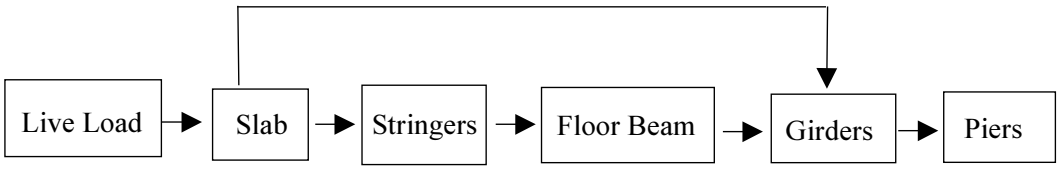

Load Path with No Contact between Slab and Floor Beam

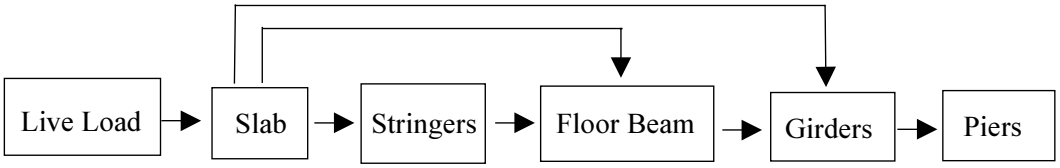

Load Path When Slab is in Contact with Floor Beam

Figure 1.2 Different Possible Load Paths of the Floor System

1.4 LOAD DISTRIBUTION MODELS

The distribution of load was examined by evaluating how a point load is distributed to the floor beams. This is important because the lateral load distribution has a significant effect on the magnitude of the floor beam moment. Three different load distribution models are outlined in the following section. Note that in the first two models, the direct load and lever rule assume simply supported stringers and floor beams and ignore the moment carried by the slab.

1.4.1 Direct Load Model

The approach adopted by AASHTO and TxDOT is a structural system that distributes load longitudinally onto the adjacent floor beams using statics. However, the load is not distributed laterally. A point load in the middle of the bridge is treated as a point load on each of the adjacent floor beams. Figure 1.3 shows the direct load method of distributing forces. This method has the advantage of being very simple to apply. The direct load approach provides a conservative estimate for the load on the floor beam since a point load will produce the maximum moment. This method ignores the lateral distribution through the slab to the stringers. The result of the other methods of distributing the load to the floor beam will be compared to this method. The floor beam moment calculated using other methods will be divided by the moment results from the floor beam loads calculated by the direct load method.

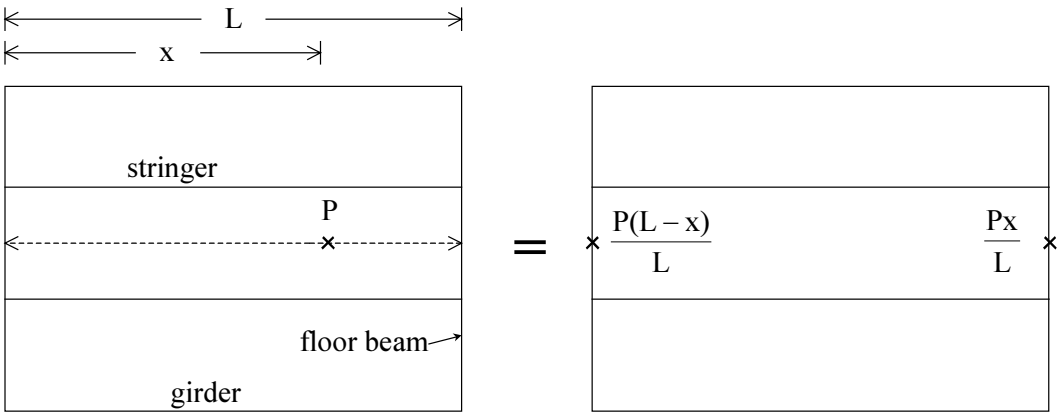

Figure 1.3 Direct Load Model for Load Distribution

1.4.2 Lever Rule Model

Another method, the lever rule, shown in Figure 1.4, transmits the entire load from the slab to the floor beams through the stringers. It treats the slab as simply supported between the stringers and statically distributes the load to each stringer. Instead of resulting in a single point load, it results in two point loads on each floor beam at the location of the stringers. This method is also simple to use and is a better model of the load path, in which the load is transferred from the slab to the floor beam through the stringers. It is also less conservative than the direct load model. If there is no contact between the floor beam and the slab, it was found that the lever rule is a good model of the floor system.

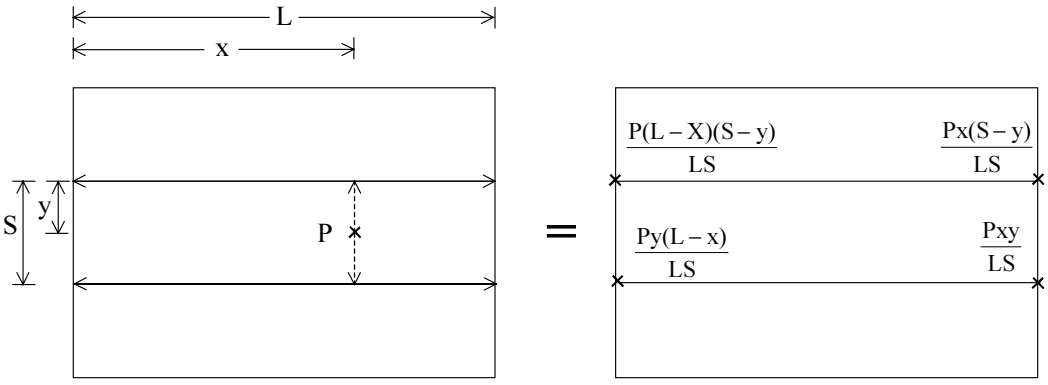

Figure 1.4 Lever Rule Model for Load Distribution

1.4.3 Slab Lateral Load Model

Assuming contact between the floor beam and slab, an example of how the load is more likely distributed is shown in Figure 1.5. Some of the load goes to the stringers and then is transmitted to the floor beams, while some of the load is transmitted from the slab to the floor beams. However, this load is not transmitted as a point load, but as a distributed load. This distributed load on the floor beam would lead to a lower maximum moment in the floor beam. It is difficult to determine how the load is distributed transversely because it depends on a number of factors such as the spacing of the system and the stiffness of the members. To gain a better understanding of the load distribution and the resulting floor beam moment, a finite element analysis was done on the bridge floor system.

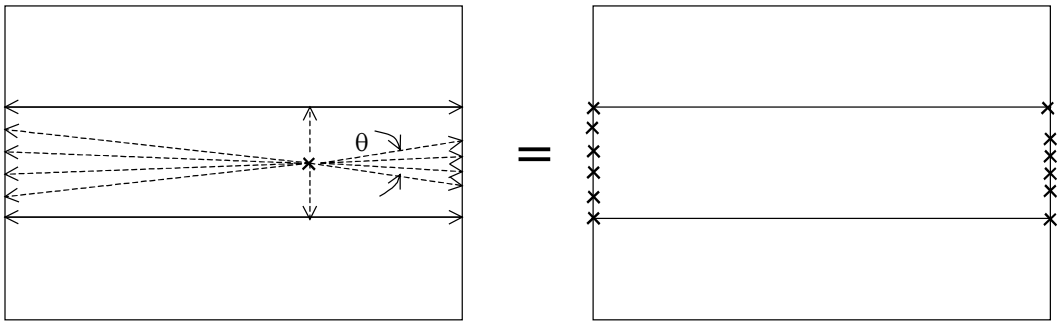

Figure 1.5 Slab Lateral Load Distribution Model

1.4.4 Comparison of Lateral Load Distribution Methods

Figure 1.6 shows the moment diagram for the floor beam caused by the different distribution methods. A 2-kip load placed in the center of the simple span shown in Figures 1.3-1.5 causes the moment diagrams shown in the figure. The distributed model assumes a distribution of the load of $\theta = 30$ degrees. The model labeled $\alpha = ½$ has half of the load following the slab lateral distribution method and half of the load following the lever rule path. This is for a floor system with a 22-foot floor beam spacing and 8-foot stringer spacing. The plot indicates that the lever rule for this single point load results in a 33% reduction from the direct load model. The slab distribution model and the combined model, $\alpha = ½$, produce calculated moments less than the current point load method and higher than the lever rule. A more refined analysis using the finite element method is used in this report.

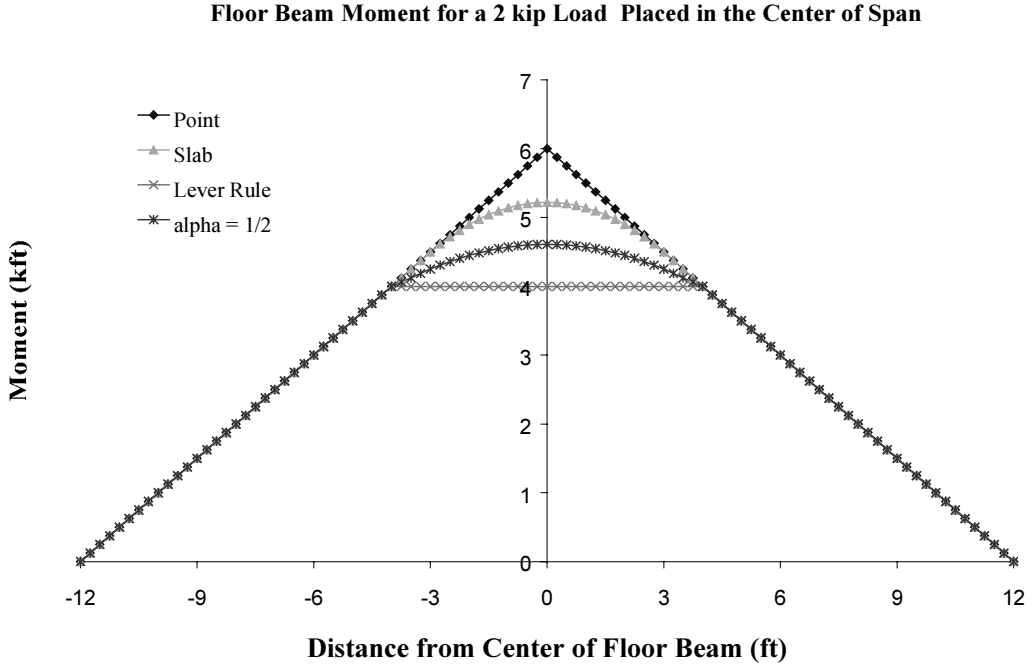

Figure 1.6 Comparison of Lateral Load Distribution Models

1.5 LOADING GEOMETRY

The load considered in this study consisted of either two HS-20 or H-20 trucks placed side by side four feet apart as per AASHTO guidelines. The HS-20 loading, shown in Figure 1.7, consists of two 4 kip wheel loads on the front axle and two 16 kip wheel loads on both rear axles. The total weight of this dual truck load is 144 kips. Wheels are spaced 6 feet apart transversely. The front axle is 14 feet from the first rear axle and the rear axles can be spaced anywhere from 14 feet to 30 feet apart. The shorter 14-foot spacing will be used for the rear axle because it results in the highest floor beam moment. The H-20 loading is exactly the same as the HS-20 loading without the rear axle. The total weight of two H-20 trucks is 80 kips. Lane loading was not considered in the analysis. For more detail on lane loading, see Chapter 5.

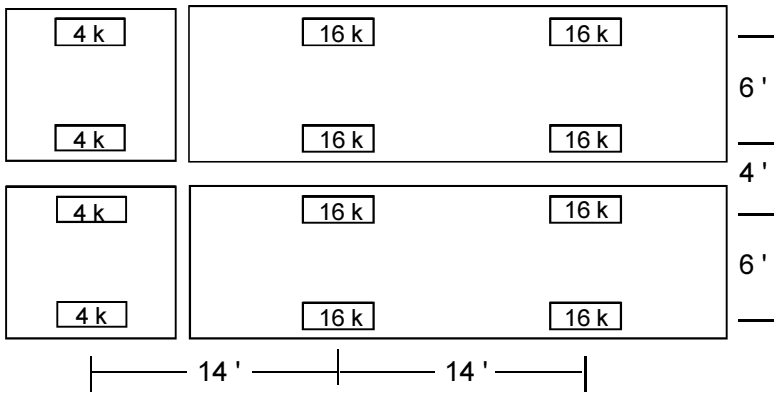

Figure 1.7 Spacing of Maximum Load (2 HS-20 trucks)

In 1978, TxDOT adopted a three-foot spacing between trucks contained in the Manual for Maintenance Inspection of Bridges published by AASHTO.[2] In 1983, however, the spacing was returned by AASHTO to four feet where it remains today.[3] However, in TxDOT's example calculations from the 1988 Bridge Rating Manual, a three-foot spacing between the trucks was still being used.[4] This closer spacing can lead to a significantly higher calculated moment in the floor beams as shown in Table 1.1. The percent increase due to the narrower stringer spacing is independent of the floor beam spacing.

Table 1.1 Percent Increase in Mid-Span Floor Beam Moment Caused by Decreasing Truck Spacing from 4 to 3 feet

Stringer Spacing (ft)	% Increase in Floor Beam Moment
6	12.5
7	9.1
7.33	8.3
7.5	8.0
8	7.1

1.6 TOPICS COVERED

To determine the forces on the floor beams, finite element analyses of various bridge geometries were conducted. The finite element modeling techniques are discussed in the next chapter and the results of the analyses are shown in Chapter 3. Results from a finite element model are then compared with data from an actual bridge test in Chapter 4. In Chapter 5, an example calculation is shown for a bridge that currently is rated inadequate and compared with the recommended method of calculating floor beam moment. Conclusions are presented in Chapter 6.

CHAPTER 2

FINITE ELEMENT MODELING

2.1 FINITE ELEMENT PROGRAM SELECTION

To examine the lateral load distribution to the transverse floor beams, the floor system was analyzed using finite elements. The goal of using the finite element modeling was to develop a more reasonable estimate for the moment in the transverse floor beams. One finite element program that was considered is BRUFEM (Bridge Rating Using Finite Element Modeling), a program developed by the Florida Department of Transportation to rate simple highway bridges. BRUFEM allowed the modeling parameters to be changed easily. However, the limitations imposed by this program on the geometry of the floor system made it a poor choice for modeling the floor system. A general-purpose finite element program, SAP2000, was chosen.[1] SAP allowed the variety of floor beam-stringer geometries to be modeled. The only limitation was that the concrete slab could not be conveniently modeled as acting compositely with the stringers.

2.2 FLOOR SYSTEM MODEL

The floor system analyzed was a twin-girder steel bridge. These girders support the transverse floor beams, which in turn support the stringers. All bridges analyzed have a 6.5-inch concrete slab resting on the stringers. Figure 1.1 shows the basic floor system geometry and terminology that will be used in this report.

Using SAP2000, the stringers, floor beams, and girders were modeled using frame elements, line elements with given cross sectional properties, and the slab was modeled using shell elements with a given thickness. The concrete slab, which overhangs the girder by two feet, was divided into one-foot by one-foot elements, wherever possible. The stringers, floor beams, and girders were also usually divided into one-foot lengths. The exception to using one-foot elements occurred only when it was required by the loading geometry. The concentrated wheel loads were placed at the joints located at the intersection of the shell elements, this resulted in some narrower shell elements in certain floor system geometries. The smallest spacing was a shell element width of 3 inches resulting in an aspect ratio of 4 to 1.

All elements were assumed to have the same centroid, which was not the case. In actual bridges, the four centroids are offset as shown in Figure 2.1. The modeling, though, is consistent with the assumption that the slab and supporting elements are not acting compositely. When the system acts in a non-composite manner, the supporting elements and slab act independent of each with the curvature of the slab unaffected by the curvature of the steel members. Figure 2.2 shows the idealized cross section used in the finite element analyses. This assumption of non-composite action is reasonable since no shear studs are specified to connect the slab to the supporting steel elements. Even if there were some composite action, the assumption of non-composite action should lead to a conservative estimate of the distribution of moments to the floor beams.

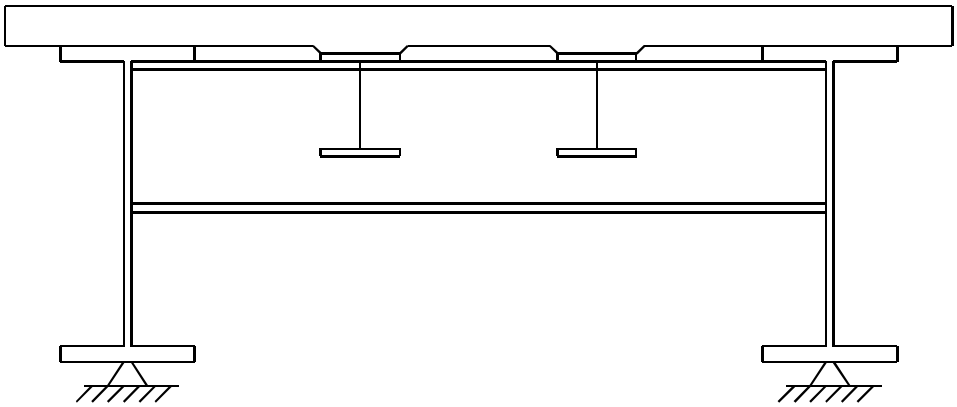

Figure 2.1 Actual Bridge Cross Section

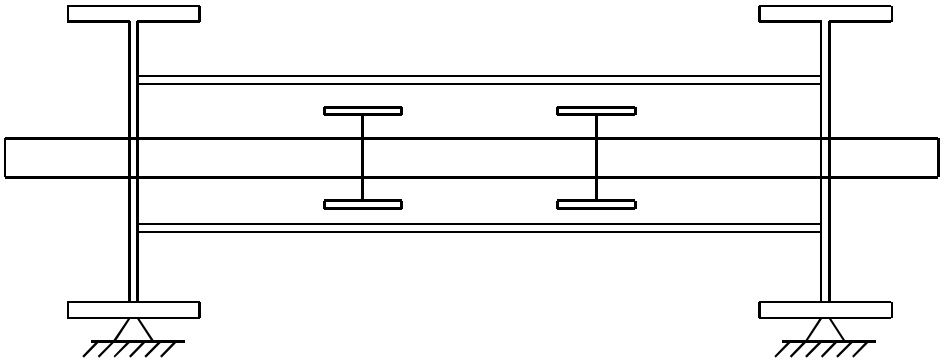

Figure 2.2 SAP2000 Idealized Cross Section

2.3 MODELING THE TRUCK LOAD

The truck load placed on each bridge model consists of two HS-20 trucks placed side by side 4 feet apart as per AASHTO guidelines shown in Figure 1.7. The maximum floor beam moment will occur with middle axle directly over the floor beam with both other axles 14 feet away as shown in Figure 2.3. As mentioned earlier, an inconvenience that arises when trying to apply loads in SAP is that the loads must be applied at the intersection of shell elements to eliminate errors in distributing the loads to adjacent nodes.

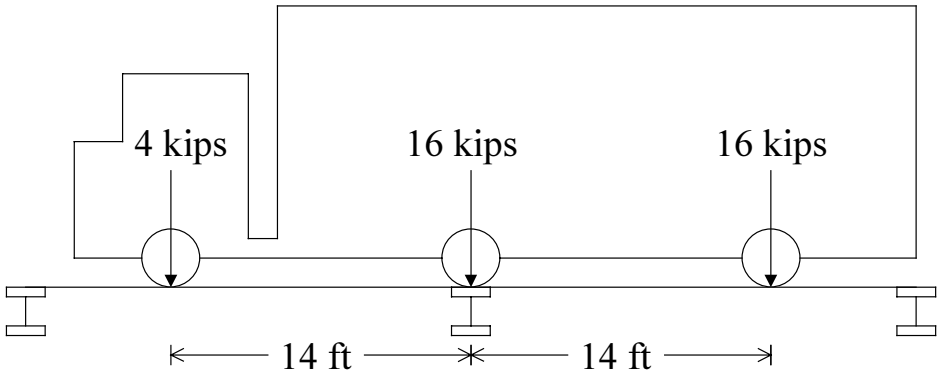

Figure 2.3 Longitudinal Position of Trucks Producing Maximum Moment

Transverse placement of the truck load was another issue in finite element modeling. The symmetric position, shown in Figure 2.4 places the two trucks side by side, each two feet away from the center of the bridge. The position that yields the maximum moment using the direct load model is two trucks placed side by side one foot from the symmetrical position, shown in Figure 2.5. This produces a slightly larger floor beam moment than placing the trucks in the symmetric position in the direct load model. Both of these truck positions were analyzed using finite element modeling and the results are discussed in Chapter 3.

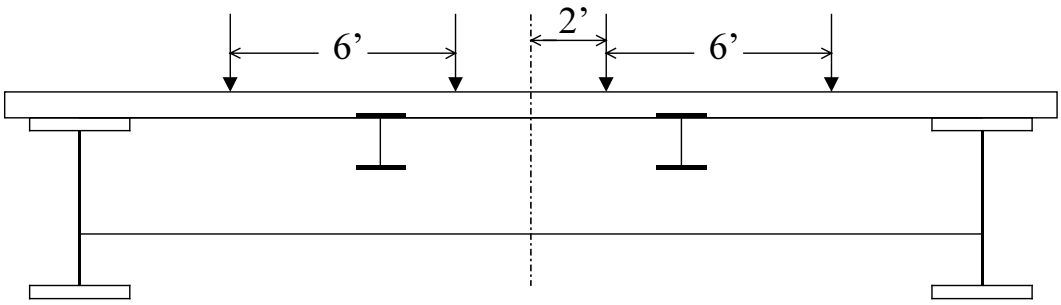

Figure 2.4 Symmetric Transverse Position of Trucks

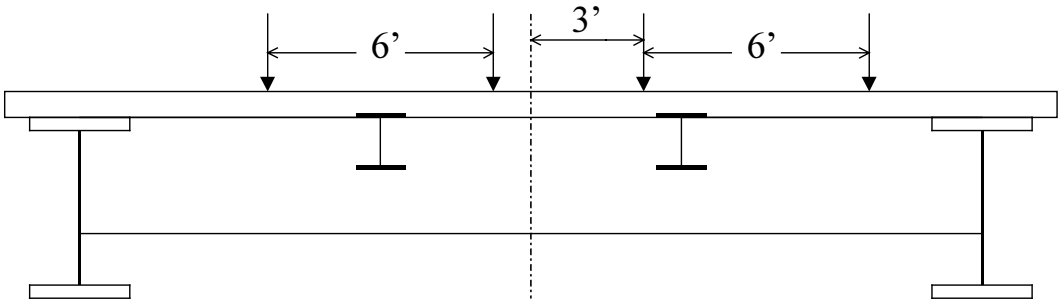

Figure 2.5 Transverse Position of Trucks to Produce Maximum Moment

2.4 MODEL SIZE

2.4.1 Small Model

There are several ways to model the bridge floor systems. The simplest model, referred to as the small model, consists of two girders and floor beams, supported at each end, with two stringers spanning between the floor beams. This model is shown in Figure 2.6. Although the model actually consists of line and shell elements, for clarity the cross-sections of the elements are also shown. Simply supported boundary conditions are used at the end of each girder. The floor beam identified is the floor beam of interest.

The vertical arrows represent the load due to two HS-20 trucks that produces the maximum moment in the center of the floor beam. This load occurs when the middle axle of each truck is directly over the floor beam and the other axles are 14 feet to either side. However, the small model uses the symmetry to reduce the model size. To use symmetry it is assumed that floor beam spacing, stringer spacing, and stringer size are the same on either side of the floor beam. Instead of applying the 16 kip load from the rear axle and the 4 kip load from the front axle on opposite sides of the floor beam the two are added together to produce a 20 kip load on one side of the floor beam. The advantage of using this small model is that it is quicker to run, much easier to input, and has fewer variables. To understand the effect of the exterior girder stiffness, the outside girders were modeled two different ways in the small model. They were modeled as much larger sections than the stringers (DSG), as shown in Figure 2.6, and as the same section as the stringers (SSG). Due to the small length of the model, however, the small model does not capture the effect of the stiffness of the exterior girders. This is discussed in more detail in Chapter 3.

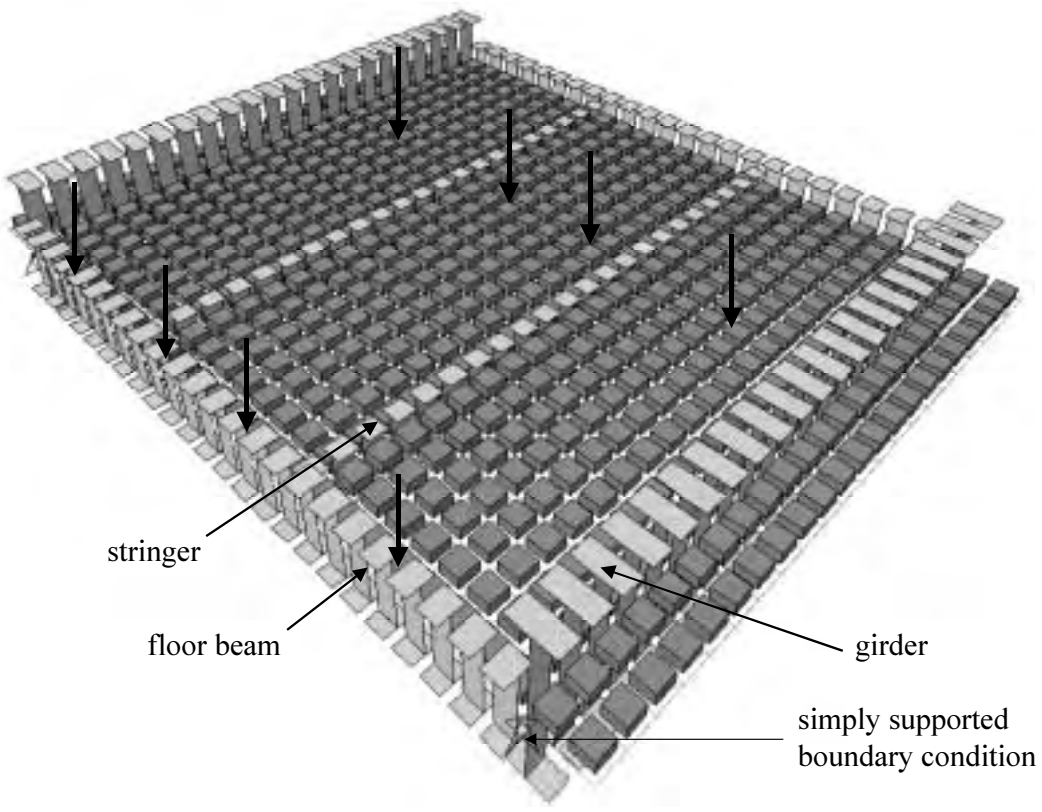

Figure 2.6 Small Floor System Model

2.4.2 Large Model

A larger, more complex model that is closer to the actual geometry of the structure was used to study the influence of the girders upon the lateral load distribution. This model consists of more than two floor beams with much longer exterior girders. Actual bridge geometries were used to generate these models. The largest span length of the bridge from support to support determines the length of the model. The girders are continuous over the length of the entire bridge with the distance spanned between inflection points of about 70 to 80% of the span length. The continuous bridge was modeled as a single span of the bridge with a span length of 80% of the distance between piers as shown in Figure 2.7.

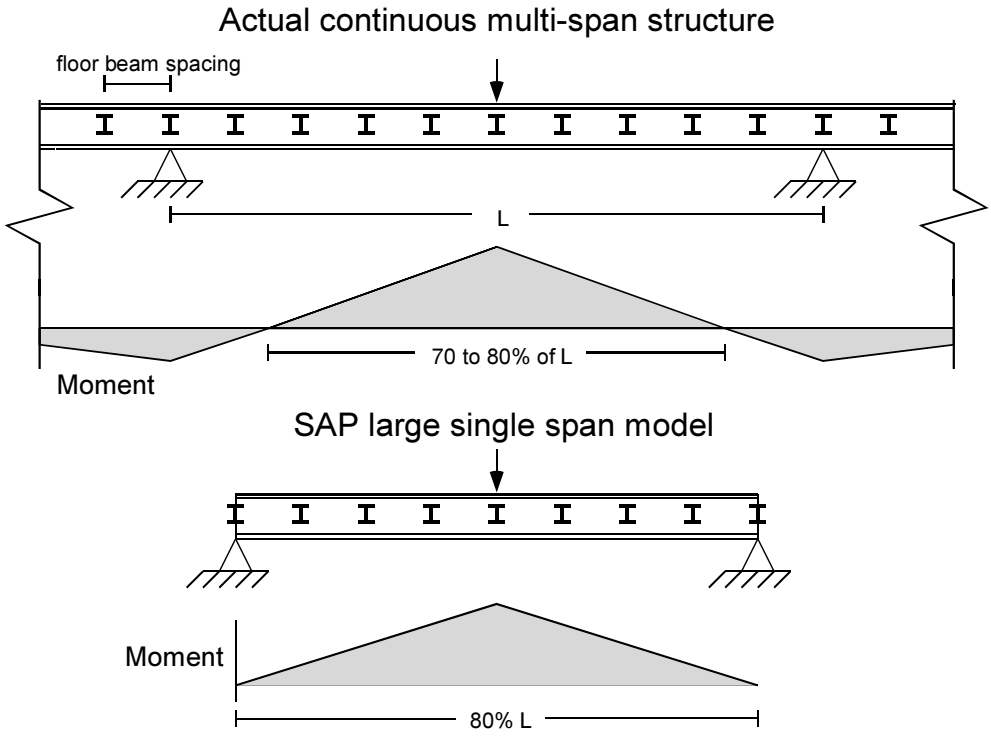

Figure 2.7 Large Model Length

The number of floor beams contained in the model determines the length of the model. The model shown in Figure 2.8 is an example of a large model containing 7 floor beams. The stringers and floor beams have rotational releases for both torsion and moment at their ends. The girders are continuous over the span of the entire model with simply supported boundary conditions at each end. The floor beam of interest is also identified in the figure.

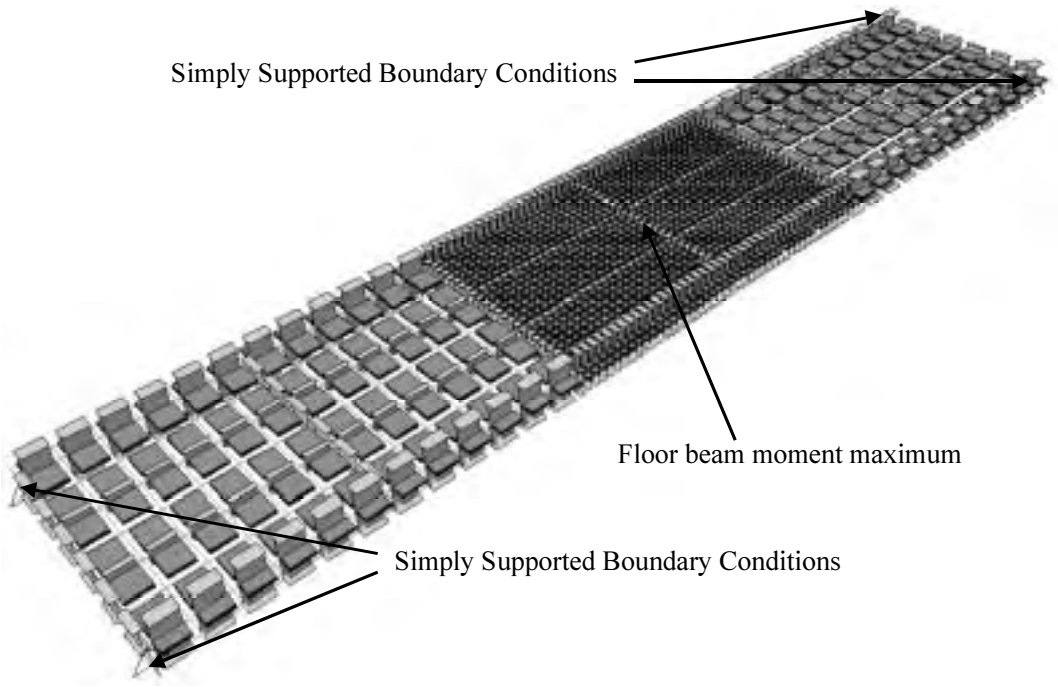

Figure 2.8 Large Floor System Model

The mesh farther away from the floor beam is less refined than the sections closer to the center floor beam. Typical mesh sizes away from the center floor beam are 3 to 4 feet. This is to reduce the analysis time without losing accuracy since the elements closer to the floor beam will have a much greater effect on the accuracy of the model.

The modeling of the slab at the floor beams is an important consideration in the large model. It can either be modeled as continuous or simply supported over the floor beam. The slab is effectively simply supported by the floor beams if it modeled as cracked over the floor beam. The influence of slab continuity up the floor beam moment was studied. The default setting in SAP would be to model the slab as continuous over the floor beams. To model the slab as cracked over the floor beams using SAP requires quite a bit more effort because the program does not provide an option for releasing shell elements.

Two methods of modeling the slab over the floor beams were used in this research. Both methods utilize a slab that ends before intersecting the floor beam. The first method is to constrain the nodes on either side the floor beam node in every direction but rotation as shown in Figure 2.9. This causes the slab to behave as if it was cracked over the floor beam. Both portions of the slab are free to rotate with respect to each other but they are forced to have the same vertical and horizontal displacements. The second method, shown in Figure 2.10, is to fill the small gap between the slab and floor beam with a shell element that has a very small stiffness. Reducing the elastic modulus reduced the stiffness.

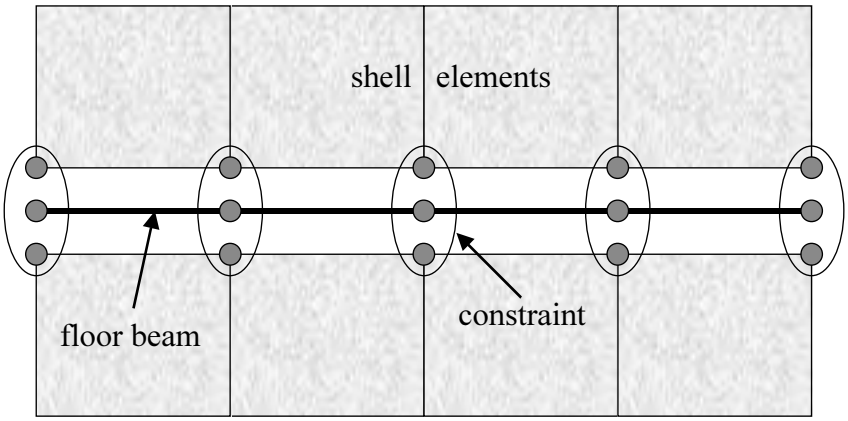

Figure 2.9 Constraint Method of Analyzing Cracked Section

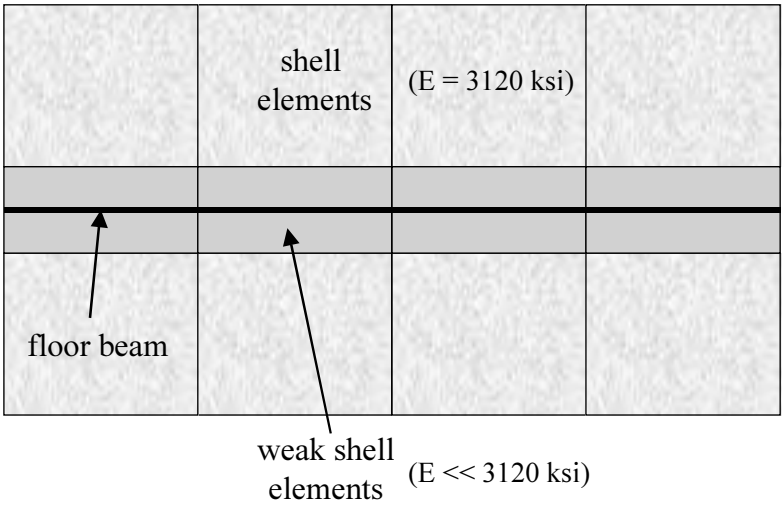

Figure 2.10 Weak Shell Method of Analyzing Cracked Section

Using constraints to model a crack over the floor beam is an inefficient method because each set of three nodes must be selected and then separately constrained. However, in the weak shell method the shell elements can all be selected and assigned a different modulus of elasticity very easily. The two methods were compared and shown to give similar results, so the weak shell method was used in the finite element models discussed in the remainder of the thesis.

2.5 INFLUENCE SURFACES

An influence surface is a useful tool for evaluating finite element models. An influence surface indicates what effect a 1 kip load placed at any location on the floor system will have upon a selected stress resultant. For our analysis, the midspan moment in the floor beam was selected. To develop an influence surface for a model, rotational releases for both torsion and moment are placed on each side of the floor beam midspan. Then equal and opposite moments are also placed on each side of the midspan of the floor beam. The displaced shape of this structure is in the same shape as the influence surface. It must then be normalized by multiplying the ordinate by the moment due to a one kip load placed directly on the floor beam at midspan divided by the displacement at midspan of the floor beam. An example of an

influence surface is shown in Figure 2.11. The example shown is from a small span model with 22-foot floor beam spacing and 8-foot stringer spacing. It is evident from the influence surface that a load placed directly on the center of the floor beam will produce the maximum moment at that location. The white rectangles in the figure show the position of the truck wheels on the influence surface for the symmetric loading case.

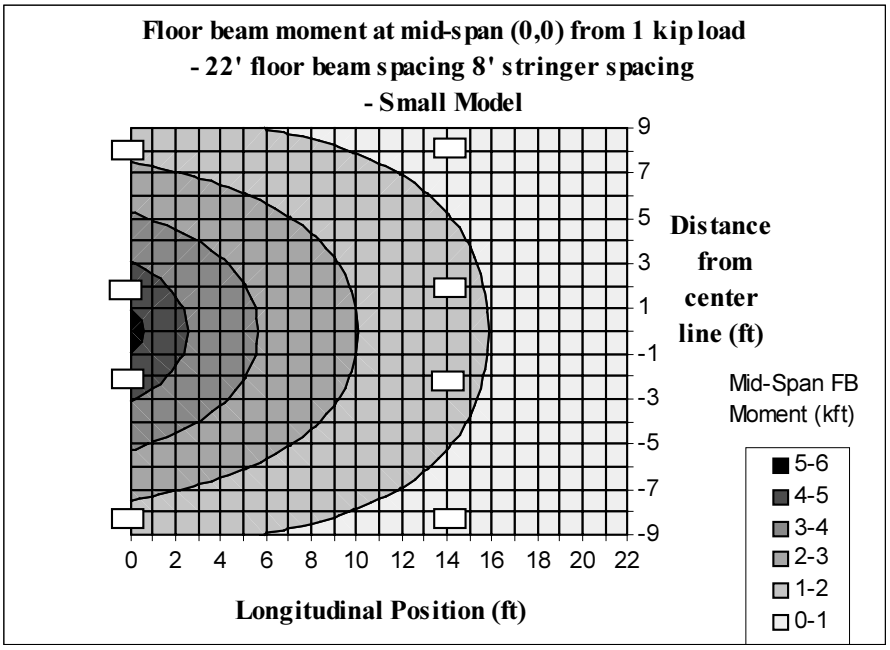

Figure 2.11 Influence Surface for Floor Beam Midspan Moment

Influence surfaces are useful because they show just what effect each wheel of each truck has on the moment and can easily show the differences between models. An influence surface can be used to predict the moments due to any loading case, although only for the moment at one specific location (in this case at the midspan of the floor beam). Using influence surfaces, it was possible to predict midspan moments within 0.1% of the value given by directly positioning the load on the floor system of the SAP model.

The most effective use of influence surfaces, though, is to generate surfaces that normalize the moment generated in a finite element model at each location by the moment generated at the same location using the direct load model, the longitudinally distributed load placed directly on the floor beam, discussed in Chapter 1. An example of an influence surface normalized by the direct load moment is shown in Figure 2.12. The shaded contour plot shows the moment generated in the finite element model as a percentage of the direct load moment. These surfaces simplify visual comparison of different models to understand which wheel loads cause the differences in models. This can help explain the characteristics or variables in each model that are responsible for the change in floor beam moment. To further simplify this comparison, the width of all influence surfaces consisted of the center 18 feet of the model. This is because the furthest wheel loads in the symmetric load case occur 8 feet on either side of the center line, while the trucks in the maximum moment load case occur 9 feet away on one side and 7 feet on the other.

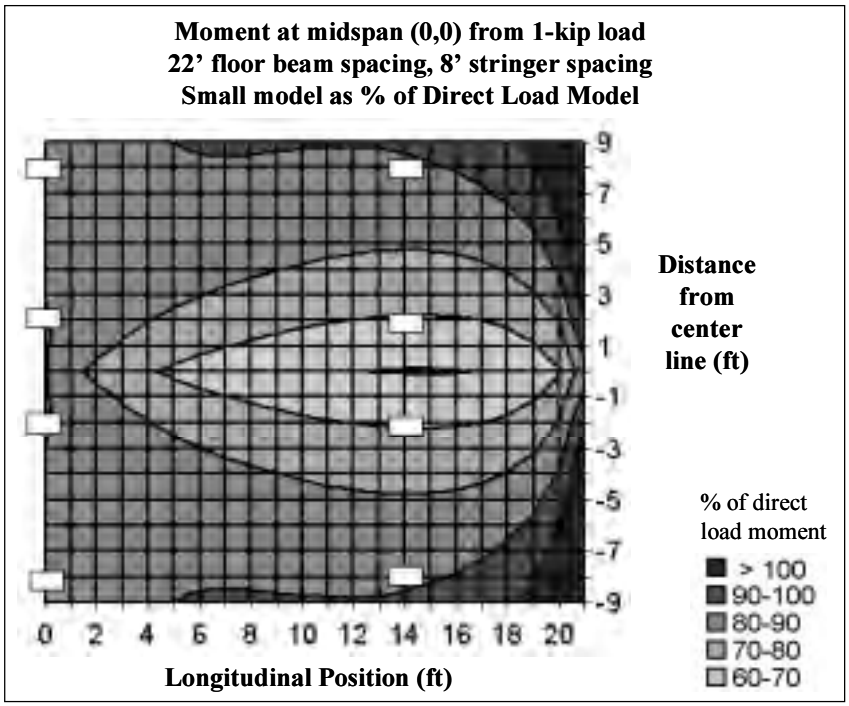

Figure 2.12 Influence Surface Comparing SAP Model to Direct Load Model

CHAPTER 3

RESULTS OF FINITE ELEMENT ANALYSIS

3.1 BRIDGE DATABASE

In order to bound the study it was necessary to identify the bridges in Texas that use this floor system. With these bridges identified, it was possible to place limits on the parameters to be studied in the finite element analysis. The type of floor system being analyzed on this project is a floor system that occurs in long span bridges built in the 1940s and 1950s. The floor system contains two continuous girders that span the length of the bridge with two intermediate stringers supported by the transverse floor beams as shown in Figure 1.1. Table 3.1 gives the floor system properties of the bridges analyzed. The cross sections of these bridges are shown in Appendix A.

Total length for each bridge is defined as the length of the section of the bridge that fits the floor system criteria. For example, if the approach span is a different section than the main span, it is not included in the total length. The span length is the largest span length of the section between supports. As can be seen, the total length of each bridge ranges from 300 feet to almost 800 feet with the longest spans between 60 and 180 feet. Three of the bridges (5, 7, and 9) have two different cross sections used over the length of the bridge. The second cross section for each structure is 5a, 7a, and 9a respectively. They were included as separate models in the finite element analysis. Floor beam spacing ranges from 15 to 22 feet and stringer spacing ranges from just under 7 feet to 8 feet. This is a fairly small range of values, especially the stringer spacing. About half of the bridges were designed for the H-20 loading and about half were designed for HS-20.

Table 3.1 Bridge Database with Floor System Properties

#	Facility Carried	Feature Intersected	Design Truck	Span Length (ft)	total length (ft)	floor beam spacing (ft)	stringer spacing (ft)
1	SH 159	Brazos River	H-20	180	662	15	8
2	FM 723	Brazos River	H-15	150	542	15	7.33
3	SH95	Colorado River	H-20	160	782	20	7.5
4	RM 1674	N Llano River	HS-20	154	528	22	7.33
5	RM 1674	N Llano River	HS-20	99.25	330	19.85	7.33
5a	RM 1674	N Llano River	HS-20	130	330	18.57	7.33
6	SH 37	Red River	H-20	180	662	15	7.33
7	US 59	Sabine River	H-20	99.3	330	19.85	8
7a	US 59	Sabine River	H-20	130	330	18.57	8
8	US 59 (S)	Trinity River	H-20	154	530	22	8
9	310	Trinity River	HS-20	60	300	20	6.92
9a	310	Trinity River	HS-20	152	380	19	6.92
Min			H-15	60	300	15	6.92
Max			HS-20	180	782	22	8

All of the bridges have a 6.5-inch thick slab. However, each bridge has different stringers, floor beams, and girders comprising the load carrying system. Those properties are shown in Table 3.2. All of the sections used are the older sections that have slightly different properties compared with the current sections from the LRFD manual and SAP2000 database. In the SAP analysis, however, the comparable current sections were used since there is very little difference in the properties. Member stiffness, an important variable in this study, is defined as the product of the moment of inertia and modulus of elasticity divided by the length. Since the modulus of elasticity of steel is constant, relative stiffness can be defined as the moment of inertia for models with a constant length.

The stringers range from a W16x40 section to a W21x73 section. The W21x73 section has approximately 3 times the moment of inertia of the W16x40 section. The floor beams have around 3 to 4 times the moment of inertia of the stringers with the values ranging from 2100 in^4 to 4470 in^4. Most of the bridges have plate girders with variable depth. A variable depth plate girder model would have been possible to input into SAP, but probably not worth the time and effort. The plate girders are modeled using a constant depth equal to the minimum depth over the length of the span, using the web and flange thickness at that location. From a preliminary analysis it was determined that this will give a conservative estimate for mid-span floor beam moment, because the stiffer the exterior girders are, the more of the load will be attracted to the outside of the bridge and away from the center. This additional load carried by the exterior girders will result in a smaller mid-span floor beam moment. The plate girders range from 4 to 8 feet in height with a moment of inertia that is from 15 to 150 times that of the stringer moment of inertia.

Table 3.2 Frame member properties

#	Stringer		Floor Beam		Plate Girder	
	Type	Moment of Inertia (in^4)	Type	Moment of Inertia (in^4)	Height (in)	Moment of Inertia (in^4)
1	18WF50	800	W27x94	3270	96	130957
2	16WF40	520	W24x76	2100	48	22667
3	18WF55	890	W27x94	3270	96	126156
4	21WF68	1480	W27x98	3450	60	42492
5	21WF63	1340	W27x98	3450	66.5	44149
5a	21WF59	1250	W27x98	3450	66.5	60813
6	18WF50	800	W27x94	3270	96	130957
7	21WF68	1480	W30x108	4470	66.5	44149
7a	21WF63	1340	W30x108	4470	66.5	60813
8	21WF73	1600	W30x108	4470	60	42492
9	21WF62	1330	W27x94	3270	50	21465
9a	21WF62	1330	W27x94	3270	50	21465
MIN	16WF40	520	W24x76	2100	48	21465
MAX	21WF73	1600	W30x108	4470	96	130957

The goal of this study was to identify parameters that might effect the maximum moment in the floor beam and determine which parameters had the greatest effect on the finite element models. Some of the parameters studied include stringer spacing, floor beam spacing, span length, and the relative stiffness of the girders, floor beams, stringers, and slab. These parameters were studied using both the large model and the small model. The lateral load distribution of the different models is compared using the direct load moment to normalize the values. All values are then given as a percent of the direct load moment.

As discussed in the first chapter, the direct load moment is only dependent on the floor beam spacing and lateral load position and not dependent on any of the member properties.

3.2 SMALL MODEL RESULTS

The first two properties examined, stringer spacing and floor beam spacing were varied along with girder stiffness. This was done holding all other factors constant using the small model. This model has the slab resting directly on the floor beam. The results are shown in Table 3.3. All of the models used W18x50 stringers, W27x94 floor beams, and 66-inch plate girders on the outside. These members are in the middle range of member sizes. The stiffness of the floor beams and plate girders is about 4 times and 70 times that of the stringers, respectively. Two different load positions were also analyzed. Trucks were placed symmetrically side by side on the bridge and at the position that will produce the maximum moment in floor beam, which occurs one foot away from the symmetric position as discussed in Chapter 2. These are located under the headings SYM and MAX for each stringer spacing.

Table 3.3 Small Model Results

			Stringer Spacing					
			7 ft		**7.5 ft**		**8 ft**	
			MAX	SYM	MAX	SYM	MAX	SYM
Floor Beam Spacing	**15 ft**	Direct Load	194.0 kip-ft	190.7 kip-ft	219.7 kip-ft	216.7 kip-ft	245.6 kip-ft	242.7 kip-ft
		Lever Rule	173.3	164.7	196.4	186.6	219.6	208.0
		% direct	**89.4%**	**86.4%**	**89.4%**	**86.1%**	**89.4%**	**85.7%**
		SAP SSG	181.7	178.4	206.1	202.8	230.4	227.2
		% direct	***93.7%***	***93.6%***	***93.8%***	***93.6%***	***93.8%***	***93.6%***
		SAP DSG	181.3	177.9	205.7	202.5	230.1	226.9
		% direct	***93.5%***	***93.3%***	***93.6%***	***93.5%***	***93.7%***	***93.5%***
	20 ft	Direct Load	246.2	242.0	278.9	275.0	311.7	308.0
		Lever Rule	220.0	209.0	249.3	236.9	278.7	264.0
		% direct	**89.4%**	**86.4%**	**89.4%**	**86.1%**	**89.4%**	**85.7%**
		SAP SSG	217	214.1	245.9	243.1	274.8	272.0
		% direct	***88.1%***	***88.5%***	***88.2%***	***88.4%***	***88.2%***	***88.3%***
		SAP DSG	211.9	208.8	241.6	238.7	271.1	268.3
		% direct	***86.1%***	***86.3%***	***86.6%***	***86.8%***	***87.0%***	***87.1%***
	22 ft	Direct Load	260.4	256.0	295.0	290.9	329.7	325.8
		Lever Rule	232.7	221.1	263.8	250.6	294.8	279.3
		% direct	**89.4%**	**86.4%**	**89.4%**	**86.1%**	**89.4%**	**85.7%**
		SAP SSG	225.9	222.9	255.8	253.0	285.7	283.1
		% direct	***86.7%***	***87.1%***	***86.7%***	***87.0%***	***86.7%***	***86.9%***
		SAP DSG	217.8	214.9	248.9	246.1	279.8	277.2
		% direct	***83.6%***	***83.9%***	***84.4%***	***84.6%***	***84.9%***	***85.1%***

Both positions were analyzed using a model with stiffer exterior girders and with girders the same size as the stringers to analyze the effect of girder stiffness. DSG (different size girders) and SSG (same size girders) represent these two cases respectively. Both of these cases as well as the lever rule are normalized by expressing them as a percentage of the direct load moment at the maximum moment position and at the symmetric load case. For each geometry, the floor beam moment calculated by the

direct load method is listed followed by the lever rule and the percentage of the lever rule moment to direct method. Similar listings are given for the SAP SSG and DSG model results.

The table is divided into nine boxes, with each box containing different models with the same floor beam and stringer spacing. For example, the box in the lower right hand corner corresponds to models with a 22-foot floor beam spacing and 8-foot stringer spacing. On the top of this grid are the direct load moments for the maximum and symmetric loading case, 329.7 and 325.8 kip-ft respectively. Looking at the left column of the box, shown next is the maximum floor beam moment calculated using the lever rule, 294.8 kip-ft or 89.4% of 329.7 kip-ft, the maximum direct load moment. The maximum moment calculated using the SSG model is 285.7 kip-ft or 86.7% of 329.7. The maximum moment in the DSG model is 279.8 kip-ft or 84.9% of 329.7. The same pattern is followed on the right column of the box for the symmetric load case.

The first thing to notice in Table 3.3 is that the direct load moment increases as both stringer spacing and floor beam spacing increase. As stringer spacing increases, the floor beam spans equal to 3 times the stringer spacing also increases, causing a higher mid-span moment. As the floor beam spacing increases, the static forces from the wheel loads 14 feet away increase on the floor beam. Moments from the SAP analysis also increase as the spacing increases. However, the increase is not in proportion to the increase found in the direct load model.

3.2.1 Truck Position

Another factor shown in Table 3.3 is the effect of truck position on the maximum floor beam moment. The two columns under each stringer spacing give the moments for the two lateral truck positions. The moment is slightly higher with the loads placed one foot away from the symmetric position for both the SAP analysis and the direct load model. However, by normalizing the moment with respect to the direct load moment, the percentages are basically the same using either loading case. Because of this, the rest of the values discussed for the finite element models will be for the symmetric loading case. However, for the lever rule analysis, the maximum loading position produces a more significant difference in the percentage for the two vehicle positions, 89% and 86%.

3.2.2 Lever Rule

The lever rule only depends on geometry and not the stiffness of the members. When normalized with the direct load method, the lever rule results in the same value of 89.4% regardless of the floor beam spacing or stringer spacing for the max load case. For the symmetric load case, the stringer spacing makes a little difference. With a 7-foot stringer spacing the moment is about 86.4% of the direct load value and with an 8-foot spacing the value falls to about 85.7%. Using the maximum value of the lever rule or 89.4% would be a conservative estimate except at smaller floor beam spacing such as 15 feet where SAP gives a value of between 93.3 and 93.7% depending on the model.

3.2.3 Floor Beam Spacing

From Table 3.3 it is evident that the floor beam spacing plays an important role in the distribution of the lateral load. As the floor beam spacing increases, the floor beam moment as a percentage of the direct load model decreases. Using a 15-foot floor beam spacing, the SAP analysis results in a floor beam moment about 94% of the direct load moment; whereas using 22-foot floor beam spacing the normalized moment is around 84%. This is because larger spacing causes more of the load to be carried to the floor beam from the far axles. For this reason, the wheel loads on either side of the floor beam that are distributed laterally have a greater effect on the total moment as the floor beam spacing increases. Table 3.4 shows this effect for an HS-20 loading. The reduction in the floor beam moment for longer floor beam spacing is also shown in Table 3.4. This table also indicates that most of the moment is caused by the loads directly over the floor beam, 92.3% for a 15-foot spacing and 68.7% for 22-foot spacing. For an

H-20 loading an even greater percentage of the moment is caused by the wheels on the floor beam, 98.3% and 91.7% for the 15-foot and 22-foot spacing respectively.

Table 3.4 Floor beam Spacing Effects for HS-20 Loading

Floor Beam Spacing (ft)	% of Total Moment Caused by Wheel Loads 14 feet away from Floor Beam	% Moment Reduction from Direct Load Model
15	7.7%	6.5%
20	27.3%	12.9%
22	31.3%	14.9%

The moment caused by wheel loads 14 feet away from the floor beam are affected much more by changing the floor beam spacing than the moments caused by the wheels placed directly on the floor beam. The wheel loads on either side of the floor beam are spread out more over the floor beam, while the load placed directly on the floor beam behaves more like the direct load model. This is demonstrated in Table 3.5, which shows that the small model moments produced by the loads over the floor beam are about 90% of the direct load model regardless of the floor system geometry. The 10% reduction in moment is due to the lateral distribution as the load goes from the slab to the floor beam. The table shows floor beam moments from the symmetric loading case using models with the same frame properties as the DSG models shown in Table 3.3. The floor beam moments for the wheels away from the floor beam are shown in Table 3.6. In contrast to the wheels placed on the floor beam, these moments vary greatly depending on the floor beam spacing and to a lesser extent, stringer spacing. This indicates that the loads placed away from the floor beam cause the differences in normalized floor beam moment when the floor beam spacing is changed. However, because these wheel loads contribute a small percentage of the total moment, it takes a substantial change in the floor beam moment caused by these loads to result in a small change in the total floor beam moment.

Table 3.5 Small Model Results with Wheels on Floor Beam Only

			Stringer Spacing		
			7 ft	7.5 ft	8 ft
Floor Beam Spacing	15 ft	Direct Load	176.0	200.0	224.0
		Small Model	159.3	180.0	200.4
		% of direct	***90.5%***	***90.0%***	***89.5%***
	20 ft	Direct Load	176.0	200.0	224.0
		Small Model	159.5	180.4	201.1
		% of direct	***90.6%***	***90.2%***	***89.8%***
	22 ft	Direct Load	176.0	200.0	224.0
		Small Model	159.5	180.4	200.8
		% of direct	***90.6%***	***90.2%***	***89.6%***

Table 3.6 Small Model Results with Wheels away from Floor Beam Only

			Stringer Spacing		
			7 ft	7.5 ft	8 ft
Floor Beam Spacing	15 ft	Direct Load	14.7	16.7	18.7
		Small Model	18.6	22.5	26.5
		% of direct	***126.8%***	***135.0%***	***142.0%***
	20 ft	Direct Load	66.0	75.0	84.0
		Small Model	49.3	58.3	67.2
		% of direct	***74.7%***	***77.7%***	***80.0%***
	22 ft	Direct Load	80.0	90.9	101.8
		Small Model	55.4	65.7	76.4
		% of direct	***69.3%***	***72.3%***	***75.0%***

The influence surfaces for a 15 and 22-foot floor beam spacing also demonstrates this effect. These influence surfaces, shown in Figure 3.1, represent the mid-span moment in the small model as a percentage of the direct load model. Using the direct load model, a load placed on the second floor beam would result in zero moment on the first floor beam. It is impossible to divide by zero, so the horizontal axis in the figure is one foot less than the floor beam spacing. The wheel loads are represented by white rectangles. First of all, the two influence surfaces have a similar shape with the minimum value occurring near the center of the model. The smallest value, 63% occurs with a 22-foot floor beam spacing. The minimum value for the 15-foot floor beam spacing is 71%. The wheel loads on the floor beam (at longitudinal position zero) generate almost the same normalized mid-span floor beam moment, though they become slightly higher as the floor beam spacing increases. However, the wheel loads positioned 14 feet away are quite different for each floor beam spacing. The model with a 22-foot spacing places the center wheel loads 14 feet away from the floor beam near the minimum value while the 15-foot spacing model places those same wheel loads at a location where the small model is greater than the direct load model.

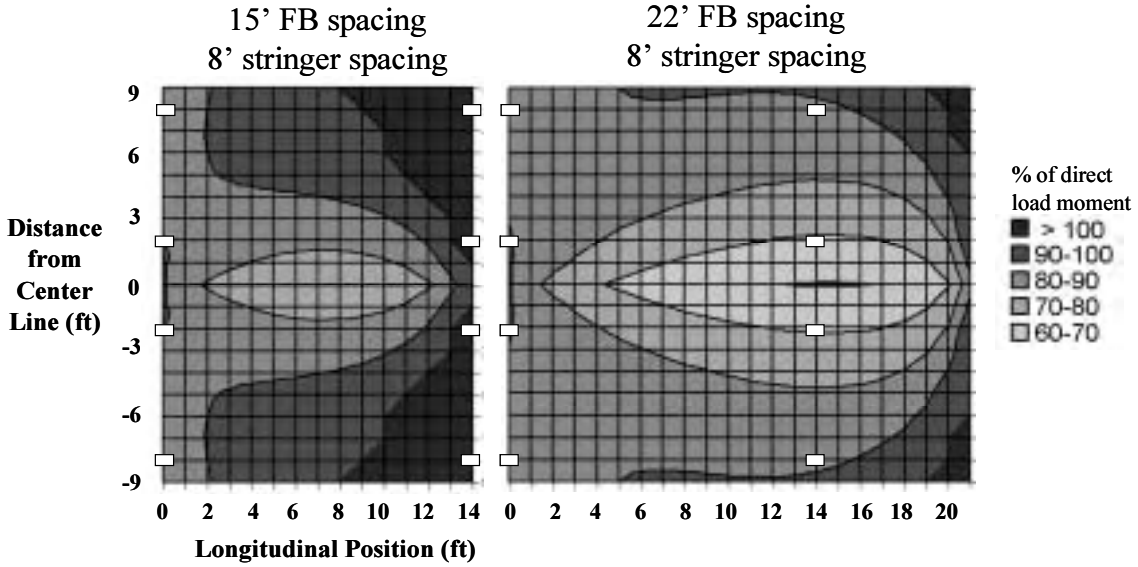

Figure 3.1 Influence Surface Comparison of Different Floor Beam Spacing

3.2.4 Stringer Spacing

When the floor beam spacing is held constant and the stringer spacing is varied, however, there is very little difference in the normalized moment. That is partly because stringer spacing is not varied over a large range. The range of stringer spacing is only from 7 feet to 8 feet. There is virtually no difference in normalized floor beam moment varying stringer spacing using the 15-foot floor beam spacing. Using the longer 22-foot floor beam spacing there is a slight decrease from 85% to 84% in the normalized moment as the stringer spacing is decreased from 8 to 7 feet. That is because when the stringer spacing is smaller, the outside wheels are closer to the stiffer exterior girders, which attract more of the load. This phenomenon is illustrated with a comparison of influence surfaces having different stringer spacing, shown in Figure 3.2. Using the same size girders in the model results in no change in the normalized moment due to the stringer spacing. This is because in the SSG model, the girders and stringers are the same size, which causes the girders to carry less load than the larger stiffer girders in the DSG model.

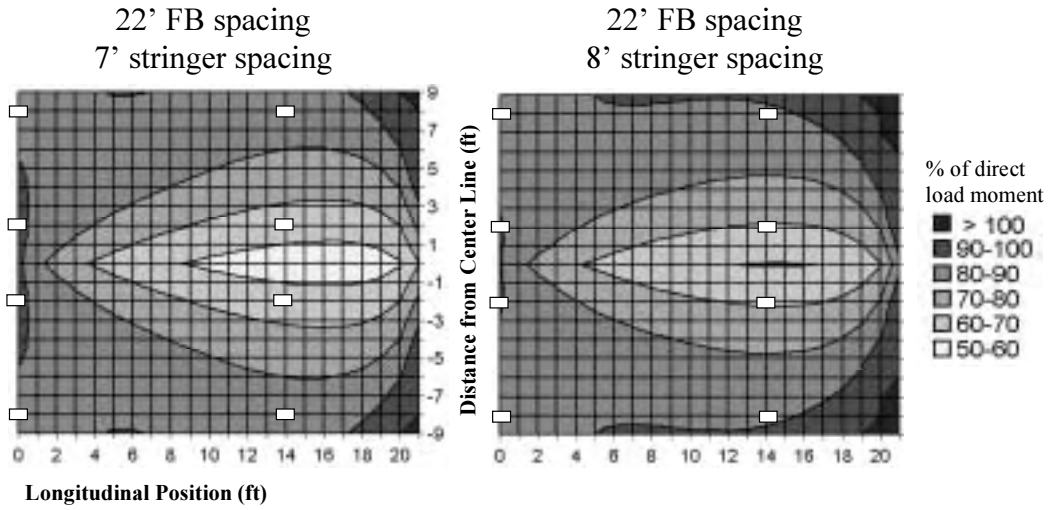

Figure 3.2 Influence Surface Comparison of Different Stringer Spacing

The wheels on the floor beam generate a slightly higher normalized moment with the narrower spacing because of the floor beam stiffness increases. However, that is counteracted by the decrease in normalized moment caused by the wheels away from the floor beam. For this case, the net change is almost negligible, with a decrease of 1.2% as the stringer spacing decreases.

3.2.5 Girder Moment of Inertia

Looking at the DSG and SSG models can show the effect of the moment of inertia of the exterior girders. The SSG model uses W18x50 stringers for the outside girders, while the DSG model has 66-inch plate girders. While the plate girders have a moment of inertia 70 times that of the stringers, there is a relatively small difference in the normalized floor beam moments using the larger exterior girders for most spacing values. The biggest difference occurs in the model with 22-foot floor beam spacing and 7-foot stringer spacing, shown in Figure 3.3. Using larger exterior girders in this model decreases the normalized moment from 87.1% to 83.9%. One would expect the maximum effect to take place in this model because with the largest floor beam spacing, the wheel loads away from the floor beam have the largest contribution to the floor beam moment. That is, the floor beam straddled by the trucks carries a greater percentage of the wheel loads away from the floor beam. Also, with the smallest stringer spacing, it places the outside wheels closest to the exterior girders, attracting the load in that direction, away from the center of the floor beam. By comparison, the 22-foot, 8-foot model goes down from 86.9% to 85.1%. Varying the girder stiffness results in virtually no change in the 15-foot floor beam spacing models.

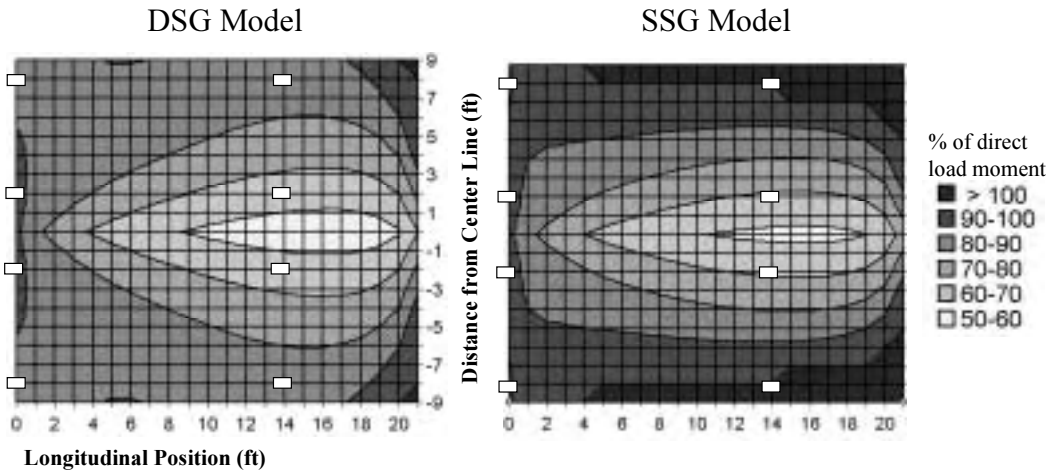

Figure 3.3 Influence Surface Comparison of Different Size Girders

3.2.6 Floor Beam Moment of Inertia

The floor beam moment of inertia can also effect the floor beam moment. A stiffer floor beam will pick up more of the moment, while a floor beam with less stiffness will cause more of the moment to be carried by the slab. This is also demonstrated with the small model. The analysis was run with both W27x94 and W30x108 floor beams using the same stringers and girders as before in the DSG model. All values shown are for the symmetric load case. The W30x108 section is about 35% stiffer than the W27x94 section. A comparison of the normalized moment values for the two different floor beams with different stringer and floor beam spacing is shown in Table 3.7. This shows that for the 22-foot and 20-foot floor beam spacing models, there is an increase in normalized floor beam moment of around 2% while the increase is around 1.5% for the 15-foot models.

The change in normalized moment caused by the floor beam stiffness is also shown in Figure 3.4. These influence surfaces are for models with 22-foot floor beam spacing and 8-foot stringer spacing. The difference in these influence surfaces is found by looking at the wheels positioned directly over the floor beam as shown in the figure. The slab and floor beam both take part of the load from these wheels. When the moment of inertia of the floor beam is increased, it carries a higher percentage of the load. That is why the influence surface for the W30x108 floor beam has higher values near the floor beam. The influence surfaces look very similar away from the floor beam.

Table 3.7 Effect of Floor Beam Stiffness

			Stringer Spacing		
			7 ft	**7.5 ft**	**8 ft**
Floor Beam Spacing	**15 ft**	Direct Load	190.7	216.7	242.7
		W27x94	177.9	202.5	226.9
		% Direct	***93.3%***	***93.5%***	***93.5%***
		W30x108	180.7	205.6	230.4
		% Direct	***94.8%***	***94.9%***	***94.9%***
	20 ft	Direct Load	242.0	275.0	308.0
		W27x94	208.8	238.7	268.3
		% Direct	***86.3%***	***86.8%***	***87.1%***
		W30x108	213.5	244.1	274.6
		% Direct	***88.2%***	***88.8%***	***89.2%***
	22 ft	Direct Load	256.0	290.9	325.8
		W27x94	214.9	246.1	277.2
		% Direct	***83.9%***	***84.6%***	***85.1%***
		W30x108	219.9	252.0	284.1
		% Direct	***85.9%***	***86.6%***	***87.2%***

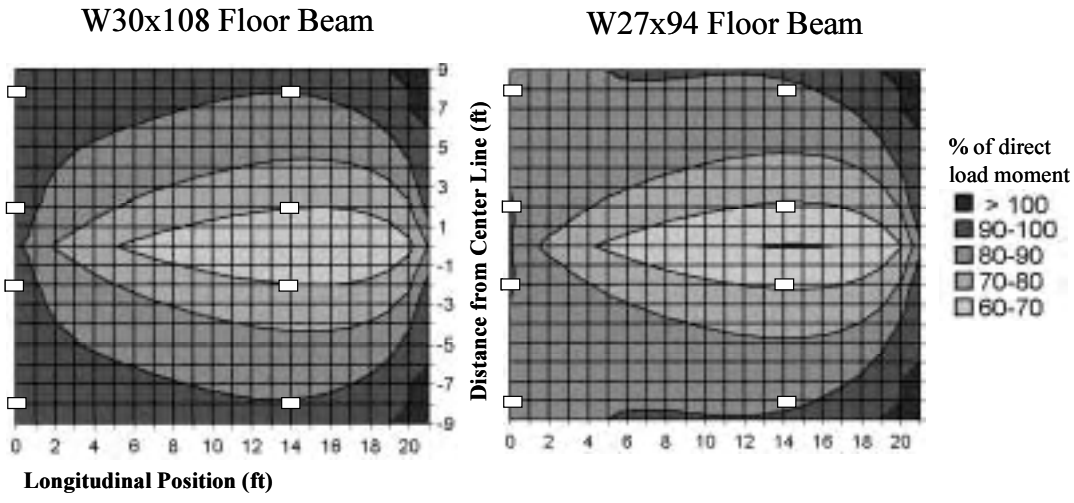

Figure 3.4 Influence Surface Comparison of Different Floor Beam Sizes

3.3 LARGE MODEL RESULTS

When analyzing the structures with the large model the effect of different input parameters changes. An important variable becomes the overall length of the model or number of floor beams in the model. The length was taken as 80% of the maximum interior span length of the bridges included in the survey of Texas bridges. This span length was rounded off to give a model length that is a multiple of the floor

beam spacing so the model starts and ends with a floor beam. The number of floor beams in the small model is two, one at each end of the span. The large model by definition has at least three floor beams. The floor beam being analyzed is always the floor beam in the middle of the model and the slab on either side of the middle floor beam is treated as discontinuous using the weak shell method. Table 3.8 shows the results from the large model of each bridge compared with the similar small model.

Table 3.8 Summary of Finite Element Results

#	Girder height (inches)	Size	Spacing (ft)	Size	Spacing (ft)	# of Floor Beams	Direct Load (kip-ft)	SSG % of direct	DSG % of direct	Large % of direct
1	96	W27x94	15.0	W18x50	8.0	11	242.7	93.5	93.4	86.5
2	48	W24x76	15.0	W16x40	7.3	9	208.0	90.6	90.3	87.5
3	96	W27x94	20.0	W18x55	7.5	7	275.0	88.3	86.8	79.3
4	60	W27x98	22.0	W21x68	7.3	7	279.3	87.3	85.6	84.7
5	66.5	W27x98	19.8	W21x63	7.3	5	262.7	88.7	87.5	81.7
5a	66.5	W27x98	18.6	W21x59	7.3	7	251.1	89.6	88.6	85.6
6	96	W27x94	15.0	W18x50	7.3	11	208.0	93.5	93.3	87.2
7	66.5	W30x108	19.8	WS21x68	8.0	5	306.5	90.8	90.1	85.2
7a	66.5	W30x108	18.6	W21x63	8.0	7	292.9	91.6	91.1	90.1
8	60	W30x108	22.0	W21x73	8.0	7	325.8	89.5	88.4	88.5
9	50	W27x94	20.0	W21x62	6.9	3	242.0	88.6	87.2	80.5
9a	50	W27x94	19.0	W21x62	6.9	7	233.9	89.4	88.3	93.0
MIN	48	W24x76	15	W16x40	7	3	208	87.3	85.6	79.3
MAX	96	W30x108	22	W21x73	8	11	326	93.5	93.4	93.0

As can be seen from the last column of the table, the results from the large model range from 79.3% to 93.0% of the direct load model. The floor beam moments from the DSG and SSG models range from 85.6 to 93.4% and 87.3 to 93.5% respectively. In every case but 9a, the results from the small model are conservative with respect to the large model. In the next few sections, the effect of different parameters on the large model results will be discussed.

3.3.1 Number of Floor Beams

The number of floor beams is a parameter that describes the overall length of the model. In the small model, there were only two floor beams, so the number of floor beams was not a variable. It will be shown here, though, that the number of floor beams or model length has a significant effect on the floor beam moment. Table 3.9 shows the results of two different bridges with the number of floor beams varied and all other parameters constant. These results show that the floor beam moment increases significantly when the number of floor beams in the model is increased.

Table 3.9 Effect of Increasing the Number of Floor Beams

Floor beam spacing (ft)	Stringer spacing (ft)	Stringer Mom. of Inertia (in^4)	Floor Beam Mom. of Inertia (in^4)	Girder Mom. of Inertia (in^4)	# of Floor Beams	% of Direct
22	8	1600	4470	42000	7	88.5
22	8	1600	4470	42000	9	90.3
19	7	1330	3270	22000	3	81.4
19	7	1330	3270	22000	5	86.3
19	7	1330	3270	22000	7	93.0
19	7	1330	3270	22000	9	99.7

For example, when the number of floor beams is increased from 3 to 9 the normalized moment increases from 81.4% to almost 100% of the direct load moment for the case with 19-foot floor beam spacing and 7-foot stringer spacing. For the case with 22-foot floor beam spacing and 8-foot stringer spacing, the floor beam moment increases from 88.5% to 90.3% when the number of floor beams is increased from 7 to 9. This occurs because as the model becomes longer, the exterior girders become less stiff and therefore carry less of the load. Notice that increasing the number of floor beams has a much greater effect on models with a smaller girder moment of inertia. The 22000 in^4 moment of inertia is the minimum moment of inertia found in any of the bridges surveyed. This value is the smallest girder section found on the bridges. Though the last row in the table shows a model that is around 100% of the direct load moment, this model geometry is unlikely. A girder size this small would not be used for a span of that length.

3.3.2 Floor Beam Moment of Inertia

The moment of inertia of the floor beams also has an effect on the floor beam moment. As the moment of inertia of the floor beams is increased, the floor beams pick up more of the load relative to the slab, similar to the results from the small model analysis. These results shown in Table 3.10 demonstrate this effect. As the floor beams are increased from 3270 to 4470 in moment of inertia, the corresponding normalized moment increases from 85.8% to 90.3% for the model using 9 floor beams. In the model with 7 floor beams, the increase is even greater, from 82.0% to 88.5%.

Table 3.10 Effect of Increasing the Size of Floor Beams

Floor beam spacing (ft)	Stringer spacing (ft)	Stringer Mom. of Inertia (in^4)	Floor Beam Mom. of Inertia (in^4)	Girder Mom. Of Inertia (in^4)	# of Floor Beams	% of Direct
22	8	1600	3270	42000	9	85.8
22	8	1600	4470	42000	9	90.3
22	8	1600	3270	42000	7	82.0
22	8	1600	4470	42000	7	88.5

3.3.3 Floor Beam Spacing

Floor beam spacing has the same effect that it had in the small model. As the spacing increases, the wheels away from the floor beam have a greater effect on the normalized floor beam moment. As the floor beam spacing decreases the normalized floor beam moment increases. This trend is shown in Table 3.11.

Table 3.11 Effect of Decreasing the Floor Beam Spacing

Floor beam spacing (ft)	Stringer spacing (ft)	Stringer Mom. of Inertia (in^4)	Floor Beam Mom. of Inertia (in^4)	Girder Mom. of Inertia (in^4)	# of Floor Beams	% of Direct	Small Model % of Direct
22	8	1600	4470	42000	7	88.5	
19.85	8	1600	4470	42000	7	93.1	
15	8	1600	4470	42000	7	94.5	
22	8	1600	3270	61000	7	78.6	85.1
19.85	8	1600	3270	61000	7	83.9	
15	8	1600	3270	61000	7	87.7	93.5

This table contains three different values for floor beam spacing with all other variables held constant. Different floor beam sections and plate girders are used in the second group. This table also demonstrates that the normalized moment decreases as the floor beam size decreases and the girder size increases. The members used in the second group of three are the same members used in the small model results shown earlier. The small model results are shown in the last column. These values are conservative for this case compared with the large model results.

3.3.4 Girder Moment of inertia

The moment of inertia of the girders becomes an important variable as the length of the model increases. This is demonstrated in Table 3.12. It is evident that changing the moment of inertia of the exterior girders has a significant effect on the floor beam moment in the longer models (the models using 5 and 7 floor beams). However, in the model with only 3 floor beams, there is very little change in moment despite increasing the girder moment of inertia by a factor of six. This was also demonstrated using the small model when there was a relatively small difference between the SSG and DSG model despite increasing the moment of inertia by a factor of 70.

Table 3.12 Effect of Increasing Girder Stiffness

Floor beam spacing (ft)	Stringer spacing (ft)	Stringer Mom. of Inertia (in^4)	Floor Beam Mom. of Inertia (in^4)	Girder Mom. Of Inertia (in^4)	# of Floor Beams	% of Direct
19.85	8	1330	4470	22000	3	87.3
19.85	8	1330	4470	42000	3	87.0
19.85	8	1330	4470	61000	3	86.8
19.85	8	1330	4470	131000	3	86.7
19.85	8	1330	4470	22000	5	92.2
19.85	8	1330	4470	42000	5	88.3
19.85	8	1330	4470	61000	5	86.9
19.85	8	1330	4470	131000	5	85.2
19.85	8	1330	4470	22000	7	99.9
19.85	8	1330	4470	42000	7	93.1
19.85	8	1330	4470	61000	7	90.7
19.85	8	1330	4470	131000	7	87.4

In the longer models, as the girder moment of inertia increases, the floor beam moment decreases significantly. This is because as the moment of inertia of the girders become larger, the stiffness increases and more of the load is attracted to the outside and away from the center of the model. However, when the model is shorter, the moment of inertia of the girders has less of an effect on the floor beam moment, because the girders are already very stiff due to their smaller length. The effect of the girder stiffness is related to the effect of the stringer stiffness. The amount of load carried by the girders is also related to the stringer stiffness. With stiffer stringers, the girders carry less of the load and the resulting floor beam moment is higher. The model with 7 floor beams shown above resulting in almost 100% of the direct load moment is not a floor system used in an actual bridge. The girder moment of inertia of 21000 in^4 is too small to be used in a span of that length.

3.3.5 Stringer Spacing

Decreasing the stringer spacing also has a minimal effect on the normalized floor beam moment. As shown in Table 3.13, when the stringer spacing decreases the normalized floor beam moment slightly increases. This is the opposite effect of what was seen using the small model. It is expected that the model with the narrower width would attract more of the load away from the center toward the outside of the bridge as was seen in the small model influence surfaces.

Table 3.13 Effect of Decreasing the Stringer Spacing

Floor beam spacing (ft)	Stringer spacing (ft)	Stringer Mom. of Inertia (in^4)	Floor Beam Mom. of Inertia (in^4)	Girder Mom. of Inertia (in^4)	# of Floor Beams	% of Direct
22	8	1600	4470	42000	7	88.5
22	7.33	1600	4470	42000	7	89.3
22	7	1600	4470	42000	7	90.2
22	**8**	**1600**	**4470**	**131000**	**7**	**81.9**
22	7.33	1600	4470	131000	7	82.4
22	**7**	**1600**	**4470**	**131000**	**7**	**82.6**
20	8	1330	3270	22000	7	89.5
20	7.5	1330	3270	22000	7	90.4
20	7	1330	3270	22000	7	92.8

Influence surfaces for the two entries in bold in Table 3.13 are shown in Figure 3.5. These influence surfaces demonstrate that there is little difference in normalized floor beam moment caused by a change in stringer spacing. As the spacing decreases, the slight normalized moment increase caused by the wheels directly over the floor beam is counteracted by the slight decrease caused by the wheels away from the floor beam. This results in a slight increase in overall normalized moment from 81.9% to 82.6%. The other models in the table had a slightly larger increase, but probably not enough to be significant.

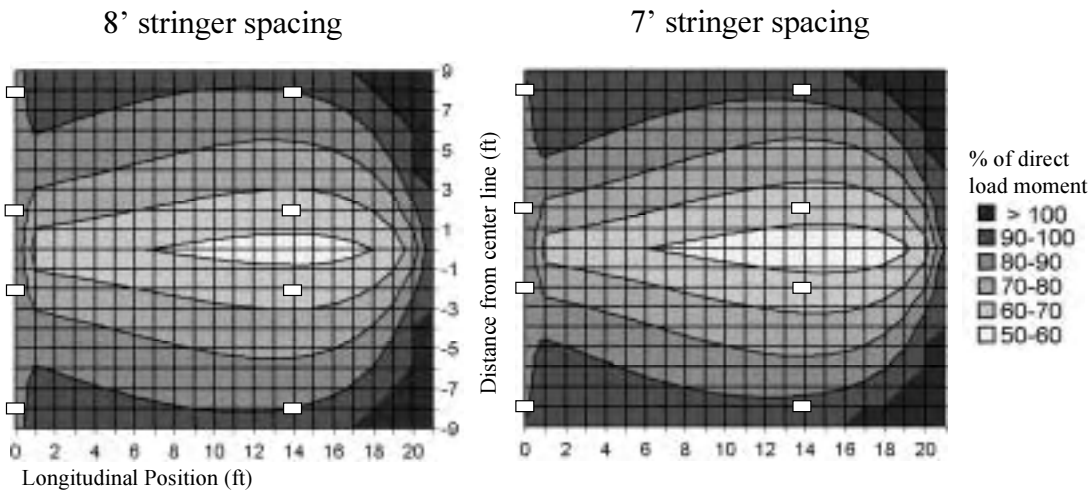

Figure 3.5 Influence Surface Comparison for Large Model Stringer Spacing

3.4 SUMMARY OF FINITE ELEMENT RESULTS

When interpreting these results, it is important to remember that the results from these finite element studies are for the case that there is contact between the floor beam and the slab, because the shell elements and frame elements share the same node. For the case when the slab does not rest on the floor beams, the lever rule is probably the appropriate method to estimate the floor beam moments.

3.4.1 HS-20 Load Case

Table 3.14 shows a summary of the effects of the various parameters studied in this chapter for the HS-20 loading. As is evident from the table, the large model shows the effects of more of the parameters. Only the floor beam spacing and floor beam moment of inertia have much effect on the normalized floor beam moment in the small model. The large model also captures the exterior girder effects. Changing the number of floor beams and the girder moment of inertia both cause a change of stiffness in the girder.

Table 3.14 Summary of Effects of Various Parameters on HS-20 Loading

Increasing this Parameter	Change in Normalized Floor Beam Moment	
	Small Model	Large Model
Floor Beam Spacing	Decrease	Decrease
Floor Beam Moment of Inertia	Increase	Increase
Girder Moment of Inertia	Slight Decrease	Decrease
Number of Floor Beams	NA	Increase
Stringer Spacing	Slight Decrease	Slight Increase

Unless a small girder size is used over a long span with relatively large stringers and floor beams, as was the case in bridge 9a, the results for the small model will be conservative compared with the large model. In bridge 9a, the plate girder moment of inertia was 21000 in^4 over a span of 114 ft. The floor beams and stringer had moments of inertia of 3270 in^4 and 1330 in^4 respectively. Using the small model, for all other cases would be a reasonable method for evaluating the floor beam moment. However, a better method is to come up with an equation that includes the different parameters shown in the above table.

3.4.2 H-20 Load Case

Though the majority of the discussion in the chapter focused on the HS-20 load case, it is also important to consider the effect of the H-20 load case. It has the same wheel loads as the HS-20 load case minus the second rear axle. Because of this there is a 4-kip wheel load away from the floor beam compared with a 16-kip wheel load on the floor beam, the effects of the 4-kip load are minimal. Almost all of the floor beam moment comes from the wheels directly over the floor beam. Figure 3.6 shows the position of the longitudinal position of the H-20 truck to produce the maximum moment.

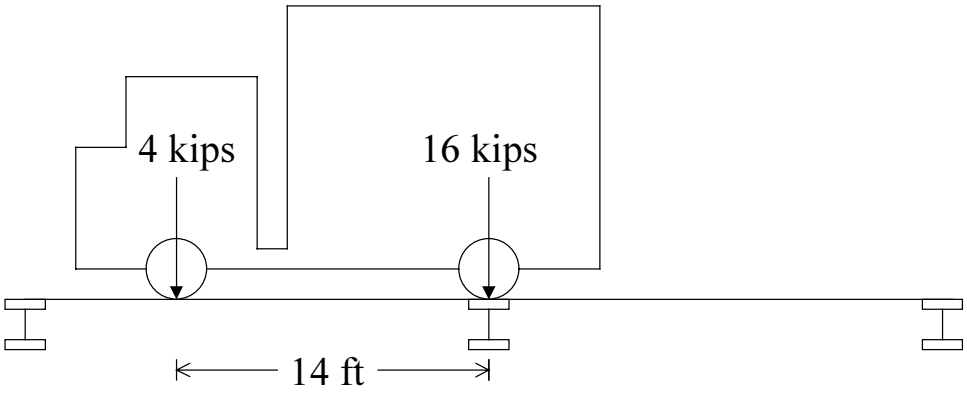

Figure 3.6 Longitudinal Position of H-20 Truck

Looking back at Table 3.5 shows that the stringer and floor beam spacing have almost no effect on the load placed directly on the floor beam. Intuitively that makes sense as well. The entire load is already on the floor beam, so there can be little effect due to load distribution. The only parameter that has an effect on the floor beam moment for this load case is the floor beam moment of inertia compared to that of the concrete slab. A higher floor beam moment of inertia causes the floor beam to carry more of the moment and a lower floor beam moment of inertia causes the slab to carry more of the moment. Table 3.15 shows the effect this ratio on the floor beam moment.

Table 3.15 Effect of Floor Beam Moment of Inertia on H-20 Load Case

Floor Beam		Slab		EI_{FB} / EI_{slab}	% of Direct
I (in^4)	EI ($k\text{-}in^2$)	I (in^4)	EI ($k\text{-}in^2$)		
2100	60900000	275	856830	71	85.5
3270	94830000	275	856830	111	89.8
4470	129630000	275	856830	151	92.2
6710	194590000	275	856830	227	94.8

Using this data it was possible to find a correlation between the floor beam to slab flexural stiffness (EI) ratio and the percent reduction of the floor beam moment. The moment of inertia for the slab was determined using a one-foot wide section of the slab. The modulus of elasticity of steel and concrete in the above table were 29000 ksi and 3120 ksi respectively. The moment of inertia of the slab was the same for every bridge examined since the same 6.5-inch thick slab was used. The moment due to an H-20 truck load can be predicted using the correlation shown in Equation 3.1. The correlation is a conservative estimate of the finite element results as shown in Figure 3.7.

$$M_{LL} = M_{direct} \cdot \left(0.08 \ln\left[\frac{EI_{FB}}{EI_{slab}} \right] + .52 \right) \tag{3.1}$$

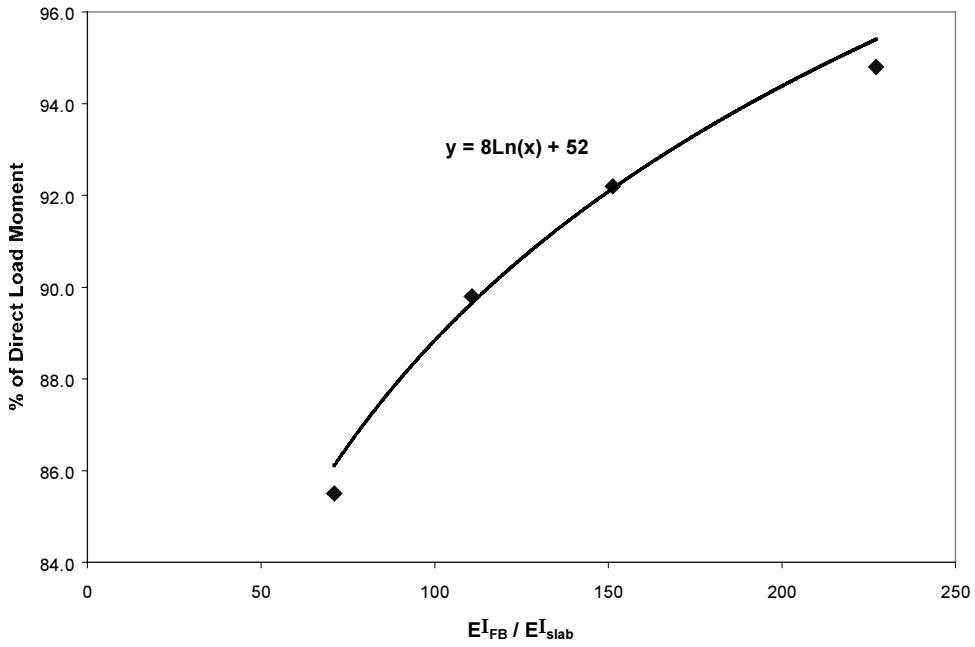

Figure 3.7 Correlation of Floor Beam Stiffness to Moment Reduction

CHAPTER 4

RESULTS OF EXPERIMENTAL TEST

4.1 LLANO BRIDGE FLOOR SYSTEM GEOMETRY

A load test was done on a bridge in Llano, TX. Charles Bowen, a Ph.D. candidate at the University of Texas, was responsible for the testing of this bridge for TxDOT's historic bridge research project, #1741. The transverse floor beams in the bridge in Llano, shown in Figure 4.1, are controlling the low load rating of the bridge. Replacement of the bridge is being considered since the floor beams have been rated deficient for the current design loads. Since this bridge was already scheduled to be tested, it was decided to use the results from this test to study of floor beam behavior and to correlate with the analytical results. The bridge was first tested on February 2, 1999.

Figure 4.1 Historic Truss Bridge in Llano, TX

Although the bridge in Llano is a truss, the floor system geometry is similar to the bridges being analyzed in this study. The bridge is made up of four identical trusses, each spanning about 200 feet. Figure 4.2 shows a plan view of a section of the floor system. This is the section adjacent to the north abutment of the bridge that was instrumented and tested. The bridge has a floor beam spacing of 22 feet, within the range of the bridges in the analytical study. There are six identical stringers as compared to the two stringers and two girders in geometry analyzed in Chapter 3. However, the distance between the outside stringers is only 22.5 feet, the same as the distance between girders in the model with 7.5-foot stringer spacing.

Having the stringers all the same size is basically the same as the SSG model looked at earlier. One difference is that in the Llano Bridge, the floor beam does not end at the outermost stringer. It continues for another 20 inches where it connects with the truss vertical. This vertical member is then connected to the bottom chord of the truss with a gusset plate. This connection is shown in Figure 4.3. Extending the floor beam past the furthest stringer leads to a longer floor beam, which, at just under 26 feet, is about 2 feet longer than the longest floor beam from the plate girder models. In the SAP model, since only the floor system is modeled, each floor beam to truss connection was modeled as a simply supported boundary condition.

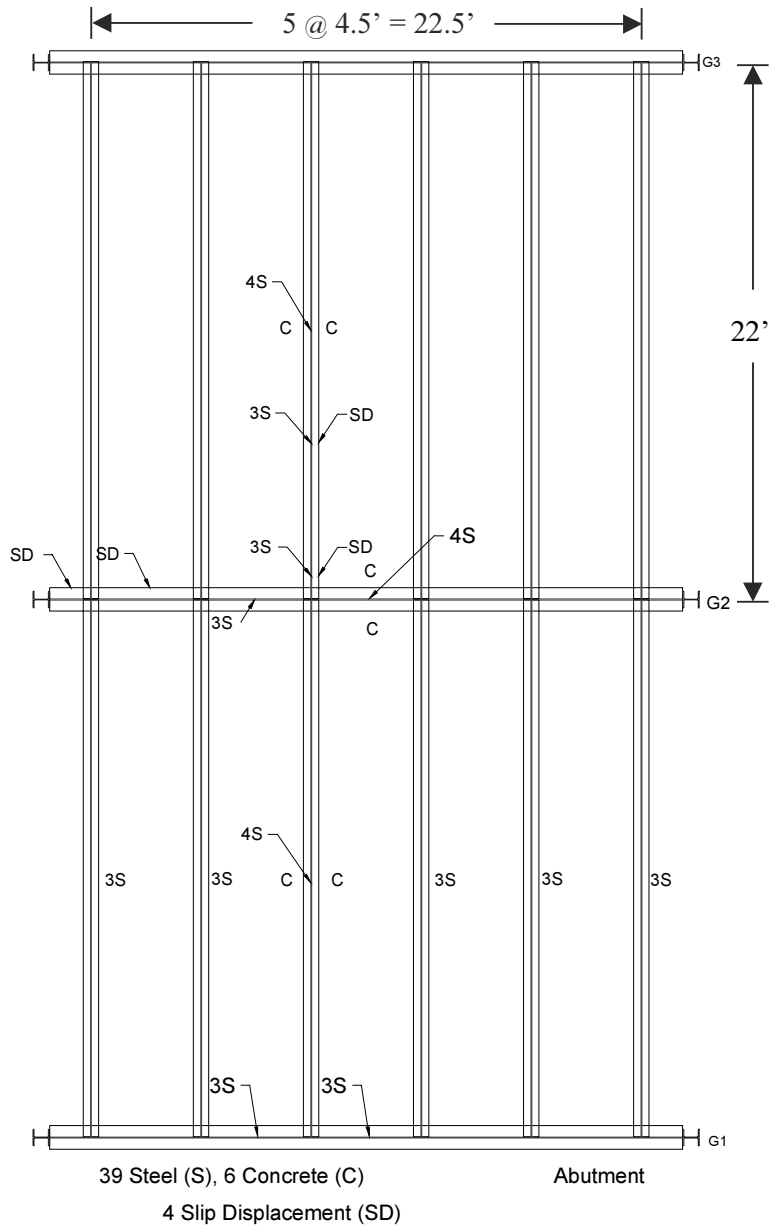

Figure 4.2 Plan View with Strain Gage Locations

The stringers in the Llano Bridge are 18WF50s and the floor beams are 33WF132s. However, the floor beams were modeled as W33x130s because this was the closest section in the SAP database. These sections are in the same approximate range as the sections studied earlier, though the floor beam is a bit larger than the maximum section used in the plate girder bridges, which was a W30x108. The slab is again 6.5 inches thick, but a low modulus of elasticity of 2850 ksi is used since it has a design strength of 2500 psi. The modulus of elasticity for the bridges in Chapter 3 was 3120 ksi for a design strength of 3000 psi. A higher floor beam stiffness and a lower slab stiffness will lead to a higher normalized moment which will be shown in with the influence surfaces later.

Figure 4.3 Connection of Second Floor Beam to Truss

4.2 LOCATION OF STRAIN GAGES

Gages were placed at various locations on the floor system, shown in Figure 4.2. Of primary interest, though, are the gages located on the floor beams. Both the first floor beam and second floor beam were instrumented at two locations, at midspan and at 4.5 feet away from midspan. The other floor beams were not easily accessible and were not instrumented.

At each location, a gage was placed on the top flange, the bottom flange, and in the center of the web. At the midspan location of the second floor beam there were gages placed on both sides of the top flange. The location of the strain gages on the floor beams is shown in Figure 4.4. Also shown in the figure are the dimensions of the wide flange section and the calculation for the section modulus of the floor beam. This section modulus (along with the modulus of elasticity) is used to convert strains to moments. This is assuming non-composite action with the neutral axis at the centroid of the floor beam. The strain at the outside of the member is determined, assuming a linear strain distribution, by multiplying the strain from the gage by the correction factor.

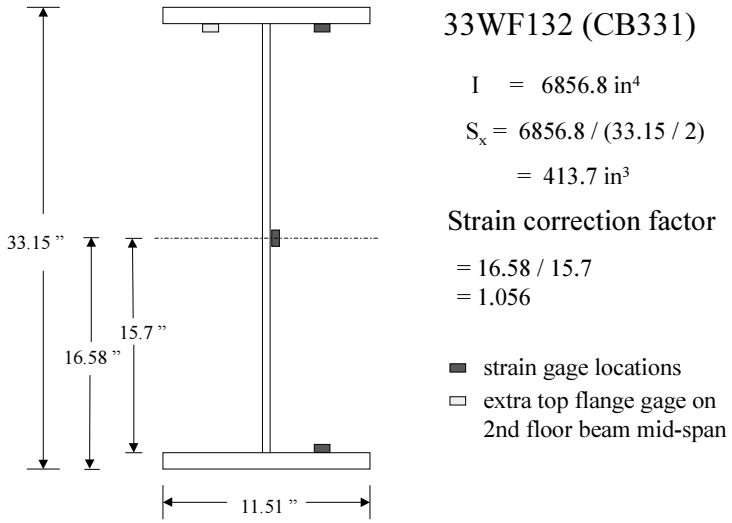

Figure 4.4 Location of Gages on Floor Beams

4.3 TRUCK LOAD

Two TxDOT dump trucks filled with sand were used in the load test of the Llano Bridge. They were almost identical in geometry and load. This made it possible to combine the trucks into one average truck for the finite element analysis. The approximate truck geometry is shown in Figure 4.5. The TxDOT vehicle is shown in Figure 4.6.

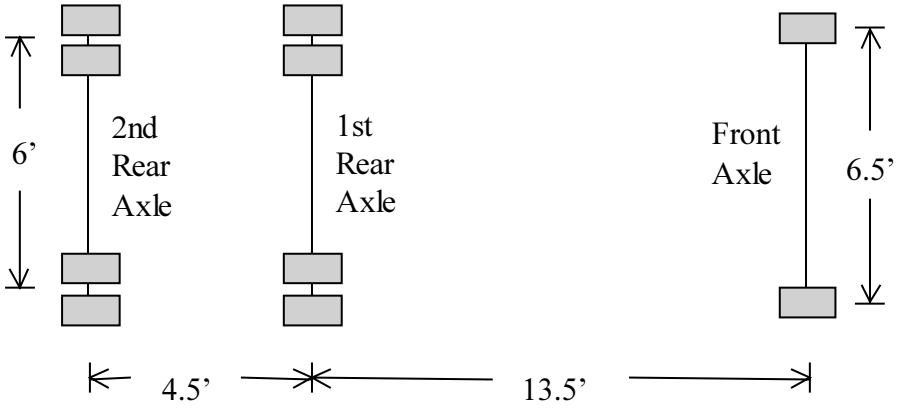

Figure 4.5 TxDOT Truck Geometry

Figure 4.6 TxDOT loading vehicle

The front axle has only two wheels, while each of the rear axles has four wheels. The total spacing of the truck is 18 feet from front to rear axle, quite a bit shorter than the 28 feet in the HS-20 model. This shorter wheel base, assuming loads of equal magnitude, would result in a higher moment in the floor beams. However, the loads are not of equal magnitude.

While there are four wheels on each of the rear axles of the loading vehicle, to simplify modeling of this truck in SAP, the pair of wheel loads on either side of the rear axles was treated as a single point loads at the centroid of the pair. These single wheel truck loads are calculated and are shown in Table 4.1. Given only the weight of the front axle and the combined weight of the two rear axles it was assumed that the load distribution of the wheels was equal. The rear tandem refers to the combined weight of the two rear axles. The final loads used in the SAP model for the Llano Bridge are shown in the final column in bold. There are two 8.66 kip loads on each rear axle spaced 6 feet apart and two 5.24 kip loads on the front axle

spaced 6.5 feet apart. These trucks have a lighter load than the HS-20 trucks with a total load of approximately 45 kips as compared with 72 kips. They have a higher percentage of the load on the front axle.

Table 4.1 Truck Loads

	Truck A Weight (kips)	Truck B Weight (kips)	Average Weight (kips)	# of Wheels	Load Per Wheel (kips)
Front Axle	10.32	10.65	10.49	2	**5.24**
Rear Tandem	35.03	34.22	34.63	4	**8.66**

The trucks were run over different lateral positions on the bridge. Most of the runs had only one truck on the bridge with one of the front wheels on one of the stringer lines. Only the center run had neither front wheel on a stringer line. There were also a few runs with two trucks on the bridge. These consisted of a side-by-side, train, and reverse train loading cases. The side-by-side loading case had the trucks 4.5 feet apart, symmetric about the centerline of the bridge. This spacing was used because it puts the front center wheel of each truck on a stringer line. The train load case had the second truck following close behind the first on the center of the bridge. The reverse train run had the second truck following in reverse close behind the first in the center of the bridge. Each different run was done twice to study repeatability. The load runs of most interest in this study are the runs with two trucks on the bridge, particularly the side-by-side load case which is most similar to the HS-20 loading case that controls the rating of the plate girder bridges. For more detail on the load runs in the first Llano test see Appendix B.

The wheel base in the TxDOT trucks is much shorter and the front axle load is higher than in the HS-20 vehicle. Both of these facts lead to a much lower percentage of the moment coming from the wheels placed directly over the floor beam according to the direct model. Table 4.2 compares the maximum HS-20 loading case to the similar side-by-side loading case using TxDOT trucks using the direct load method. The wheels directly over the floor beam, labeled FB Wheels in the table, contribute about 50% of the total floor beam moment for test trucks. The wheels directly on the floor beams with the HS-20 vehicle contribute close to 70% of total floor beam moments. Also shown in the table is that the smaller test load leads to a lower total design moment despite the shorter wheel base of the TxDOT trucks.

Table 4.2 Comparison of Direct Load Moments

Direct Load	HS-20s		TxDOT trucks	
	FB Wheels	Total	FB Wheels	Total
Moment (kip-ft)	254.1	369.6	128.9	262.5
% of Total	68.8%		49.1%	

4.4 FINITE ELEMENT MODEL RESULTS

The finite element models used to calculate the moments in the Llano Bridge were similar to the models used in the previous chapters. The floor system was modeled using SAP again with one-foot wide shell and frame elements. The stringers were released at the connection with the floor beams. Several different models were studied to evaluate the influence of the model size upon the results. The models analyzed were a single-span model with two floor beams, a 2-span model (3 floor beams), and a 4-span

model (5 floor beams). The two-span and four-span models were modeled with the slab continuous and cracked over the floor beam.

Figure 4.7 shows the 4-span model used to calculate the moment in the floor beam due to the load applied by the TxDOT vehicle. It also shows the location of the floor beam strain gages in the finite element model. Each truss actually consists of 10 floor beams, but using more than four spans did not produce a difference in the results. No difference was found when the slab was modeled as cracked when more than two stringer spans were used in the model. The results from the gages located in the midspan of the second floor beam, shown as a star in the figure, will be compared with the results from the finite element models. The strains measured in the bottom flange there are converted to moment and compared with the moments predicted using finite element models. The earlier models assumed that the highest floor beam moment would occur on the middle floor beam. However, since only the first two floor beams in Llano were instrumented, these are the locations in the SAP model that were studied.

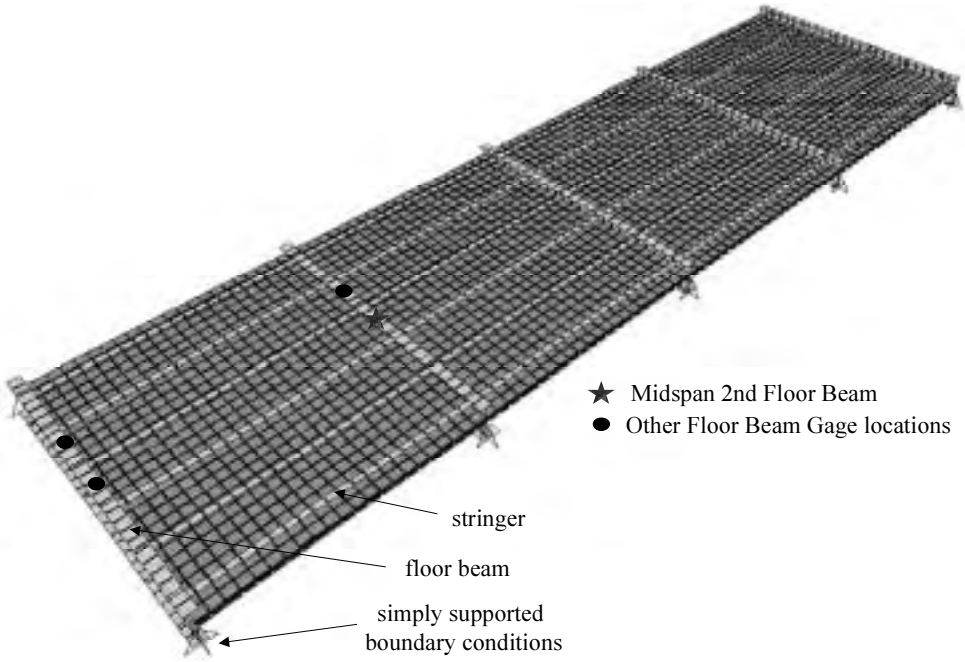

Figure 4.7 Llano Bridge 4-span Finite Element Model

As mentioned before, the Llano small model is similar to the previous small models that were analyzed. This is shown in Figure 4.8, which compares the influence surface of the Llano small model to a small model with 22-foot floor beam spacing and 8-foot stringer spacing. The wheels shown in the figure represent the wheels from the TxDOT vehicles used in the Llano test. The middle group of four wheels shown in the figure would actually be on the left side of the floor beam, but is placed on the right side in this model by symmetry. Both influence surfaces showing normalized floor beam moment have the same trends and shape. However, the Llano model has a larger value for normalized moment. That is because it has a larger floor beam moment of inertia and a smaller slab modulus of elasticity. The Llano model has W33x130 floor beams compared with W30x108 in the plate girder model. The slab modulus of elasticity is 2,850 and 3,120 ksi respectively.

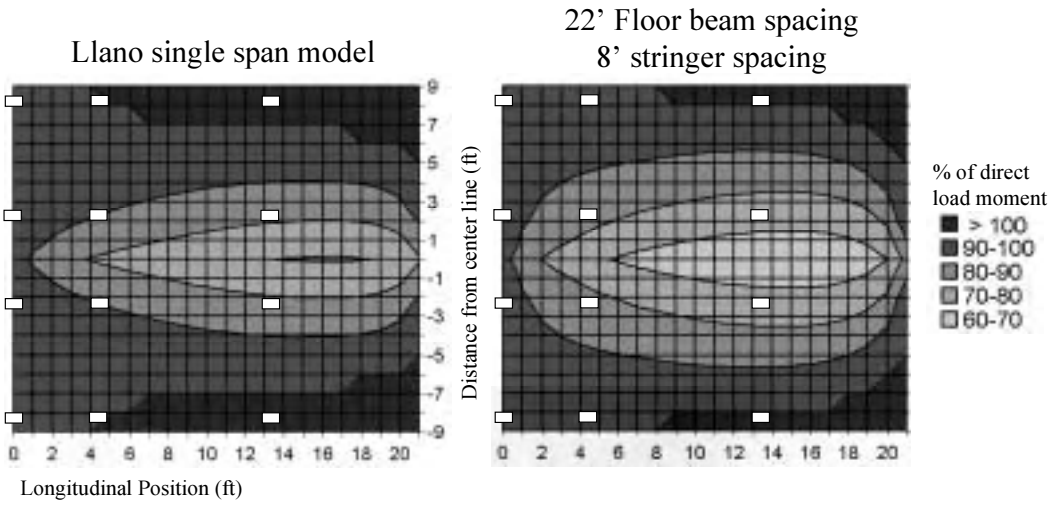

Figure 4.8 Comparison of Llano Small Model with Plate-Girder Model

A comparison of the different Llano model results for the side-by-side load case is shown in Table 4.3. The first column for each truck type is the ratio of the calculated moment divided by the direct load moment for only the truck axles placed directly over the floor beam. The second column is the ratio of the calculated total moment of all the truck axles to the moment from a direct load calculation. The direct load moments are shown in Table 4.2. The axle loading is slightly smaller in the TxDOT loading model because the trucks are placed 4.5 feet apart instead of 4 feet apart. The small model has the largest prediction of total floor beam moment at almost 94% of the direct load for the TxDOT loading vehicles. The other models predict a floor beam moment in the high 80% range. The one-span model has a larger moment because even though slab may be modeled as cracked over the floor beam, it still has to bend transversely as the floor beam deflects and therefore will pick up some of the moment. For the single-span small model, there only exists a slab on one side of the floor beam so the slab picks up less of the moment.

Table 4.3 Comparison of Finite Element Models

Model	% of Direct Load			
	HS-20s		TxDOT Trucks	
	Axle	Total	Axle	Total
Small model	95.2%	93.2%	95.1%	93.9%
2-span continuous	79.5%	85.9%	79.3%	85.4%
2-span cracked	90.8%	88.7%	90.7%	89.2%
4-span continuous	83.3%	87.9%	83.1%	88.1%
4-span cracked	90.8%	88.8%	90.7%	89.3%

As the length of the model increases, the moment stays the same in the model with a cracked slab over the floor beam. This is different than what was shown in the plate girder models. This is because in the Llano models with a cracked slab, there is no continuity at the floor beam. In the other models, the plate-girders were continuous over the length of the bridge and there were only supports at corners of the model. When using more than two spans in the Llano model with the cracked slab, there is no change at all in the influence surface generated. This is shown in the almost identical influence surfaces in Figure

4.9. In the other models, though, with continuous girders supported only at their ends, the girder stiffness decreased as the length increased. This led to a higher midspan floor beam moment.

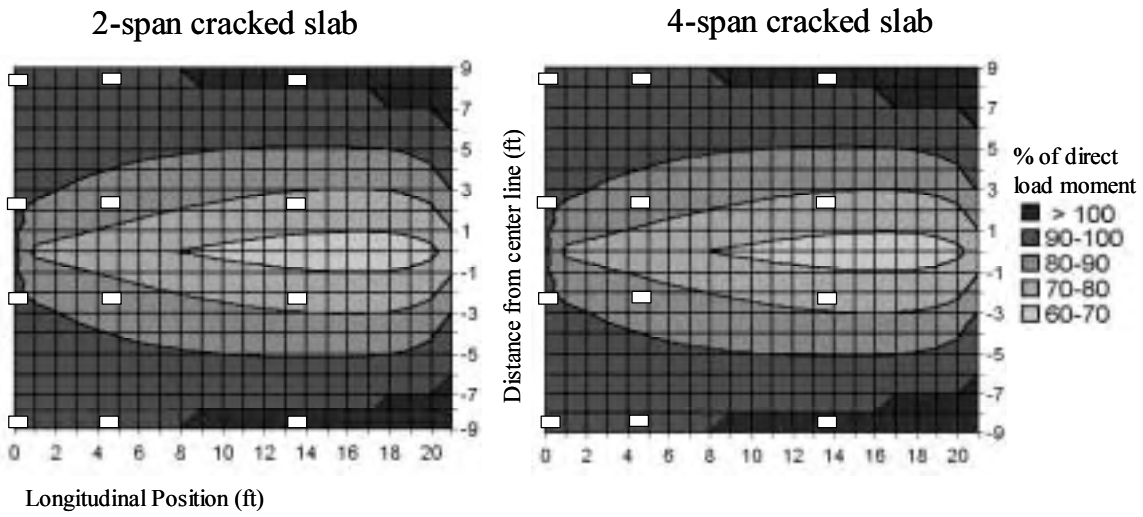

Figure 4.9 Comparison of 2- and 4-Span Cracked Slab Models

However, in the model with a continuous slab, the moments increase slightly as the length of the model increases. This is also different from the effect found in the earlier analysis. This effect is shown in Figure 4.10.

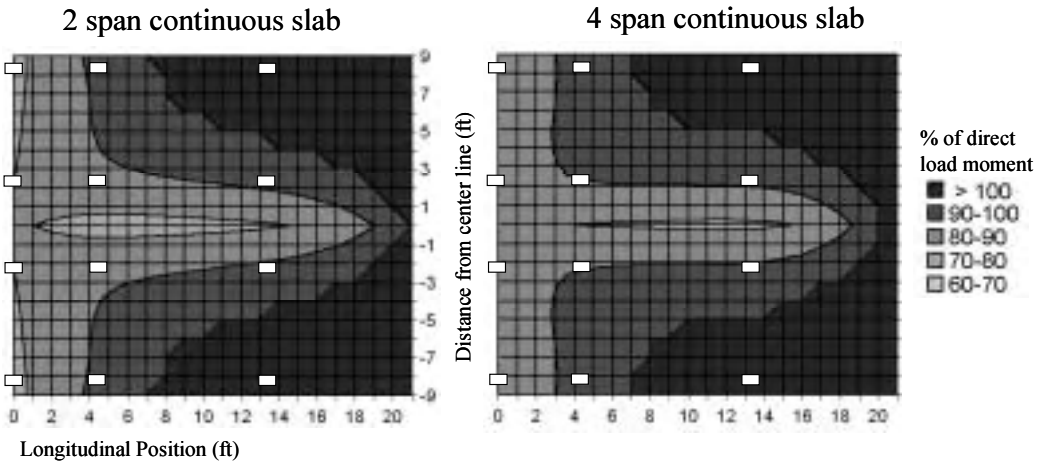

Figure 4.10 Comparison of 2- and 4-Span Continuous Slab Models

4.5 EXPERIMENTAL RESULTS

The experimental results that were analyzed were from the four gage locations shown earlier. The results showed little to no composite behavior between the floor beam and the slab since the bottom flange and top flange stresses were of similar magnitude and the gage at middepth of the web had almost zero strain. The results from the strain gages on the first floor beam are shown for the side-by-side load case in Figure 4.11. This load case was repeated three times with the results shown here from Run 1b, the second run.

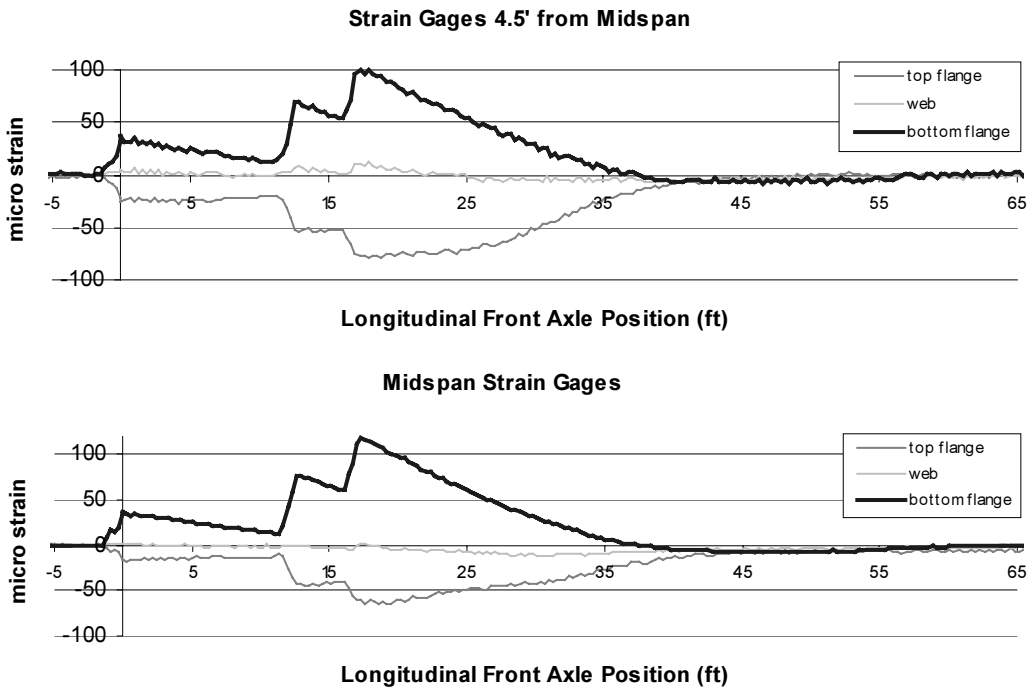

Figure 4.11 Results from First Floor Beam for Side-by-Side Load Case

These results show that the strain in the first floor beam has three peaks. Each peak occurs when an axle of each truck is positioned over the floor beam. The highest peak occurs when the third axle is positioned over the floor beam and the other two axles of each truck are on the same span. The plots also show that the magnitude of the bottom flange strain is slightly higher for the midspan gage. A comparison of the top and bottom flanges of the midspan gage would indicate some composite action, but the middepth gage on the web does not. However, the other location indicates almost no composite action. The results do seem to indicate that there is some continuity between spans, because the moment reverses sign as the truck moves to the next span. However, the negative moment values as the truck moves to the next span are very small. These results can be compared with the results from the gages found on the second floor beam for the same load case, shown in Figure 4.12.

The top flange (o) gage refers to the gage on the opposite side of the web from the other gages. However, this gage seems to give better readings than the top flange gage on the same side. The two gages gave about the same maximum strains, but the gage on the same side as the bottom gage reads a maximum strain about ten feet later than expected. This trend was repeated on every single load run. The gages on the second floor beam show a higher value for maximum strain than the same gages on the first floor beam. This trend is the same for all of the load runs, shown in Appendix E. This is predicted by the finite element analysis as well, however this difference is larger than expected. The results from the finite element model would predict only a 6% decrease at midspan and a 4% decrease 4.5' away. The much lower moments are in the first floor beam are probably caused by the greater amount of restraint in the first floor beam connection than second floor beam. The two connections are shown in Figure 4.13.

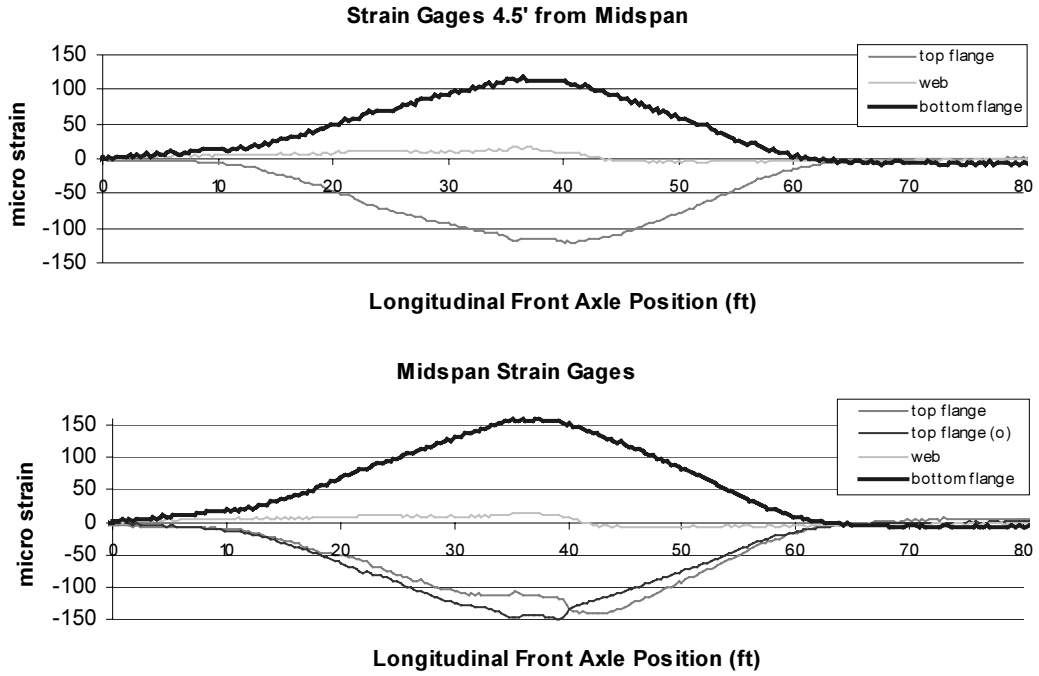

Figure 4.12 Results from Second Floor Beam Gages for Side-by-Side Load Case

Figure 4.13 Floor Beam to Truss Connections

These gages also show very little composite action with the top and bottom flange maximum stresses being approximately equal. The neutral axis for this floor beam was calculated and is shown in Figure 4.14. The axis is calculated from the top and bottom flange strains for the middle portion of the run where the strains are highest and the calculation is less affected by noise. The calculation was done using the top flange gage on the opposite side of the bottom flange gage because of the problem with the other top flange gage. The predicted neutral axis is located at middepth of the floor beam indicating non-composite action. Appendix C shows neutral axis calculations for other load runs. In Appendix D, the percent difference between the bottom flange and top flange gages is shown.

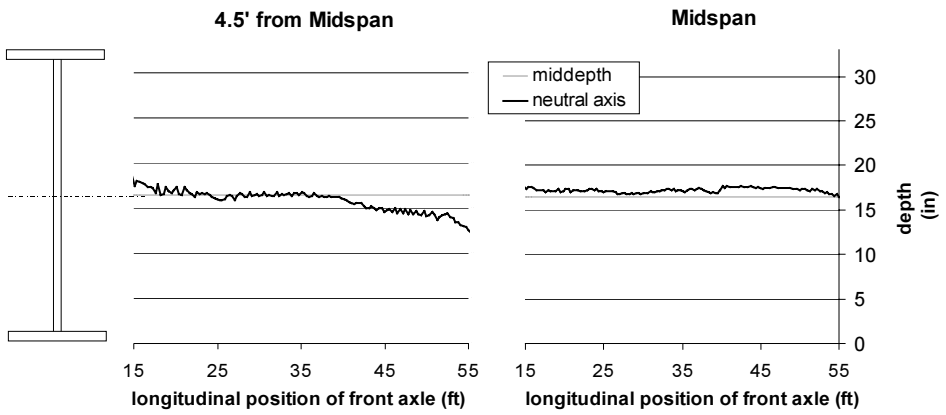

Figure 4.14 Neutral Axis Calculation for Second Floor Beam

4.6 COMPARISON OF RESULTS

The goal of this experimental test in this study was a comparison with the results from the finite element analysis. The most useful comparison is the comparison of the midspan floor beam moment in the second floor beam. This comparison is shown in Figure 4.15. The three side-by-side runs are shown compared to the different models for predicting the floor beam moment.

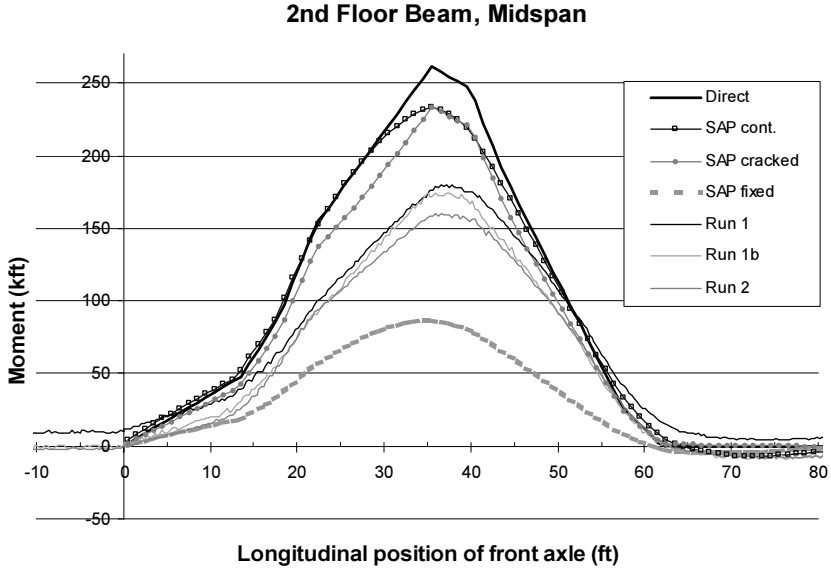

Figure 4.15 Comparison of Second Floor Beam Moments

The direct load model predicts the highest results as was shown earlier. The model identified as the SAP continuous model is a four-span model that models the slab as continuous over the floor beams. The next model, the SAP cracked model, is a four-span model with the slab modeled as cracked over every floor beam. It is evident that this model is not as smooth as the continuous model, as would be expected. These two models, however, have a similar value for maximum moment, with the continuous model only slightly higher. The fourth analytical model, called SAP fixed, is a model that treats the floor beam to truss connection as a fixed support instead of a pinned support. This moment is significantly less than the models with pinned supports.

On these three experimental runs, the agreement between the runs was not as good as it was for the other load runs. The other runs are shown in Appendix F. Run 1 did not start at or return to zero. This would indicate that the gage was not properly zeroed before the run began. In Run 2, one of the trucks was about a foot and a half in front of the other, which produced the additional peaks in the data taken at the first floor beam shown in Figure 4.16. Instead of three peaks, there were six. Run 1b gives the best estimate for floor beam moment due to two trucks placed side by side.

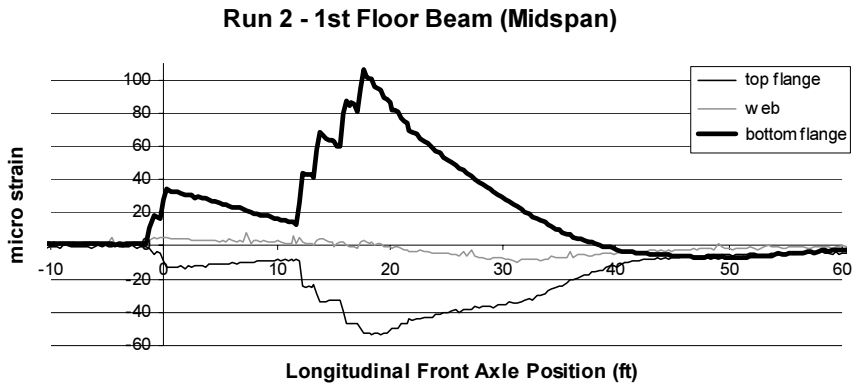

Figure 4.16 Two Trucks out of Alignment in Run 2

The experimental runs have the same general shape as the analytical models, although they seem to follow the smoother pattern of the continuous model. This and the fact that there is a slight sign reversal as the load passes over the floor beam indicates that there is some continuity over the floor beam. However, from inspection of the Llano bridge it was evident the there were cracks over the floor beams as shown in Figure 4.17. The cracks may not go to full depth of the concrete and the stringer to floor beam connections may have some fixity as well.

Table 4.4 shows the comparison of the different models for each load case. It compares the calculated moments from the experimental test with both the SAP cracked model and to the direct load model. Shown in the third column is the transverse position of the center of the truck load on the bridges (zero for a symmetrical load). Shown in the fifth column of the table is the longitudinal location of the truck in each experimental run that produced the maximum moment in the floor beam. The load cases with one truck or the two trucks side by side should have the maximum moment occur when the middle axle is on the floor. This means that the front axle is 35.5 feet onto the bridge. The average occurrence of the maximum value for the experimental runs is about 1 foot later at 36.6 feet. What this value may mean is that the rear axles of the truck are actually a little bit heavier than the middle axle, so the maximum moment actually occurs slightly after the middle axle crosses the floor beam, when the rear axle is closer.

Figure 4.17 Cracked Slab over Floor Beam

Truck Information			Experimental Results				SAP Cracked		SAP Continuous		SAP fixed		Direct Load
Run Description (2 truck runs)		Center (ft)	M_{max} (kft)	Loc. of M_{max} (ft)	% of Direct	% of SAP	M_{max} (kft)	% of direct	M_{max} (kft)	% of direct	M_{max} (kft)	%of direct	M_{max} (kft)
1	side by side	0	180.1	37.2	69%	77%	233.7	89%	233.3	89%	87.2	33%	261.4
1b	side by side	0	174.5	37.2	67%	75%	233.7	89%	233.3	89%	87.2	33%	261.4
2	side by side	0	160.4	36.6	61%	69%	233.7	89%	233.3	89%	87.2	33%	261.4
3	train	0	129.6	40.0	66%	74%	174.2	88%	182.2	92%			197.1
4	train	0	131.2	47.1	67%	75%	174.2	88%	182.2	92%			197.1
20	reverse train	0	161.4	48.9	68%	78%	206.5	86%	223.0	93%			239.0
21	reverse train	0	162.8	48.1	68%	79%	206.5	86%	223.0	93%			239.0
avg					66%	75%		88%		91%		33%	
(1 truck runs)													
7	R4	-5.5	79.2	36.4	61%	68%	116.8	89%	116.6	89%	43.6	33%	130.7
8	R4	-5.5	75.3	36.0	58%	64%	116.8	89%	116.6	89%	43.6	33%	130.7
9	*L5*	*-3.5*	*82.7*	*35.1*	*50%*	*58%*	*143.0*	*86%*	*143.4*	*86%*	*60.5*	*36%*	*165.8*
10	L5	-3.5	94.4	35.0	57%	66%	143.0	86%	143.4	86%	60.5	36%	165.8
17	R3	-1	112.0	38.0	64%	73%	153.4	88%	154.6	89%	65.3	37%	174.6
18	R3	-1	114.3	35.6	65%	74%	153.4	88%	154.6	89%	65.3	37%	174.6
5	center	0	113.0	38.7	65%	73%	154.0	88%	155.2	89%	65.4	37%	174.6
6	center	0	110.4	38.5	63%	72%	154.0	88%	155.2	89%	65.4	37%	174.6
11	L4	1	111.8	38.5	64%	73%	153.4	88%	154.6	89%	65.3	37%	174.6
12	L4	1	108.8	36.0	62%	71%	153.4	88%	154.6	89%	65.3	37%	174.6
15	R2	3.5	100.5	34.8	61%	70%	143.0	86%	143.4	86%	60.5	36%	165.8
16	R2	3.5	94.1	34.8	57%	66%	143.0	86%	143.4	86%	60.5	36%	165.8
13	L3	5.5	79.9	37.7	61%	68%	116.8	89%	116.6	89%	43.6	33%	130.7
14	L3	5.5	80.1	37.5	61%	69%	116.8	89%	116.6	89%	43.6	33%	130.7
avg				36.6	61%	69%		88%		88%		36%	

Also, the method in which truck position is estimated on the experimental run has an error of +/- 0.3 feet. Truck position is estimated by manually closing a switch as the truck passes over a known location. This interrupts the excitation making it possible to determine when the truck is located in a known location. In the Llano test, these "clicks" were spaced 11 feet apart. Interpolation is used to determine the truck position between these various locations. This interpolation assumes a constant truck speed. There can be a slight error in manually closing the switch or in the interpolation due to a changing truck speed. Each data point represented about 0.3 ft of truck movement.

Another trend noticed both in Table 4.4 and in Figure 4.15 is that the moments from the experimental runs were significantly lower than the first three analytical models, but higher than the SAP model with using fixed boundary conditions at the ends of the floor beams. These experimental values for the second floor beam midspan location were between 65% and 80% of the values predicted by the SAP cracked model. This indicates that the floor beam connection with the truss is somewhere between fixed and pinned. All connections are somewhere between perfectly fixed and perfectly pinned, but the degree of fixity is hard to determine. Unfortunately, the floor beam was not instrumented more thoroughly in this first test to have a better understanding of the moment diagram of the floor beam.

Also, if the concrete has a modulus of elasticity higher than the value of 2850 ksi that was assumed for the analysis, this also would lead to a lower floor beam moment. That is because the slab would carry more of the moment. The value of 2850 ksi assumes of compressive strength of 2500 psi. The concrete is probably much stronger than this estimated value.

4.7 SECOND EXPERIMENTAL TEST

The second load test of the Llano bridge took place about 2 months later on the 15th of April 1999. The goals of this test were to demonstrate repeatability and to come to a better understanding of why the forces in the members were significantly lower than the finite element results indicated. In this test, the second floor beam would be more fully instrumented to get a better understanding of the fixity of the connections.

4.7.1 Repeatability of Test

To determine if the test demonstrates repeatable results every effort was made to keep all field conditions the same for both tests. Gages were placed in many of the same locations as the first test and the same runs were repeated. For both tests to have the same results, the loading vehicles would have to be the same as well.

The trucks used in the second experimental test had the same geometry as the trucks from the first test, but the weights were not the same. The difference in truck weights is noticeable in the experimental results. The truck weights used in the second test are shown in Table 4.5. The weight of the rear tandem of Truck B is about 5% less than Truck A. The weight of Truck A is almost exactly the same as the weight of the average vehicle from the first run. Therefore, the maximum floor beam values predicted by the first test should coincide with the values from Truck A. The values from the Truck B should be about 5% lower.

Table 4.5 Comparing Truck Weights from Both Tests

	1st Test Avg.	Truck A	Truck B	% less than A
Front Axle	10.49	10.46	10.22	2.3%
Rear Tandem	34.63	34.44	32.78	4.8%
Total	45.11	44.90	43.00	4.2%

The results from both tests were very similar, as shown in Table 4.6 and Table 4.7. These tables compare the maximum calculated moments from the same load runs on both tests. The load runs that are compared are the side-by-side load run and the load run with a single truck on the center of the bridge. Both runs being examined are symmetric about the center of the bridge in order to check lateral symmetry. The first column in both tables tells which floor beam the gage is mounted on and the distance the gage is from the midspan of the floor beam.

Table 4.6 Maximum Moment Comparison for Side-by-Side Load Case

Gage Location	Maximum Moments (kip-ft)		
Floor Beam # (distance from midspan)	1st Test Run 1b	2nd Test Run 0	2nd Test Run 1
2nd (0)	174.5	176.7	181.6
2nd (4.5)	128.8	140.0	141.2
1st (0)	127.9	118.9	124.74
1st (4.5)	110.3	102.9	113.94

Table 4.7 Maximum Moment Comparison for Single Truck in Center

Gage Location	Maximum Moments (kip-ft)		
Floor Beam # (distance from midspan)	1st Test Average	2nd Test Truck A	2nd Test Truck B
2nd (0)	111.7	124.3	116.3
2nd (4.5)	80.3	94.7	91.9
1st (0)	86.9	86.1	82.0
1st (4.5)	76.3	77.3	72.3

The moment comparisons of the two tests demonstrate the repeatability of the moments. The values for floor beam moment from the two tests are fairly consistent. Run 0 and Run 1 in Table 4.6 should be the same as each other and slightly less than the values from the first test. However, the noise level of the second floor beam, midspan gage caused the slight increase in the calculated moment from the first test to the second test at that location. Also, the gage located 4.5 feet away from the center of the second floor beam gave a moment that was 10 to 15% higher in the second test for some unknown reason. In addition, in Table 4.7, moment values for Truck B are around 5% less than for the Truck A run, consistent with the decrease in the weights of the rear axles.

4.7.2 Floor Beam Moment Diagram

To have a better understanding of the floor beam moment diagram, the floor beams were more thoroughly instrumented in the second test than in the first test. Figure 4.18 shows the SAP model of two stringer spans of the bridge with the gage locations employed in the both load tests. In the first test, the floor beams were instrumented in four locations as shown by the stars in the figure. Four locations were added in the second test to determine the moment diagram of the floor beam and to check on the symmetry about its centerline. All gages are located midway between the stringer connections, 4.5 feet apart. All locations have gages at the top flange, middepth of the web, and at the bottom flange, the same as the first test. Other gages were placed at other depths, but many were very noisy and the results were not useful.

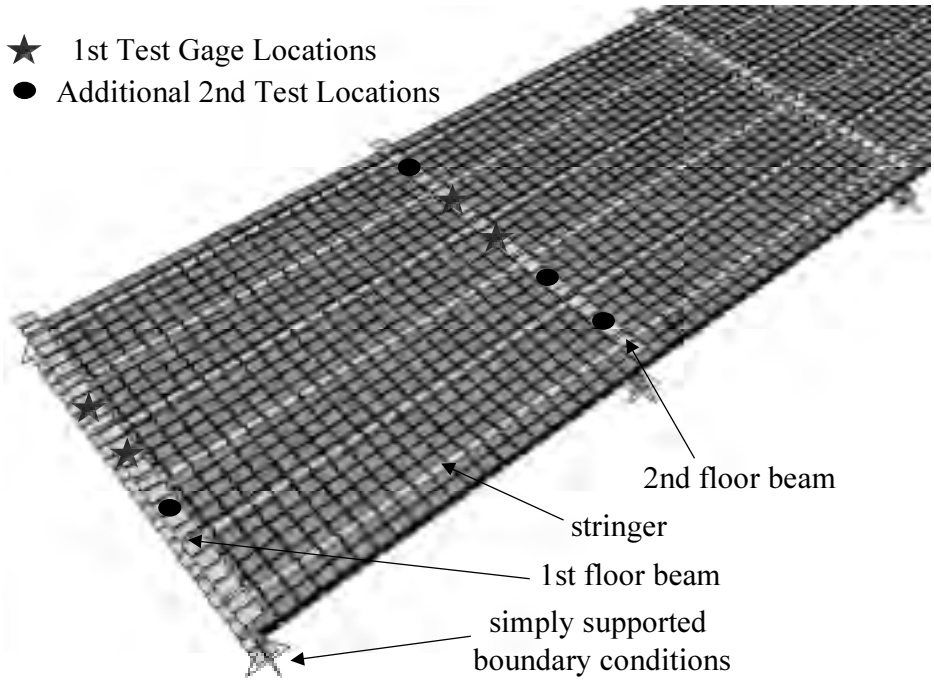

Figure 4.18 Location of Gages in Both Load Tests

In the first test, only two locations along each floor beam were instrumented so it was impossible to generate an accurate picture of the moment diagram from two points. The second floor beam was instrumented in five different locations to get a more accurate representation of the moment diagram. That moment diagram for the load case with Truck A running over the transverse center of the bridge is shown in Figure 4.19. Also shown in the figure are the moment diagrams for the direct load moment diagram and the moment diagram from a SAP analysis. Moment diagrams for other load runs are shown in Appendix H. The moment diagrams shown occur when the truck is positioned with its center axle over the second floor beam. The x-axis in the figure shows the distance from the center of the floor beam. As was mentioned previously, the values for the bending moment in the floor beam in the SAP model are around 85 to 90% of the direct load moment values. It is also evident that there is more lateral load distribution in the SAP model, because the moment diagram is more rounded than the moment diagram for the direct load model. At midspan of the floor beam, the experimental value for moment 76% of the SAP value and 67% of the direct load value.

It is hard to determine the amount of fixity in the connections from this moment diagram. However, it is possible to get an idea as to whether there is some fixity or not. In Figure 4.19, a straight line is drawn between the points at 4.5 feet and 9 feet and extended to the location of the connection at 12.94 feet. The same thing is done on the other side. The extensions are shown as broken lines in the figure. If there were no restraint provided by the connection, the line would terminate at zero moment at the location of the connection. However, from the figure, it is evident that there may be restraint in the connections. Using the extended line, the predicted moment at the connections is approximately -13 kip-ft, about 10% of the maximum moment.

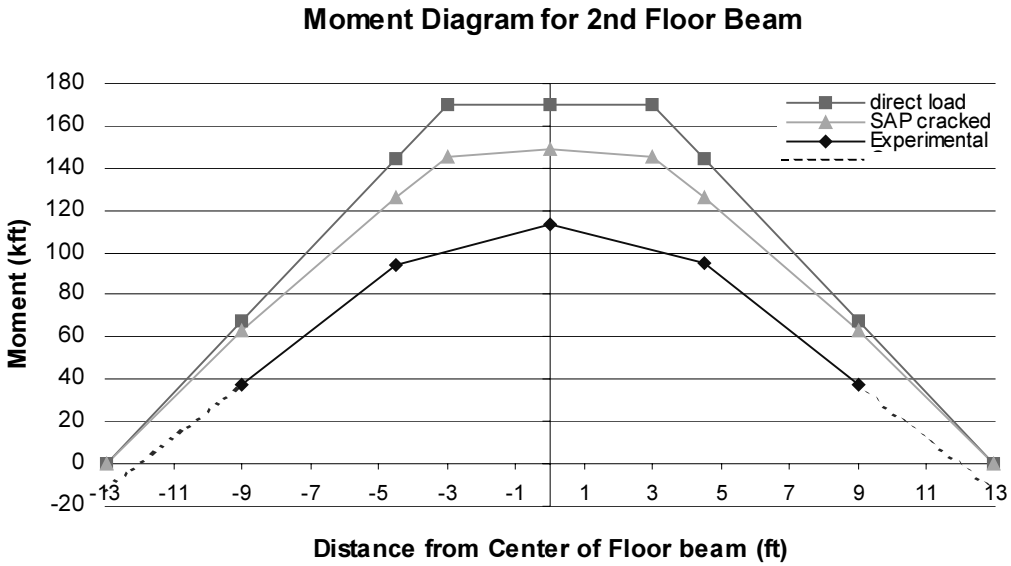

Figure 4.19 Moment Diagram for Second Floor Beam, Center Run, Truck A

Figure 4.20 illustrates what the moment diagram would look like if the average amount of these two values were added to the entire moment diagram. The moment diagram is still only 85% of the moment diagram for the SAP model. The remaining 15% difference between the experimental model and the SAP model is probably caused by underestimating the stiffness of the slab in the SAP model. The slab is probably thicker than the 6.5 inches due to overlays and the modulus of elasticity is probably higher than 2850 ksi based on the compressive strength specified in the plans. Both factors would cause the slab to carry a higher percentage of the moment, thereby reducing moment in the floor beam.

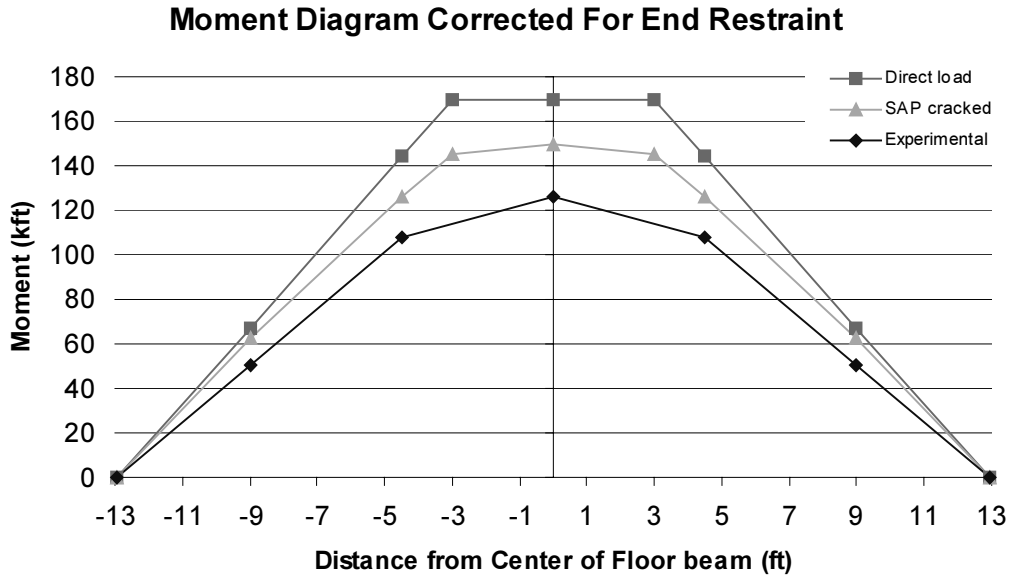

Figure 4.20 Moment Diagram without Restraint for Center Run, Truck A

4.8 CONCLUSIONS FROM THE EXPERIMENTAL TEST

The experimental test of the bridge located in Llano demonstrated that the floor beam moments due to a truck load on the bridge are much smaller than the moments predicted by the direct load method. The moments are also significantly smaller even than the moments predicted by the finite element models. This can likely be attributed to the fixity of the floor beam to truss connections and underestimation of slab stiffness in the finite element model.

The experimental test does demonstrate that the moment values predicted by the finite element model are conservative compared with the actual moments seen in the bridge. This means that even though the moments from the finite element models may not match the experimental values, they give a better estimate of the actual forces in the floor beam than the direct load model. The behavior of floor systems in trusses is continuing with the further experimental and analytical studies in Project 0-1741.

CHAPTER 5

DETERMINING FLOOR BEAM REQUIREMENTS

5.1 LIMIT STATE DESIGN

The rating system used to determine the capacity of bridges has changed since AASHTO moved from Allowable Stress Design in favor of Limit State Design. Limit State Design includes both Load Factor Design (LFD) and Load and Resistance Factor Design (LRFD). In both specifications, to determine if the floor beam meets the necessary requirement for moment, the allowable moment, M_n (multiplied by a resistance factor in LRFD), must be greater than or equal to the required moment, M_u as shown in Equation 5.1. The required moment is determined for a number of different limit states, which require different load factors.

$$\phi M_n \geq M_u \tag{5.1}$$

5.2 REQUIRED MOMENT

The right side of Equation 5.1 is the required moment. It is the sum of the moments caused by each type of load on the bridge multiplied by a load factor unique to that type of load. The required moment is computed from one of two provisions discussed in the following section.

5.2.1 Load & Resistance Factor Design

Load & Resistance Factor Design, or LRFD, is the most recent provision to determine the required moment for a bridge member.[5] There are many different limit states that must be checked to determine the required moment. However, only the Strength I Limit State, shown in Equation 5.2, will be examined. Strength I, the "basic load combination relating to the normal vehicular use of the bridge without wind," most often determines the required strength of the floor beam.

$$M_u = 1.75(LL + IM) + 1.5DW + 1.25DC \tag{5.2}$$

The live load in LRFD includes both the lane loading and the truck loading. The lane loading used by LRFD consists of a uniform load of 0.064 ksf distributed over the length of the bridge longitudinally and over a ten-foot width transversely. This lane load does not include any concentrated loads and must correspond in lateral position with the truck load. That is, if the trucks are off center by one foot, the lane loads must be as well. There should always be a two-foot space between the lane loads. The impact factor of 1.33 is applied to the truck load but not the lane load. The dead load is divided into the load from the wearing surface and utilities, DW, and the load from the components and attachments, DC. For the floor beam analysis, DC would is the load from the stringers and floor beams, while DW would is the load from the 6.5 inch concrete slab.

5.2.2 Load Factor Design

Load Factor Design, the specification prior to the introduction of AASHTO-LRFD, is also still used today.[6] The LFD provision for required strength is shown in Equation 5.3. In this specification, either the

lane load or the truck load is used as live load, but not both. Because of this fact, there is a larger factor, about 2.17, on the live load in the LFD equation. For the bridges in this study, the truck load will always control the floor beam rating. Only for longitudinal members in longer span bridges will the lane load control. Also, the same load factor of 1.3 is applied to all dead load moments regardless of whether the moments are caused by the wearing surface or steel components in the LFD equation.

$$M_u = 1.3(DL + 1.67(LL + IM) \tag{5.3}$$

5.3 ALLOWABLE MOMENT

The left side of Equation 5.1 is the allowable moment. This determines the resistance of the floor beam to moment. The equation to determine the allowable moment in the LRFD specification is shown in Equation 5.4. This equation is 6.10.4.2.6a-1 from the AASHTO-LRFD manual.[5] Since the floor beams in this study are not hybrid girders, the factor R_h is 1. A conservative estimate of C_b=1 is used in this study. I_{yc} is the moment of inertia of the compression flange about the vertical axis in the plane of the web and "d" represents the depth of the floor beam. The unbraced length of the compression flange, L_b, in this case is the stringer spacing. That is because the stringers brace the compression flange, which in this case is the top flange. Because of the relatively small unbraced length, this equation is governed by yield moment, M_y. The resistance factor used in the LRFD specifications for yield moment is 1.

$$M_n = 3.14EC_bR_h\left(\frac{I_{yc}}{L_b}\right)\sqrt{0.772\left(\frac{J}{I_{yc}}\right) + 9.87\left(\frac{d}{L_b}\right)^2} \le R_hM_y \tag{5.4}$$

5.4 BRIDGE RATING EXAMPLE

To demonstrate the use of these equations, a bridge from the study will be examined in detail. The bridge under consideration is located in Polk County. It carries US Highway 59 over the Trinity River and is Bridge 8 from Chapter 3. The cross section of the bridge is shown in Figure 5.1. Shown in the figure are the dimensions of the floor system. The stringers are spaced 8 feet apart and the floor beams are spaced 22 feet on center. Also, notice that there is a two-inch gap between the floor beam and the slab indicating that the all of the load transferred from the slab to the floor beam must go through the stringers. The floor beam on this bridge did not rate sufficiently according to the current LRFD provisions. We will look at these provisions in relation to this bridge in more detail in this chapter. The bridge, designed for an H-20 loading, will be analyzed for the same loading.

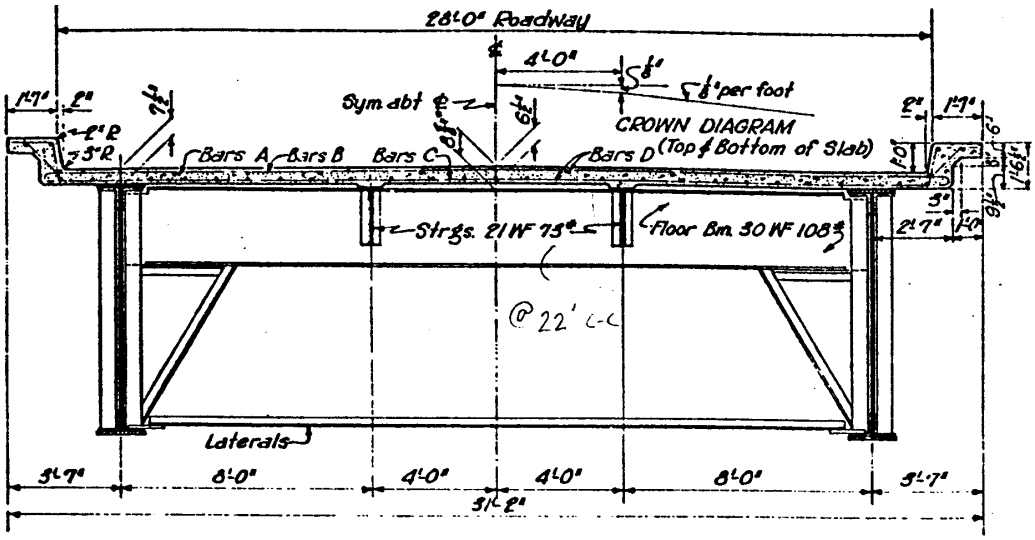

Figure 5.1 Cross Section of Trinity River Bridge

5.4.1 Rating for LRFD and LFD

5.4.1.1 Allowable Moment

The first step is to compute the allowable moment of the floor beam. The properties of the W30x108 section along with the properties of the other floor beam sections are shown in Table 5.1.

Table 5.1 Properties of Floor Beam Sections

Section	D (in)	I_{yc} (in^4)	B_f	S_x (in^3)	J (in^4)	M_y kip-ft
W24x76	23.91	41.22	8.99	175.4	2.68	526.2
W27x94	26.91	62.06	9.99	242.8	4.03	728.4
W27x98	27	66	10.00	255.3	4.6	765.9
W30x108	**29.82**	**72.98**	**10.48**	**299.2**	**4.99**	**897.6**

The calculation for allowable moment according to the LRFD specification is shown in Equation 5.5. Because the unbraced length of the compression flange is small, the allowable moment is actually equal to the yield moment of 897.6 k-ft. The yield moment is calculated assuming a steel yield strength of 36 ksi. Since the resistance factor for flexure is equal to 1.0, the resulting M_n from the equation is the allowable moment.

$$M_n = 3.14 * 29000 * 1 * 1 * \left(\frac{72.98}{96}\right) * \sqrt{0.772\left(\frac{4.99}{72.98}\right) + 9.87\left(\frac{29.82}{96}\right)^2}$$

$$= 69580\,k \cdot in = 5800\,k \cdot ft \geq 897.6\,k \cdot ft \quad \therefore Mn = 897.6\,k \cdot ft \qquad (5.5)$$

5.4.1.2 Required Moment

To determine the required moment of the floor beam it was necessary to find the moment due to each type of load and apply a load factor for each different type of load. Figure 5.2 shows the floor beam moment caused by a pair of H-20 trucks according to the direct load method. The 16-kip loads directly over the floor beam are added to the percentage of the 4-kip loads that are longitudinally distributed to the floor beam using statics. H-20 trucks are used because that is the load that the bridge was rated for originally. The lanes are offset by one foot to produce the maximum moment. The trucks are always positioned two feet away from the edge of the lane as shown in the figure. Results for the HS-20 loading are shown later in the chapter.

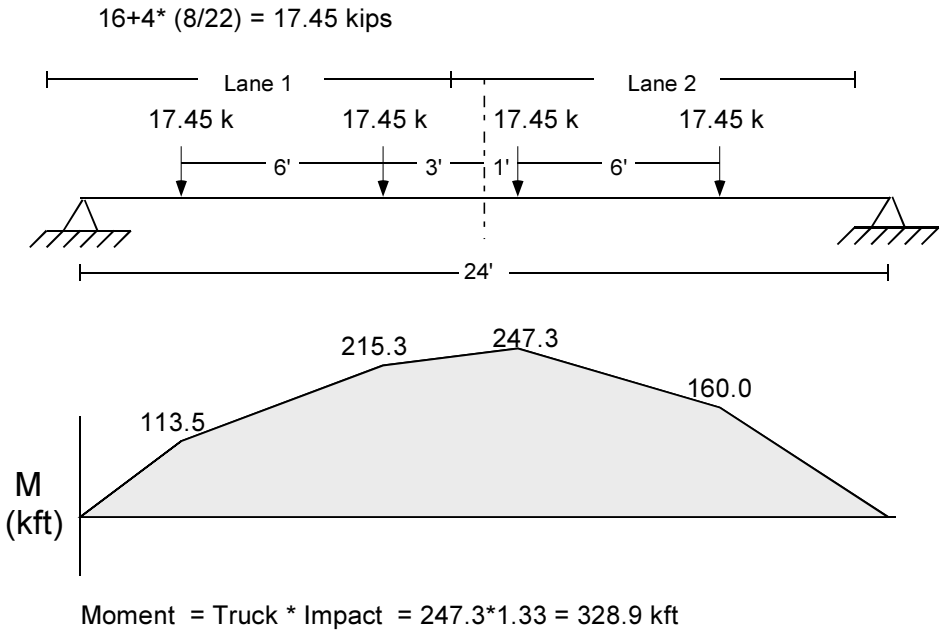

Figure 5.2 H-20 Truck Moment Calculation Using Direct Load

The lane load moment is calculated using the same 12-foot lanes as the truck load. There is a minimum of one foot between the edge of the lane and the distributed lane load. This results in the two 10-foot lanes spaced 2 feet apart. The calculation for the moment caused by lane load is shown in Figure 5.3. The distributed load on the floor beam from the lane load is calculated by multiplying the 0.064 ksf lane by the floor beam spacing of 22 ft.

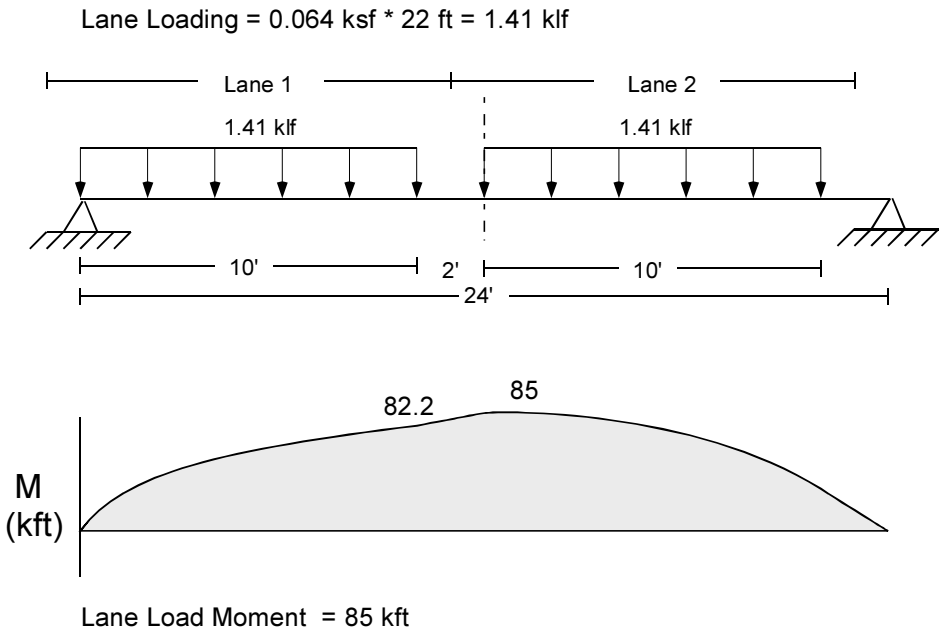

Figure 5.3 H-20 Lane Loading Moment Using Direct Load

The loads from the slab, stringers, and floor beam can easily be calculated using statics. The load from the slab is treated as a distributed load on the floor beam. The moment values from the different loads are shown in Table 5.2. The load factors for both LFD and LRFD are then used to calculate the total required moment for each specification. Notice the high percentage of the moment caused by the truck loading in the LRFD specifications. This is the reason most of this research has gone into determining if the method for distributing the truck load is accurate. With an allowable moment of 897.6 kft, this floor beam does not meet the specifications using either design method. The under-strength is around 1% for the LFD method and 5% for the LRFD method.

Table 5.2 Calculation of Required Moment

	M_i	LFD		LRFD	
	(kft)	γ_i	$\gamma_i M_I$	γ_i	$\gamma_i M_I$
Slab	128.7	1.3	167.3	1.5	193.1
Stringers	12.8	1.3	16.7	1.25	16.1
Floor beams	7.8	1.3	10.11	1.25	9.7
Lane	85			1.75	148.8
Truck + IM	328.9	2.171	714	1.75	575.5
Sum			**908**		**943.2**

5.4.2 Rating Using Allowable Stress Design

The TxDOT approach is taken from the 1988 TxDOT bridge rating manual.[4] The basic rating equation, shown below follows an allowable stress approach. The allowable load is determined by using 55% of the yield stress as the allowable stress in the member for the inventory rating and 75% of the yield stress for the operating rating. In this study, only the inventory rating will be examined.

$$H - Rating = H - \left[20 * \frac{M_{all} - M_{DL}}{M_{LL}(H - 20\,Vehicle)} \right] \tag{5.6}$$

TxDOT uses the information shown in Table 5.3 to compute the allowable moment, M_{all}. To determine the load rating allowable stress is rounded to a value and a correction is made with respect to the unbraced length. The rounded value of allowable stress is represented by A while the correction for unbraced length is represented by B in Table 5.3 and in Equation 5.7. The allowable moment is then calculated by multiplying the allowable stress in the floor beam, F_b, by the section modulus, S_x.

Table 5.3 TxDOT Table to Compute Allowable Stress for Inventory Rating

F_y (ksi)	0.55 F_y (ksi)	Rounded Allowable A	Bracing Factor B
26	14.3	14.0	0.0039
30	16.5	16.0	0.0052
33	18.1	18.0	0.0063
36	**19.8**	**20.0**	**0.0075**
45	24.7	24.0	0.0117
50	27.5	27.0	0.0144
55	30.3	30.0	0.0174

$$F_b\,(Inventory) = A - B\left(\frac{L_b}{b_f}\right)^2 \quad \rightarrow \quad M_{all} = F_b \cdot S_x \tag{5.7a}$$

$$F_b\,(Inventory) = 20 - 0.0075 \cdot \left(\frac{8 \cdot 12}{10.48}\right)^2 = 19.3\ ksi \tag{5.7b}$$

$$M_{all} = \frac{19.3 \cdot 299.2}{12} = 481.2\ k\,ft \tag{5.7c}$$

The live load moment is determined using the direct load method for an H-20 or HS-20 loading vehicle. The live load used in this equation is also multiplied by a smaller impact factor that has a maximum value of 1.3. The dead load is also determined using the direct load method. However, all dead load is treated as a distributed load over the length of the floor beam. This is appropriate for the self-weight of the floor beam. However, the weight from the stringers should be treated as concentrated loads at the connection to the floor beam. If the slab were in contact with the floor beam, it would be appropriate to treat the weight of the slab as a distributed load over the floor beam. However, if the slab weight is all transferred through the stringers, it should be included in the stringer reactions on the floor beam. Using the moment values determined previously, and shown in Table 5.2, the calculation of dead load moment is shown in Equation 5.8a. Equation 5.8b shows the calculation of the live load moment and Equation 5.8c shows the final rating value for the floor beam using allowable stress design.

$$\text{MDL} = \text{Mslab} + \text{Mstr} + \text{MFB} = 128.7 + 12.8 + 7.8 = 149.3\ \text{kft} \tag{5.8a}$$

$$MLL = \text{H-20 Load} * \text{Impact Factor} = 247.3*1.3 = 321.5 \text{ kft} \quad (5.8b)$$

$$H - Rating = H - \left[20 \cdot \frac{481.2 - 149.3}{321.5} \right] = H - 20.6 \quad (5.8c)$$

Because the rating is greater than H-20, the floor beam meets the requirements for an H-20 loading. Therefore, if the live load from the direct load model were used, the floor beam would meet the specifications following the ASD provisions, but not the provisions from LFD or LRFD.

5.4.3 Rating Using the Lever Rule

If there is no contact between the floor beam and the slab, the lever rule is a more appropriate way to rate the floor beam. It is still a conservative estimate, though, because a higher percentage of the load is attracted to the stiffer outside girder, thereby causing less moment in the midspan of the floor beam. This was demonstrated using finite element modeling.

The lever rule affects the way both live load and dead load moments are calculated. The dead load affected is the load from the slab. Instead of calculating the dead load from the slab as a uniformly distributed load along the floor beam, the dead load from the slab can be treated as point loads at the location of the stringer connections. Moving the load away from the midspan of the floor beam toward the stringer connections reduces the moment due to the slab weight.

Both the lane load and truck load moment are affected by using the lever rule. The lever rule actually slightly increases the value of the lane moment because instead of being uniformly distributed along 2 ten-foot widths, it is transmitted through point loads at the stringer connections. The difference between the lane loading and slab dead load is that the lane loads do not occur over the entire 24 feet and are placed eccentrically on the bridge to match the truck loads. The lane load has no effect on the LFD method or ASD method because truck loading controls those specifications.

Using the lever rule instead of the direct load model significantly reduces the moments from the design truck, which make up the largest percentage of the total moment. The lever rule, as shown in Chapter 3, reduces the maximum moment, independent of the floor beam spacing, to 89.4% of the direct load moment. This same value was calculated with the floor beam spacing anywhere from 6 feet to 12 feet. The range of floor beam spacing in Texas is from 7 to 8 feet. The 0.894 factor then could be applied to all bridges with this geometry rather than recalculating the lever rule moment. Using the new moment values for the slab, lane, and truck loads, the calculations for required moment are shown in Table 5.4. Notice that using the lever rule, the allowable moment of 897.6 kip-ft is now greater than the required moment using both the LRFD and LFD specification.

Table 5.4 Calculation of Required Moment Using Lever Rule

	M_i	LFD		LRFD	
	(kft)	γ_I	$\gamma_i M_I$	γ_I	$\gamma_i M_i$
Slab	114.4	1.3	148.7	1.5	171.6
Stringers	12.8	1.3	16.7	1.25	16.06
Floor beams	7.8	1.3	10.1	1.25	9.72
Lane	89.2	0	0.0	1.75	156
Truck + IM	294.0	2.17	638.0	1.75	514.5
Sum			**813.5**		**868**

5.4.4 Rating Using Finite Element Results

If the slab is in contact with the floor beam, the simple lever rule could not be applied as easily. The floor beam moment diagram would have to include the effects from load transmitted directly to the floor beam. Because the truck used to rate this bridge is an H-20 and not an HS-20, most of the load is positioned directly over the floor beam. Because of this, there is not as much distribution of the H-20 truck load. However, the slab does take some of the moment. Using the small model, which is conservative in most cases, the reduction would depend only on the floor beam to slab ratio. The calculation for live load is shown in Equation 5.9. Using the trend developed in Chapter 3 for a 6.5-inch slab the live load is then multiplied by the factor determined from the equation.

$$M_{LL} = M_{direct} \cdot \left(0.08 \ln(\frac{EI_{FB}}{EI_{slab}}) + .52 \right) \tag{5.9a}$$

$$M_{LL} + IM = 1.33 \cdot \left[247.3 \cdot \left(0.08 \ln\left(\frac{4470 \cdot 29000}{275 \cdot 3120} \right) + 0.52 \right) \right] = 303.1 \; kft \tag{5.9b}$$

Table 5.5 shows the how this factor affects the overall rating of the bridge. Both of these values are slightly larger than the lever rule but smaller than the direct load method. Notice that the LFD required moment is well under the allowable moment using this provision and the LRFD required moment is now less than 0.1% too high. A more detailed finite element model could be used in this case to get a more exact value for the floor beam moment.

Table 5.5 Calculation of Required Moment Using Equation 5.9

	M_i (kft)	LFD		LRFD	
		γ_I	$\gamma_i M_I$	γ_I	$\gamma_i M_i$
Slab	128.7	1.3	167.3	1.5	193.05
Stringers	12.8	1.3	16.7	1.25	16.06
Floor beams	7.8	1.3	10.1	1.25	9.72
Lane	85.0	0	0.0	1.75	148.75
Truck + IM	303.1	2.17	657.7	1.75	530.43
Sum			**851.8**		**898.0**

5.5 BRIDGE RATINGS WITH H-20 LOADING

Using the methods outlined above, all of twelve bridge sections were examined for the H-20 truck load, except for one bridge, Brazos 2, which was designed for the H-15 truck loading. The results are shown in Table 5.6. The bridges italicized in the table were designed for two HS-20 trucks, but were rated here for H-20 vehicles. The percentages show the amount of over-strength using each different design method. Negative percentages, shown in bold, represent floor beams that have insufficient strength. Notice that using the direct load method, there are four floor beams that are do not meet the LRFD specification and three that do not meet LFD. Using the lever rule, all of the bridges have sufficient strength. Using the Equation 5.9 to factor in slab moment, only two floor beams have marginally insufficient strength according to LRFD and none for LFD. Trinity 8 was the bridge used in the example calculations earlier in the chapter.

Table 5.6 Over-Strength Factors for the 12 Cross Sections for H-20 Trucks Using LRFD and LFD Specifications

		Mn	Direct		Lever Rule		Equation 5.9	
		(kft)	LRFD	LFD	LRFD	LFD	LRFD	LFD
1	Brazos	728.4	**-7.3%**	**-8.5%**	1.3%	2.2%	**-0.3%**	0.1%
2	Brazos*	526.2	**-0.8%**	**-1.7%**	8.5%	9.8%	9.0%	10.5%
3	Colorado	728.4	**-2.4%**	1.5%	6.0%	13.3%	4.1%	10.4%
4	*N Llano*	*765.9*	*1.9%*	*7.4%*	*10.4%*	*19.8%*	*8.2%*	*16.2%*
5	*N Llano*	*765.9*	*0.4%*	*2.3%*	*9.2%*	*14.2%*	*7.1%*	*11.1%*
5a	*N Llano*	*765.9*	*3.6%*	*4.6%*	*12.8%*	*16.7%*	*10.6%*	*13.7%*
6	Red	728.4	8.9%	7.0%	18.8%	19.5%	17.1%	17.1%
7	Sabine	897.6	0.0%	2.3%	8.8%	14.1%	5.1%	9.0%
7a	Sabine	897.6	3.2%	4.6%	12.4%	16.7%	8.6%	11.6%
8	Trinity	897.6	**-4.8%**	**-1.2%**	3.4%	10.3%	**-0.1%**	5.3%
9	*Trinity*	*728.4*	*6.7%*	*8.4%*	*15.9%*	*21.0%*	*14.1%*	*18.2%*
9a	*Trinity*	*728.4*	*9.2%*	*10.2%*	*18.7%*	*23.0%*	*17.0%*	*20.2%*

* This bridge was rated for H-15 loading instead of H-20

It is evident that even though the reductions from the lever rule and slab moment are small, around 10%, it can have a critical effect on whether a bridge meets the rating standards. Note that all calculations from the table above were based on a yield stress of 36 ksi. Calculations using 33 ksi steel, the expected yield strength for bridges built during this time period according to the TxDOT Bridge Rating Manual, are shown in Table 5.7.

Table 5.7 Over-Strength Factors with 33 ksi Steel Using H-20 Trucks

		Mn	Direct		Lever Rule		Equation 5.9	
		(kft)	LRFD	LFD	LRFD	LFD	LRFD	LFD
1	Brazos	667.7	**-15.0%**	**-16.1%**	**-7.1%**	**-6.3%**	**-8.6%**	**-8.3%**
2	Brazos	482.4	**-9.0%**	**-9.9%**	**-0.5%**	0.6%	**-0.1%**	1.3%
3	Colorado	667.7	**-10.5%**	**-6.9%**	**-2.9%**	3.9%	**-4.5%**	1.2%
4	*N Llano*	*702.1*	***-6.6%***	***-1.6%***	*1.2%*	*9.8%*	***-0.8%***	*6.5%*
5	*N Llano*	*702.1*	***-8.0%***	***-6.2%***	*0.1%*	*4.7%*	***-1.8%***	*1.8%*
5a	*N Llano*	*702.1*	***-5.0%***	***-4.1%***	*3.4%*	*7.0%*	*1.4%*	*4.2%*
6	Red	667.7	**-0.2%**	**-1.9%**	8.9%	9.5%	7.4%	7.3%
7	Sabine	822.8	**-8.4%**	**-6.3%**	**-0.3%**	4.6%	**-3.7%**	**-0.1%**
7a	Sabine	822.8	**-5.4%**	**-4.1%**	3.0%	7.0%	**-0.5%**	2.3%
8	Trinity	822.8	**-12.8%**	**-9.4%**	**-5.2%**	1.1%	**-8.4%**	**-3.5%**
9	*Trinity*	*667.7*	***-2.2%***	***-0.6%***	*6.2%*	*11.0%*	*4.6%*	*8.4%*
9a	*Trinity*	*667.7*	*0.1%*	*1.0%*	*8.8%*	*12.8%*	*7.2%*	*10.2%*

The over-strength factors using allowable stress design are shown in Table 5.8 for both 33 and 36 ksi yield stress. Using 36 ksi steel, all but one floor beam rates sufficiently, even with the direct load method. However, using 33 ksi steel, only three of the floor beams rate sufficiently with the direct load method.

Using the lever rule and Equation 5.9 with a 33 ksi yield stress, almost all of the floor beams rate satisfactorily. These tables demonstrated that a small difference in the yield strength of steel can make a significant difference to the rating of a bridge. By determining the actual yield stress of the steel could determine whether a bridge is rated acceptable or unacceptable.

Table 5.8 Over-Strength Factors for ASD Using H-20 Trucks

		36 ksi				33 ksi			
		M_{all} (kft)	Direct	Lever	Eq. 5.9	M_{all} (kft)	Direct	Lever	Eq. 5.9
1	Brazos	390.7	**-3.2%**	12%	8%	352.4	**-15.9%**	**-2%**	**-6%**
2	Brazos	281.8	3.4%	20%	20%	254.3	**-10.9%**	4%	3%
3	Colorado	392.4	8.2%	26%	21%	353.9	**-7.0%**	9%	4%
4	*N Llano*	*413.1*	*16.2%*	*35%*	*29%*	*372.6*	***-0.2%***	*17%*	*11%*
5	*N Llano*	*413.1*	*10.8%*	*28%*	*23%*	*372.6*	***-4.2%***	*12%*	*6%*
5a	*N Llano*	*413.1*	*14.8%*	*33%*	*27%*	*372.6*	***-0.3%***	*16%*	*11%*
6	Red	392.9	19.9%	38%	34%	354.3	4.9%	21%	17%
7	Sabine	483.0	10.1%	28%	19%	435.6	**-4.9%**	11%	3%
7a	Sabine	483.0	14.2%	32%	24%	435.6	**-0.9%**	15%	7%
8	Trinity	483.0	3.8%	21%	13%	435.6	**-10.9%**	5%	**-3%**
9	*Trinity*	*394.2*	*20.5%*	*39%*	*34%*	*355.4*	*4.6%*	*21%*	*17%*
9a	*Trinity*	*394.2*	*23.5%*	*42%*	*38%*	*355.4*	*7.4%*	*24%*	*20%*

As is evident from the results in the preceding tables, a better estimate of the forces actually on a floor beam can cause a member previously rated deficient to have enough strength to meet the design requirements. Also evident from the tables is the change in the rates is dependent upon the specification. As you move from ASD to LFD to LRFD, the requirements become harder to meet. Floor beams that meet requirements for ASD do not necessarily meet the requirements of the other specifications.

5.6 BRIDGE RATING USING HS-20 LOADING

Though the bridges were designed for H-20 design trucks, the same procedure can be followed to examine the floor beam for an HS-20 truck load. The lever rule would apply exactly the same way for a slab not in contact with the floor beam. However, a different equation would have to be used to determine the moment reduction when the slab sits directly on the floor beam. This equation would take into account more factors than only the floor beam and slab stiffness. According to the direct load method, the HS-20 truck loading causes a moment that is up to 33% higher than the moment caused by the H-20 loading. With a larger floor beam spacing, the extra axle will have a greater effect on the floor beam moment. The over-strength factors are shown for LRFD and LFD in Table 5.9 for the HS-20 loading. Table 5.10 shows the over-strength factors for Allowable Stress Design using the HS-20 loading. Both tables show the results from the direct load and lever rule only.

Table 5.9 Over-Strength for HS-20 Loading, 36 ksi Steel

			Direct Load		Lever Rule	
		Mn	LRFD	LFD	LRFD	LFD
1	Brazos	728.4	**-11.2%**	**-13.3%**	**-2.9%**	**-3.1%**
2	Brazos	526.2	**-5.0%**	**-6.8%**	3.9%	4.1%
3	Colorado	728.4	**-22.5%**	**-23.9%**	**-15.3%**	**-15.0%**
4	*N Llano*	*765.9*	***-20.8%***	***-21.9%***	***-13.6%***	***-12.8%***
5	*N Llano*	*765.9*	***-14.7%***	***-16.4%***	***-6.9%***	***-6.7%***
5a	*N Llano*	*765.9*	***-10.2%***	***-12.2%***	***-1.9%***	***-2.0%***
6	Red	728.4	3.9%	1.2%	13.6%	13.0%
7	Sabine	897.6	**-14.8%**	**-16.2%**	**-6.9%**	**-6.4%**
7a	Sabine	897.6	**-10.2%**	**-11.9%**	**-1.9%**	**-1.7%**
8	Trinity	897.6	**-20.9%**	**-21.7%**	**-13.6%**	**-12.6%**
9	*Trinity*	*728.4*	***-9.8%***	***-11.9%***	***-1.6%***	***-1.6%***
9a	*Trinity*	*728.4*	***-6.2%***	***-8.6%***	*2.3%*	*2.0%*

Table 5.10 ASD Over-Strength Factors for HS-20 Loading

		36 ksi			33 ksi		
		M_{all} (kft)	Direct	Lever	M_{all} (kft)	Direct	Lever
1	Brazos	390.7	**-9.1%**	5%	352.4	**-21.1%**	**-8%**
2	Brazos	281.8	**-3.3%**	13%	254.3	**-16.7%**	**-2%**
3	Colorado	392.4	**-24.1%**	**-12%**	353.9	**-34.7%**	**-23%**
4	*N Llano*	*413.1*	***-21.8%***	***-9%***	*372.6*	***-32.8%***	***-21%***
5	*N Llano*	*413.1*	***-13.3%***	*0.4%*	*372.6*	***-25.0%***	***-13%***
5a	*N Llano*	*413.1*	***-7.1%***	*7%*	*372.6*	***-19.3%***	***-6%***
6	Red	392.9	12.2%	29%	354.3	**-1.9%**	13%
7	Sabine	483.0	**-13.6%**	0.2%	435.6	**-25.4%**	**-13%**
7a	Sabine	483.0	**-7.3%**	7%	435.6	**-19.6%**	**-7%**
8	Trinity	483.0	**-22.2%**	**-9%**	435.6	**-33.2%**	**-22%**
9	*Trinity*	*394.2*	***-6.4%***	*8%*	*355.4*	***-18.7%***	***-6%***
9a	*Trinity*	*394.2*	***-1.5%***	*14%*	*355.4*	***-14.3%***	***-1%***

CHAPTER 6

CONCLUSIONS

6.1 PURPOSE OF RESEARCH

The main goal of the research was to more accurately determine the moments in the transverse floor beams in twin girder steel bridges. This was accomplished by modeling actual bridge geometries with the SAP2000 finite element program. These results from this analysis were then compared with the moment resulting from the current provisions and with the moments from experimental results. Using these results, it was possible to quantify the force experienced by the floor beam for a given loading condition.

6.2 OVERVIEW OF FINDINGS

6.2.1 Current Analysis Methods Are Over-Conservative

Using finite element modeling as well as simple statics, it was determined that the floor beams in the bridge do not experience the force estimated by the current rating procedures. The amount of reduction due to the lateral load distribution and moment carried by the slab is about 10%. Though 10% may not seem like much, it often makes the difference between rating the member as adequate of inadequate, as was shown in Chapter 5.

6.2.2 Suggested Changes in Load Distribution Methods

If the floor beam does not come into contact with the slab, the lever rule should be used to determine the moment in the floor beam. This is a relatively simple calculation. In fact, if the system has only two stringers spaced from 6 to 12 feet, the value for the maximum moment using the lever rule is determined by simply multiplying the direct load moment by 0.894. This is still conservative with respect to moment values in the floor beam predicted by finite element analysis.

If the floor beam does come into contact with the slab, the load is transferred in a more complex manner. To avoid having to take the time to use a finite element model for each bridge, it was necessary to come up with an equation that gives a moment value closer to the actual value, yet still conservative. The equation shown in chapter 3 accomplishes this for the H-20 load case. This specification uses the ratio of floor beam stiffness to slab stiffness to predict the percentage of moment taken by the floor beam and slab. An equation for HS-20 truck loading is not available at this time.

6.2.3 Comparison of Experimental and Analytical Results

The experimental test of the Llano bridge confirmed what was demonstrated using finite element modeling, that the direct load model results in moments that are much higher than those actually experienced. Even the results from the SAP analyses are quite a bit higher than the moments calculated using the experimental results. The reason for this could be attributed to the fixity of the connections and the higher stiffness of the concrete deck. However, it is not known with certainty why the experimental moments were lower. It does imply, though, that using a finite element model with simply supported floor beams is still a conservative approach.

6.3 PRACTICAL RESULTS OF RESEARCH

The result of the research was not the development of a new design method. In fact, new bridge construction rarely includes the type of bridges analyzed in this study. The research looks primarily at existing structures to determine if they are being rated properly. The result of this research is a more realistic assessment of the floor beam moment, which will lead to a more rational rating of the bridge. Bridges that are functioning at an acceptable level should be rated accordingly. This would make available both time and money to use on structures that should demand more attention. Another result of this research should be a new interest in transverse load distribution. This subject has been long overlooked by the codes and it is the hope of the authors that more work will be done to determine exactly how load is distributed transversely. There is still much that can be done in this area.

APPENDIX A

BRIDGE CROSS SECTIONS

Brazos 1

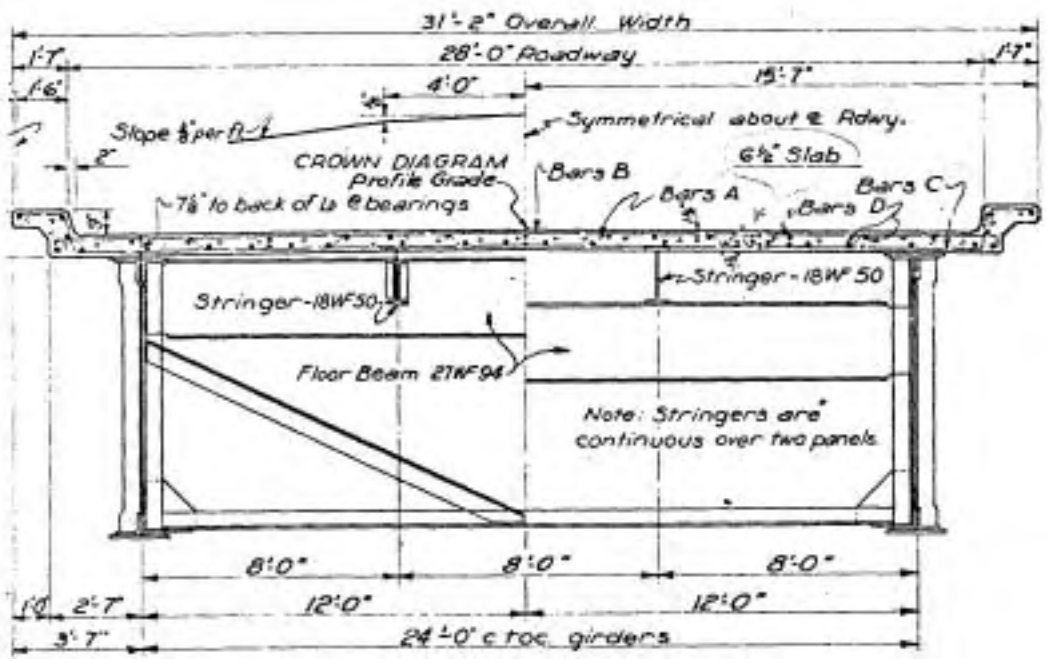

Brazos 2

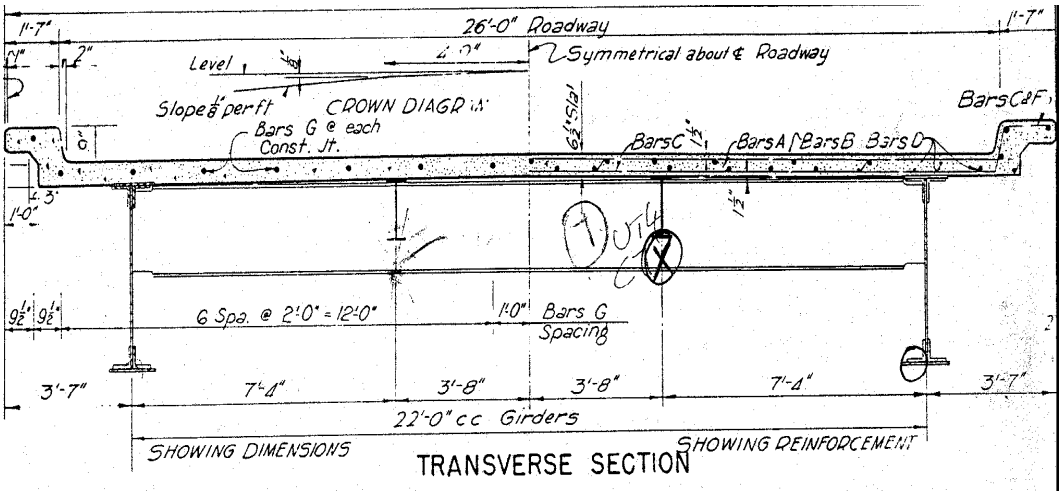

Colorado 3

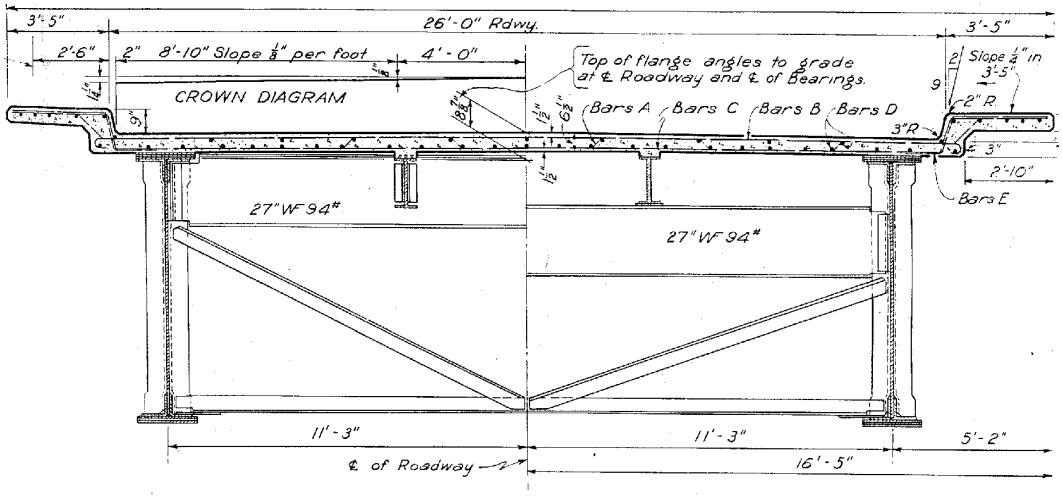

N. Llano 4

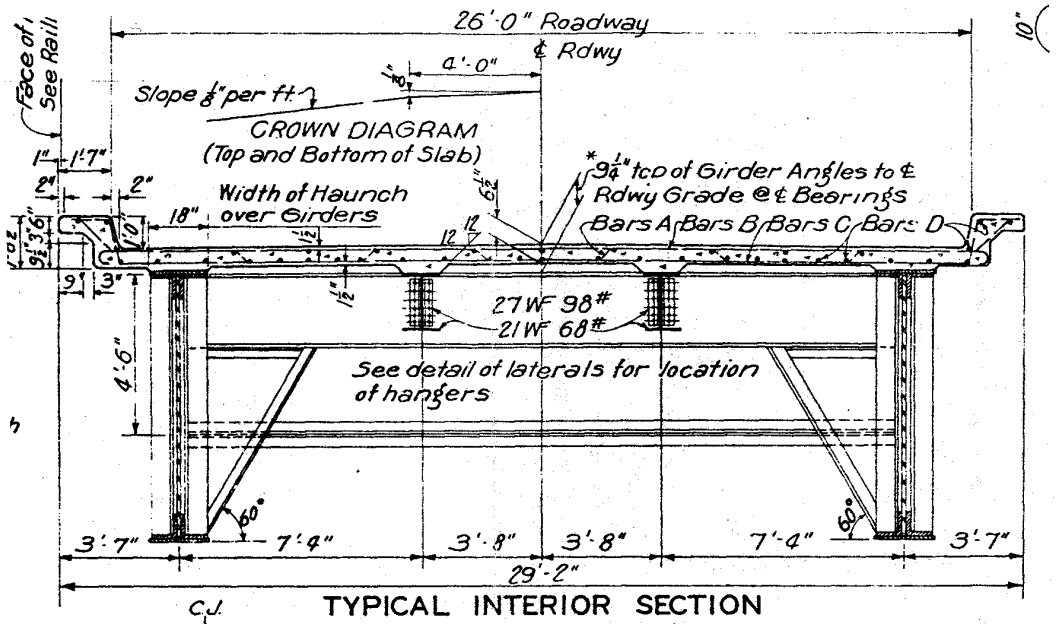

N. Llano 5 & 5a

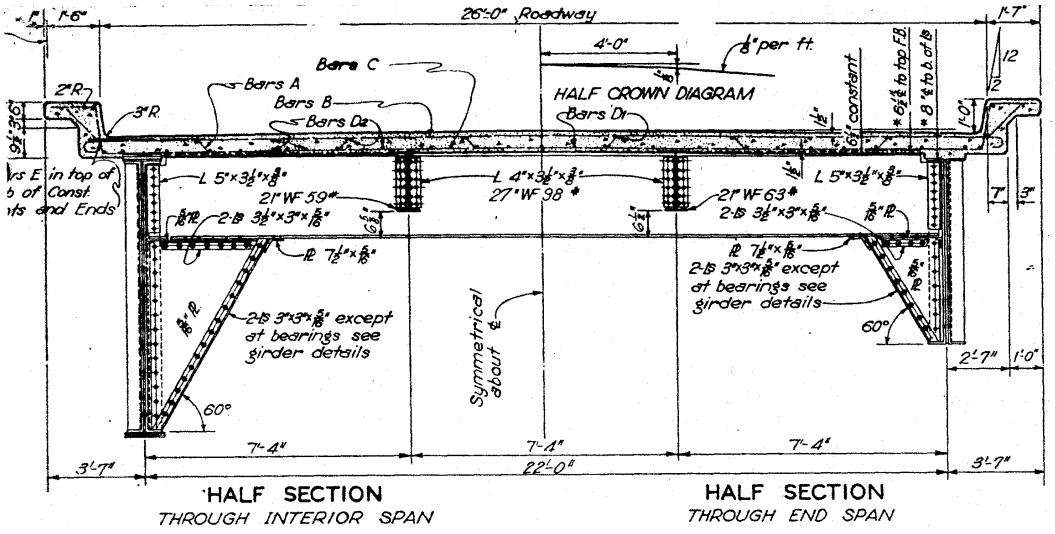

Red 6

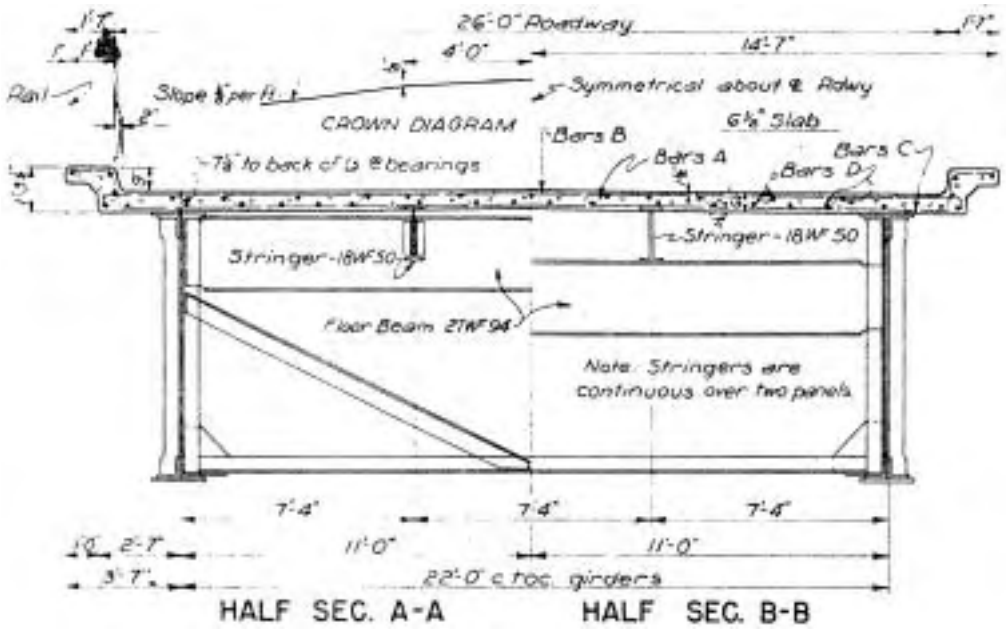

Sabine 7 & 7a

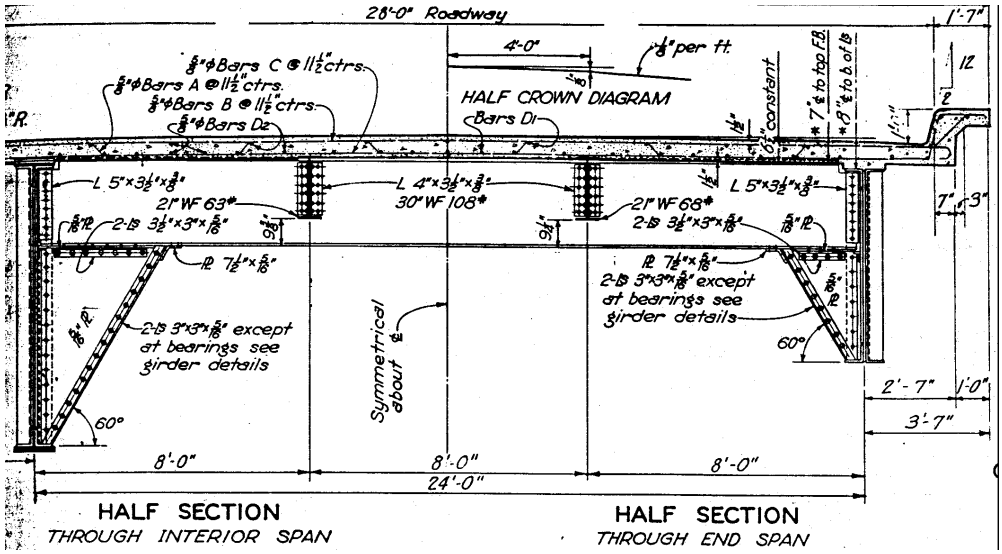

Trinity 8

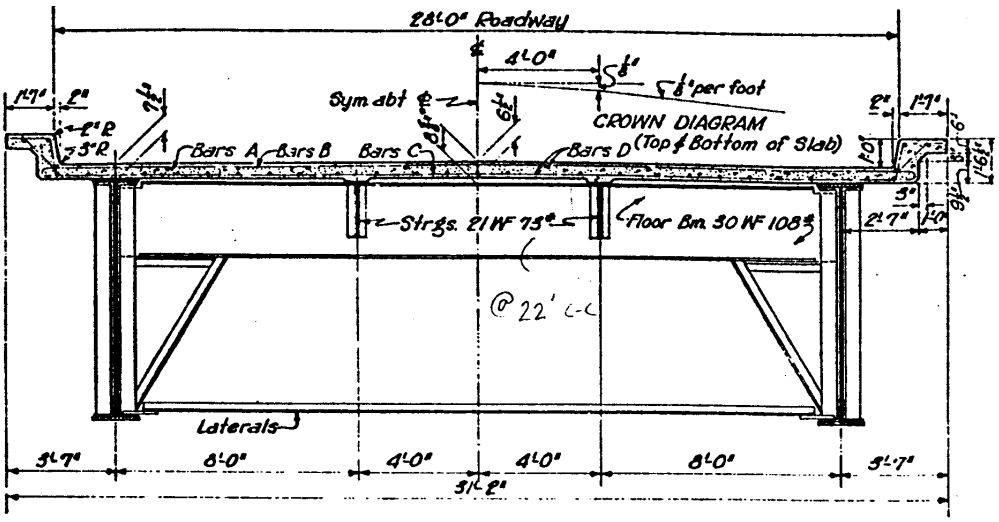

TYPICAL INTERIOR SECTION

Trinity 9 & 9a

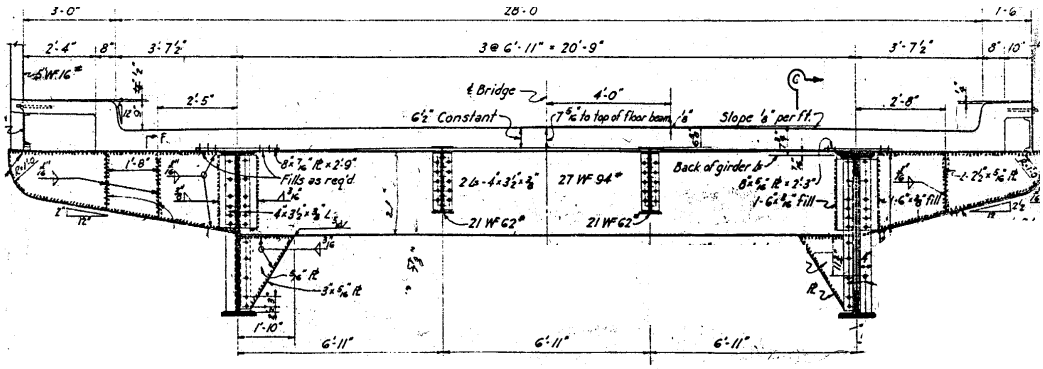

SECTION A-A

APPENDIX B

LOAD RUN DESCRIPTIONS FOR FIRST LLANO TEST

Run	Truck	Description of Run (Transverse Location of Center of Load, ft)
1	A & B	Two Trucks, Side by Side (0)
1B	A & B	Two Trucks, Side by Side (0)
2	A & B	Two Trucks, Side by Side (0)
3	A & B	Two Trucks, Train (0)
4	A & B	Two Trucks, Train (0)
5	A	One Truck, Center (0)
6	B	One Truck, Center (0)
7	A	One Truck (-5.5)
8	B	One Truck (-5.5)
9	A	One Truck (-3.5)
10	B	One Truck (-3.5)
11	A	One Truck (1)
12	B	One Truck (1)
13	A	One Truck (5.5)
14	B	One Truck (5.5)
15	A	One Truck (3.5)
16	B	One Truck (3.5)
17	A	One Truck (-1)
18	B	One Truck (-1)
19	A & B	Two Trucks, Reverse Train (0)
20	A & B	Two Trucks, Reverse Train (0)
21	A & B	Two Trucks, Reverse Train (0)

APPENDIX C

SELECTED NEUTRAL AXIS CALCULATIONS FOR FIRST LLANO TEST

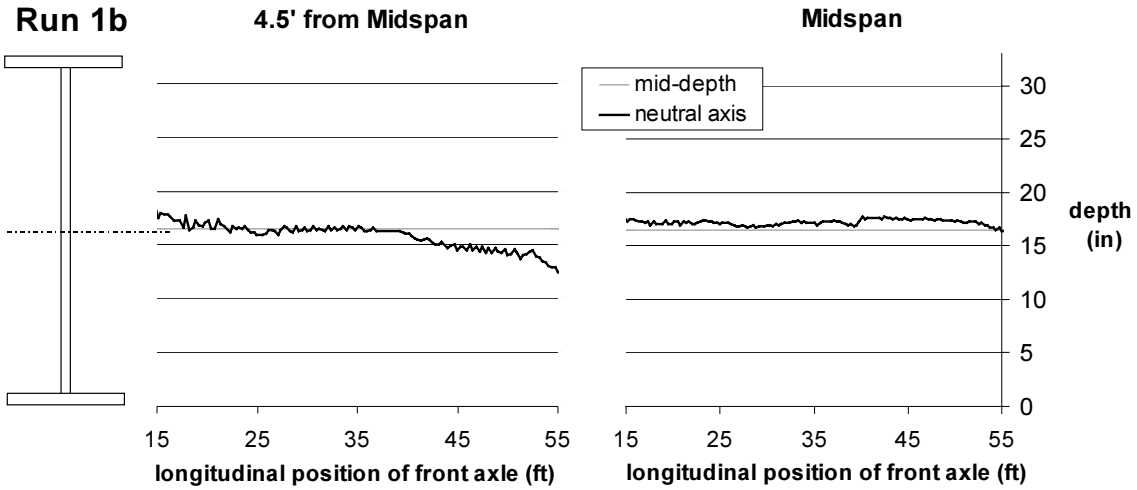

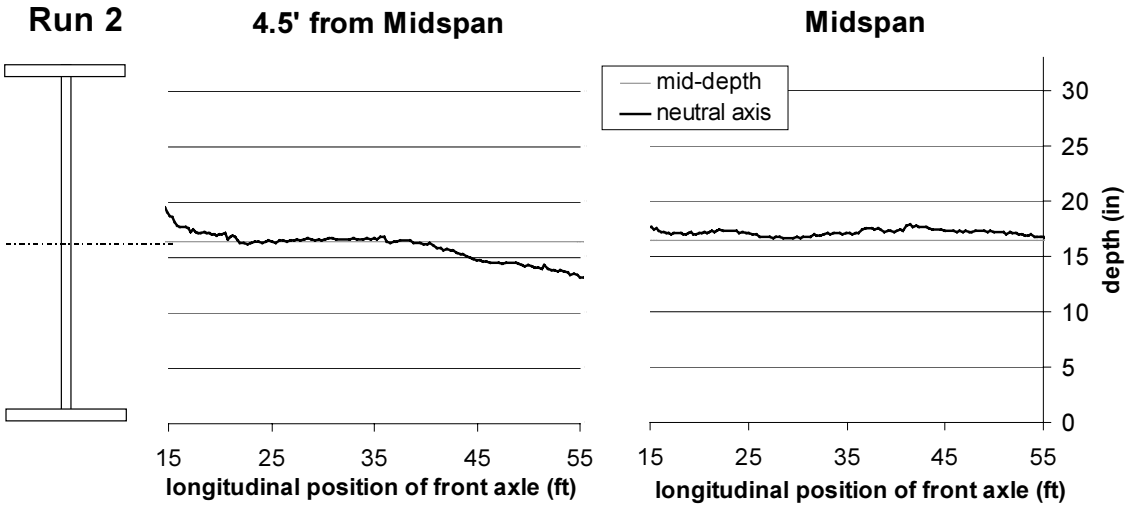

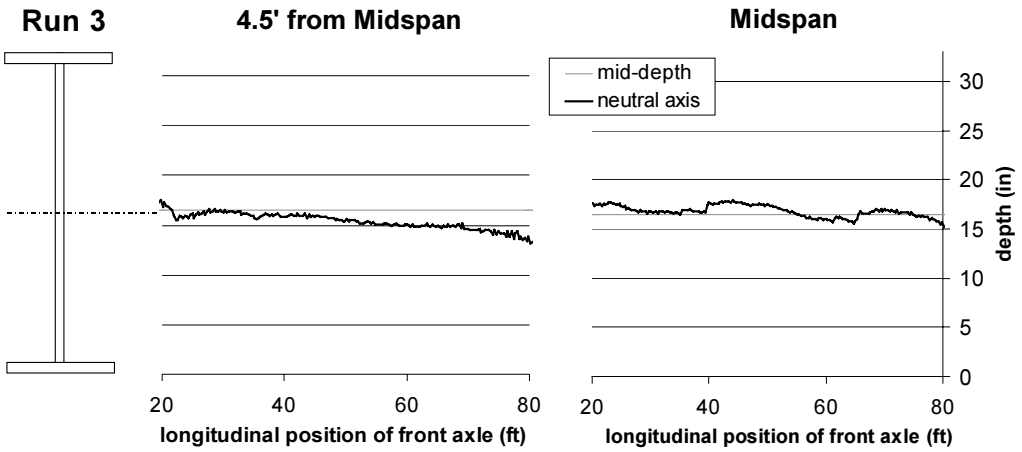
Run 3
4.5' from Midspan
Midspan
mid-depth
neutral axis
depth (in)
0
5
10
15
20
25
30
20
40
60
80
longitudinal position of front axle (ft)

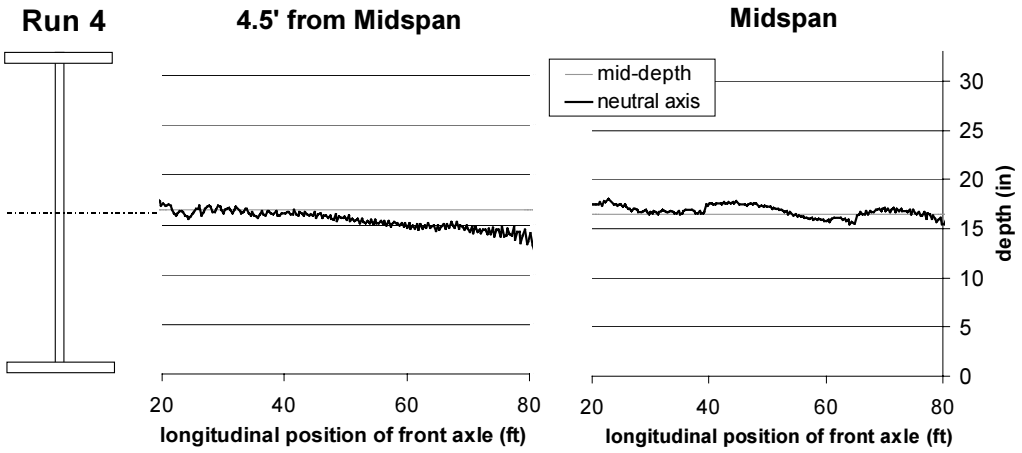
Run 4
4.5' from Midspan
Midspan
mid-depth
neutral axis
depth (in)
0
5
10
15
20
25
30
20
40
60
80
longitudinal position of front axle (ft)

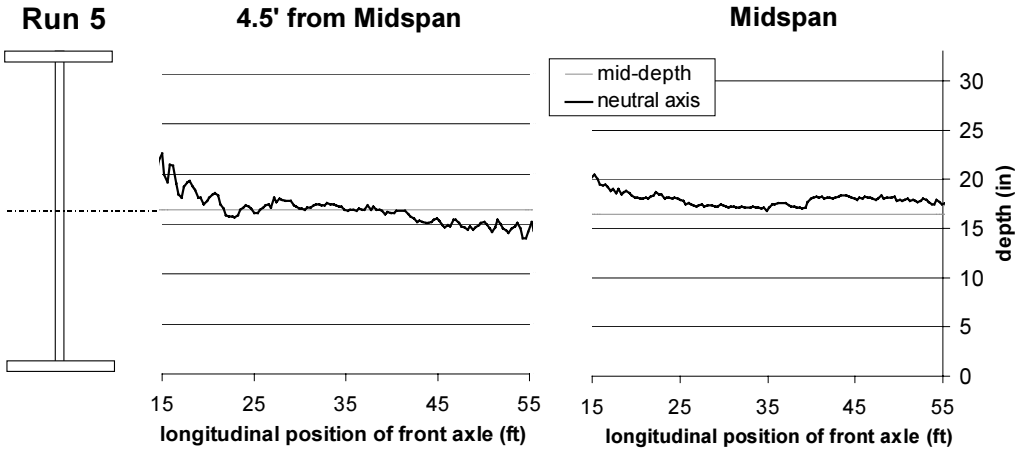
Run 5
4.5' from Midspan
Midspan
mid-depth
neutral axis
depth (in)
0
5
10
15
20
25
30
15
25
35
45
55
longitudinal position of front axle (ft)

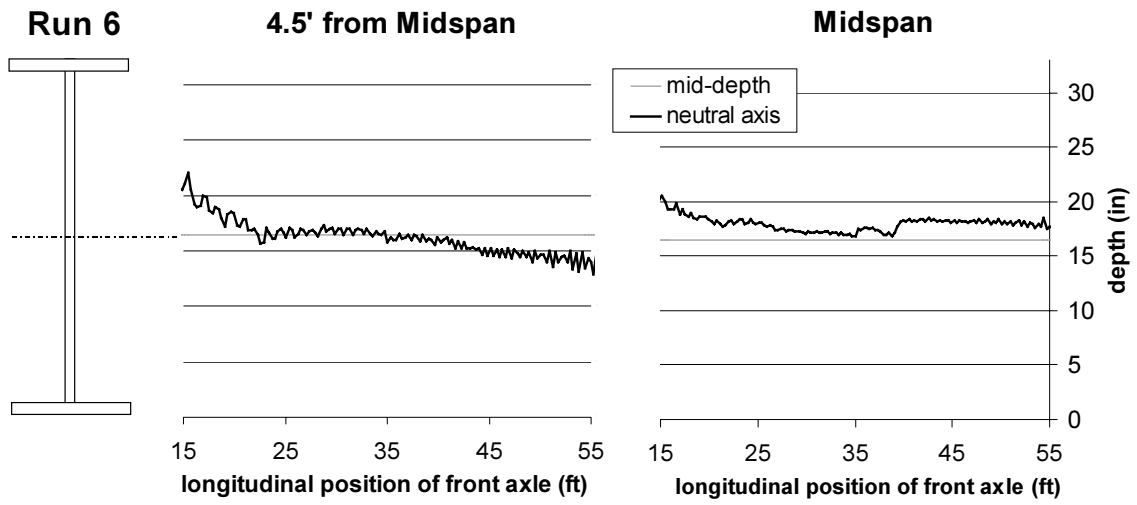
Run 6
4.5' from Midspan
Midspan
mid-depth
neutral axis
30
25
20
15
10
5
0
depth (in)
15
25
35
45
55
longitudinal position of front axle (ft)
15
25
35
45
55
longitudinal position of front axle (ft)

APPENDIX D

COMPARISON OF TOP TO BOTTOM FLANGE STRAINS IN FIRST LLANO TEST

Run	% top flange max is less than bottom flange max			
	FB1 -mid	FB2-mid	FB1-4.5'	FB2-4.5'
1	48%	19%	18%	-6%
1b	44%	7%	22%	-2%
2	50%	7%	19%	-4%
3	40%	1%	-1%	-11%
4	41%	0%	-3%	-8%
5	38%	5%	1%	-1%
6	46%	7%	-2%	-3%
7	54%	28%	23%	5%
8	59%	25%	18%	3%
9	50%	-29%	18%	4%
10	54%	9%	20%	6%
11	40%	-1%	2%	-4%
12	49%	1%	-2%	-3%
13	32%	9%	-2%	-2%
14	42%	14%	-2%	-2%
15	39%	5%	5%	-3%
16	42%	3%	3%	-9%
17	43%	6%	3%	-7%
18	48%	14%	4%	-2%
20	45%	7%	-10%	-11%
21	46%	8%	-3%	-4%
Avg.	45%	7%	6%	-3%

APPENDIX E

COMPARISON OF SECOND FLOOR BEAM TO FIRST FLOOR BEAM STRAINS

Run	Mid-Span			4.5' Away		
	FB2 (με)	FB1 (με)	% smaller	FB2 (με)	FB1 (με)	% smaller
1	164.6	108.0	34%	110.6	94.0	15%
1b	159.5	116.9	27%	117.8	100.8	14%
2	146.6	106.1	28%	109.3	95.0	13%
3	118.5	83.1	30%	83.6	69.7	17%
4	119.9	84.1	30%	85.4	69.5	19%
5	103.3	80.1	22%	73.4	71.1	3%
6	101.0	78.8	22%	73.4	68.4	7%
7	72.4	55.5	23%	72.0	69.9	3%
8	68.8	54.3	21%	70.1	65.5	7%
9	75.6	72.8	4%	80.2	76.8	4%
10	86.3	67.6	22%	76.9	73.6	4%
11	102.2	82.3	19%	68.3	67.2	2%
12	99.5	81.2	18%	68.5	63.8	7%
13	73.0	60.1	18%	38.8	33.6	13%
14	73.2	57.3	22%	38.8	33.6	13%
15	91.8	73.2	20%	53.4	48.8	9%
16	86.0	70.1	18%	49.5	42.8	13%
17	102.4	79.6	22%	75.7	74.5	2%
18	104.4	77.6	26%	76.5	73.8	4%
20	147.5	96.5	35%	102.9	81.5	21%
21	148.8	94.9	36%	106.2	79.9	25%
Avg.			24%			10%
Comparison of Experimental to SAP and Direct Load using Run 1b						
Exp.	159.5	116.9	27%	117.8	100.8	14%
SAP	233.7	219	6%	203	194.7	4%
Direct	261.4	237.8	9%	226.3	205.9	9%

APPENDIX F

RESULTS FROM LOAD RUNS IN FIRST LLANO TEST

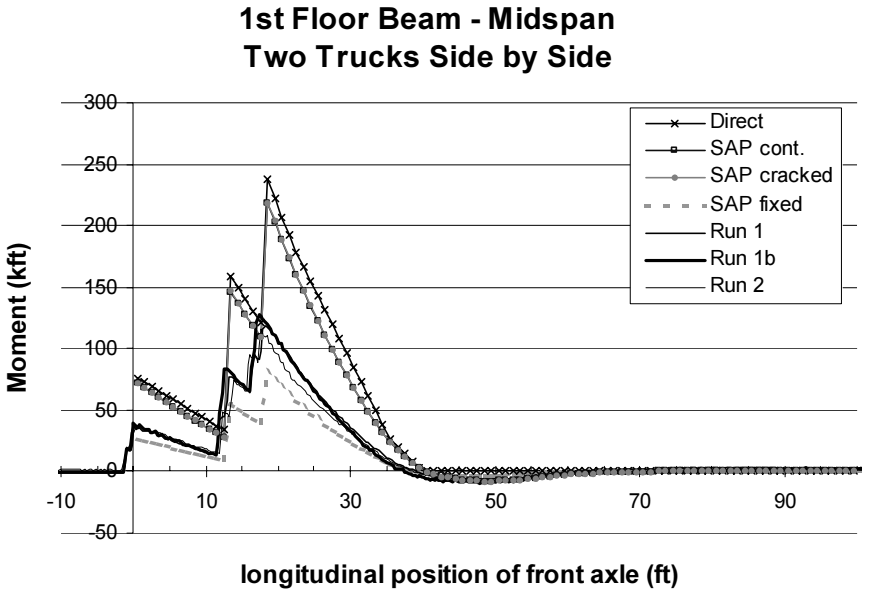

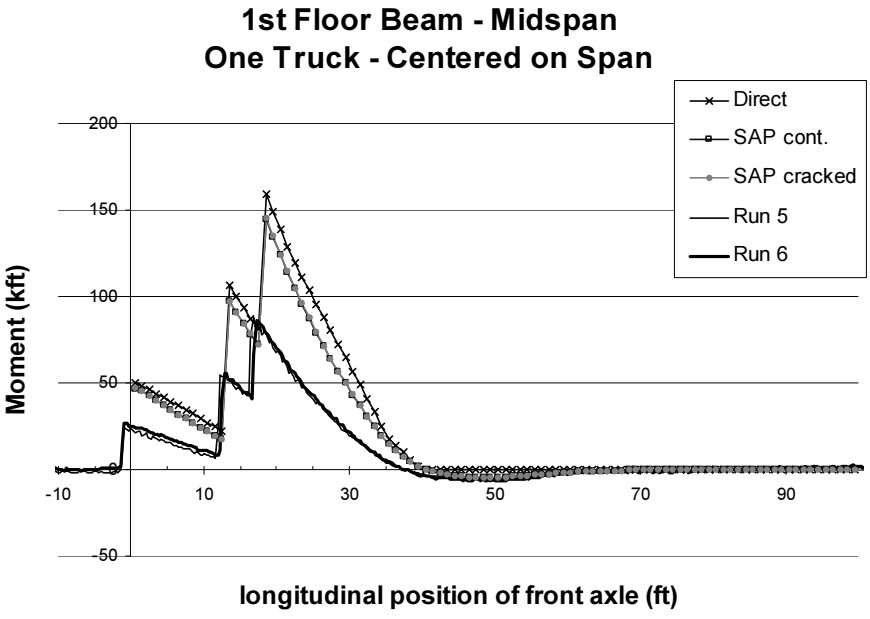

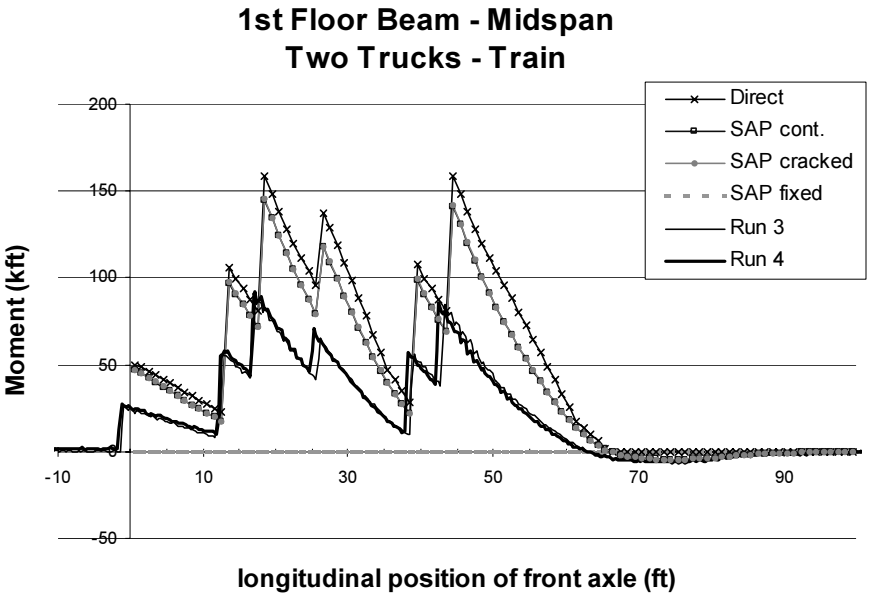
1st Floor Beam - Midspan
Two Trucks - Train
Direct
SAP cont.
SAP cracked
SAP fixed
Run 3
Run 4
Moment (kft)
200
150
100
50
0
-50
-10
10
30
50
70
90
longitudinal position of front axle (ft)

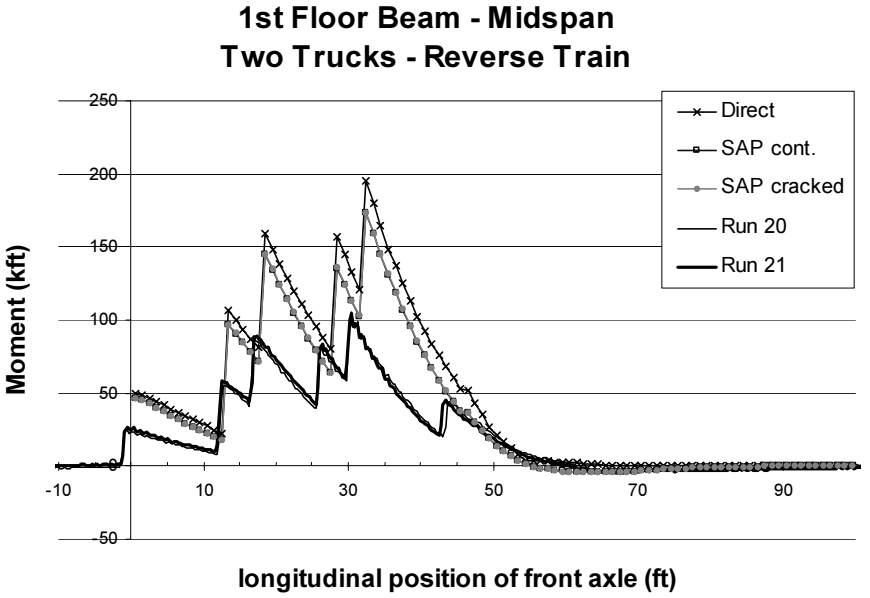
1st Floor Beam - Midspan
Two Trucks - Reverse Train
Direct
SAP cont.
SAP cracked
Run 20
Run 21
Moment (kft)
250
200
150
100
50
0
-50
-10
10
30
50
70
90
longitudinal position of front axle (ft)

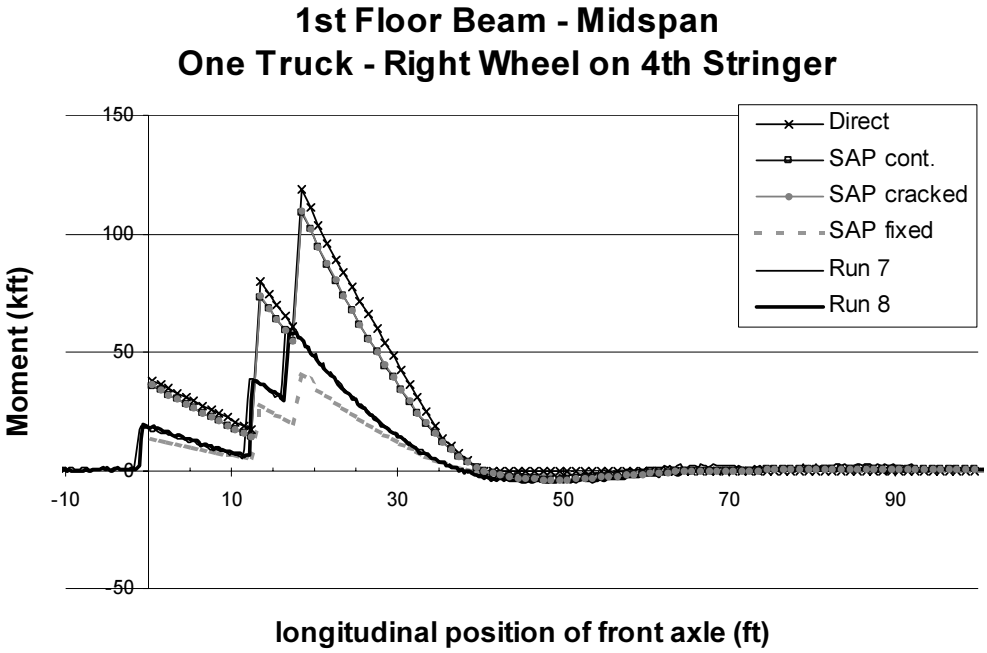
1st Floor Beam - Midspan
One Truck - Right Wheel on 4th Stringer
Moment (kft)
150
100
50
0
-50
-10
10
30
50
70
90
longitudinal position of front axle (ft)
Direct
SAP cont.
SAP cracked
SAP fixed
Run 7
Run 8

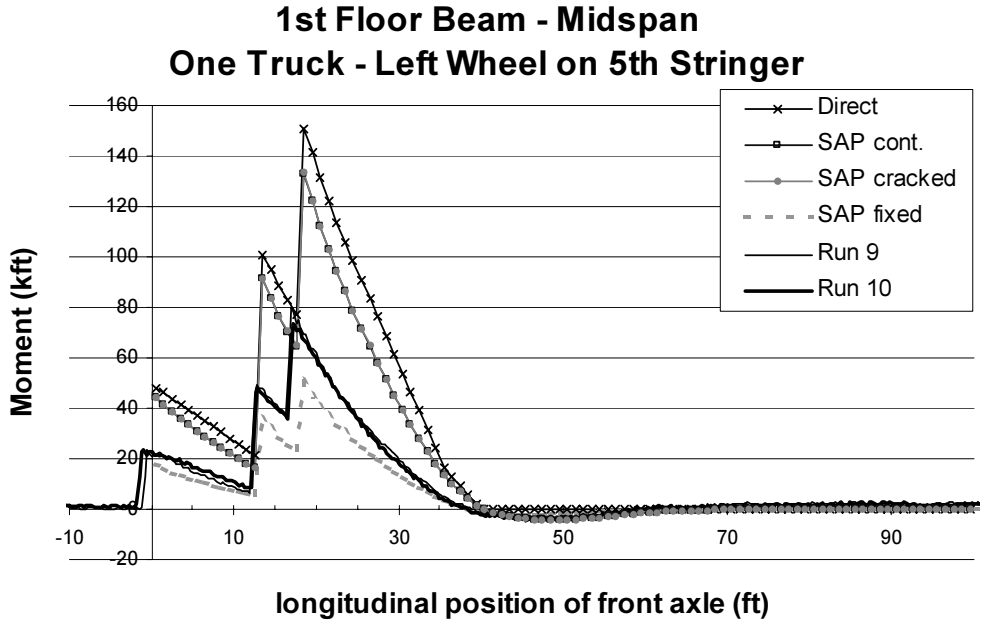
1st Floor Beam - Midspan
One Truck - Left Wheel on 5th Stringer
Moment (kft)
160
140
120
100
80
60
40
20
0
-20
-10
10
30
50
70
90
longitudinal position of front axle (ft)
Direct
SAP cont.
SAP cracked
SAP fixed
Run 9
Run 10

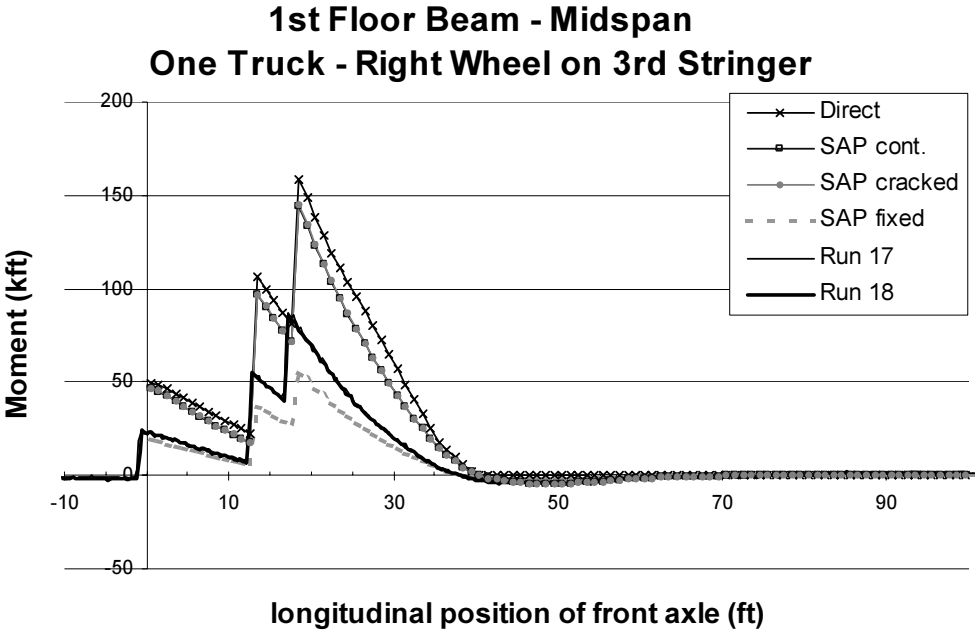
1st Floor Beam - Midspan
One Truck - Right Wheel on 3rd Stringer
Moment (kft)
200
150
100
50
0
-50
-10
10
30
50
70
90
Direct
SAP cont.
SAP cracked
SAP fixed
Run 17
Run 18
longitudinal position of front axle (ft)

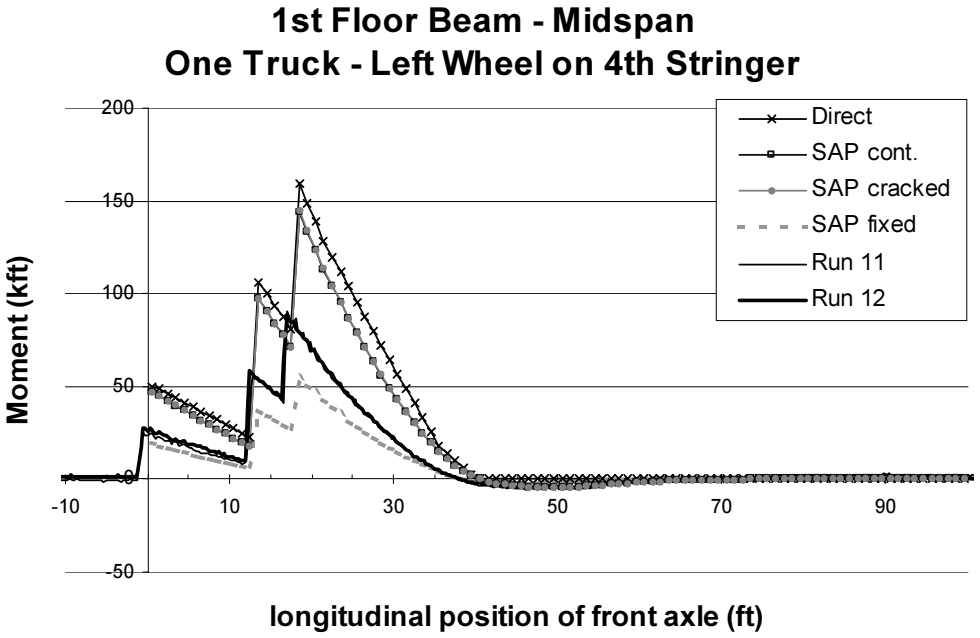
1st Floor Beam - Midspan
One Truck - Left Wheel on 4th Stringer
Moment (kft)
200
150
100
50
0
-50
-10
10
30
50
70
90
Direct
SAP cont.
SAP cracked
SAP fixed
Run 11
Run 12
longitudinal position of front axle (ft)

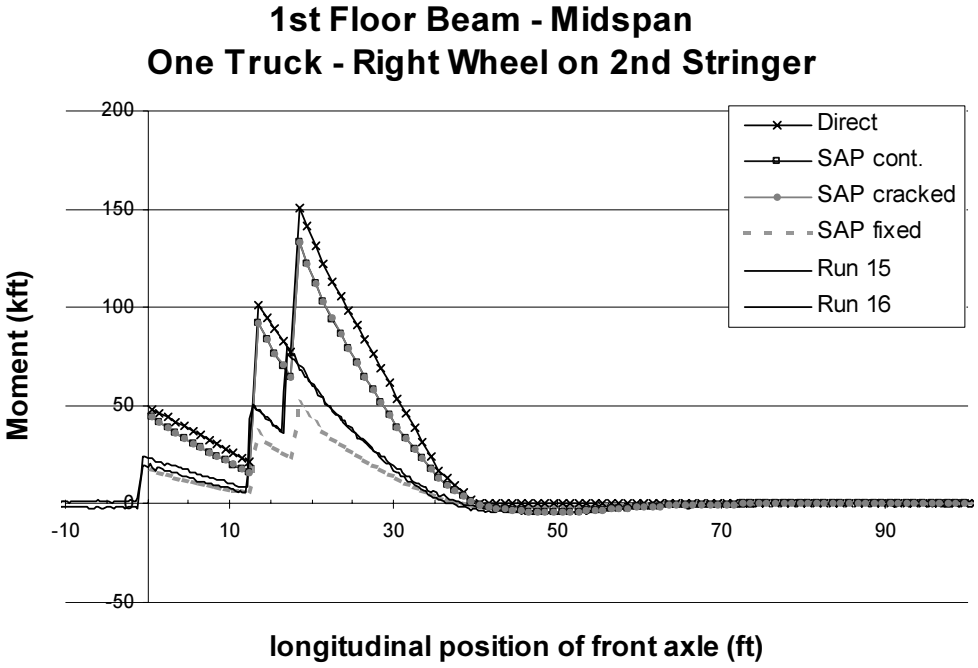
1st Floor Beam - Midspan
One Truck - Right Wheel on 2nd Stringer
Moment (kft)
200
150
100
50
0
-50
-10
10
30
50
70
90
Direct
SAP cont.
SAP cracked
SAP fixed
Run 15
Run 16
longitudinal position of front axle (ft)

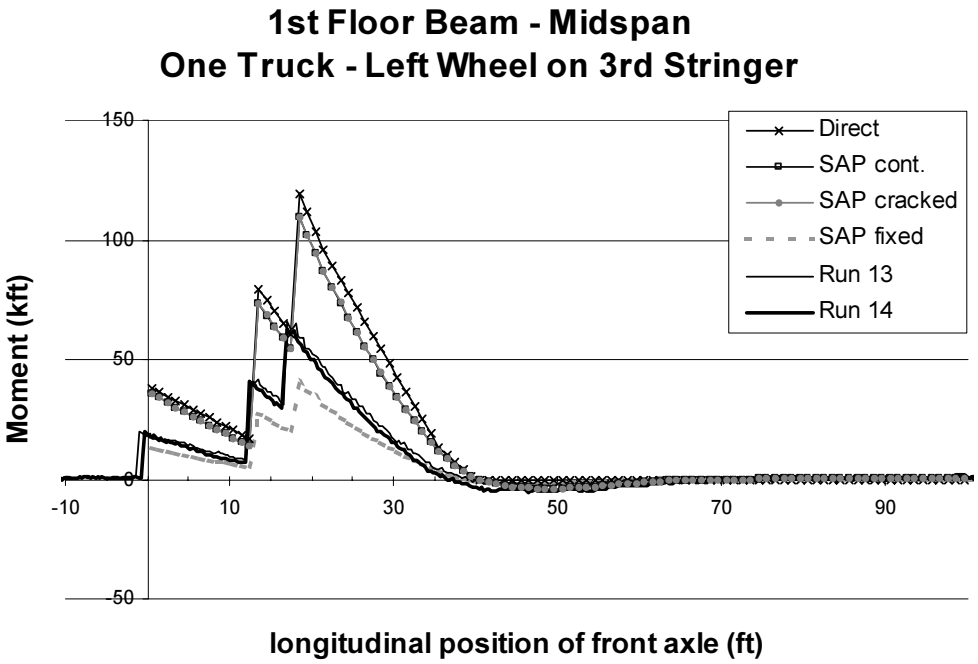
1st Floor Beam - Midspan
One Truck - Left Wheel on 3rd Stringer
Moment (kft)
150
100
50
0
-50
-10
10
30
50
70
90
Direct
SAP cont.
SAP cracked
SAP fixed
Run 13
Run 14
longitudinal position of front axle (ft)

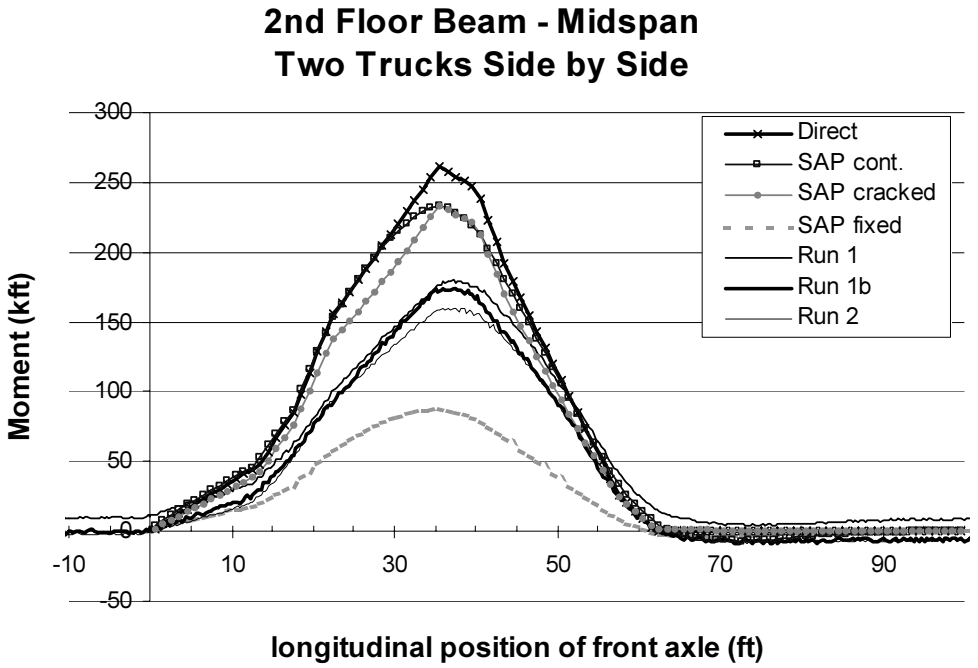
2nd Floor Beam - Midspan
Two Trucks Side by Side
Moment (kft)
300
250
200
150
100
50
0
-50
-10
10
30
50
70
90
Direct
SAP cont.
SAP cracked
SAP fixed
Run 1
Run 1b
Run 2
longitudinal position of front axle (ft)

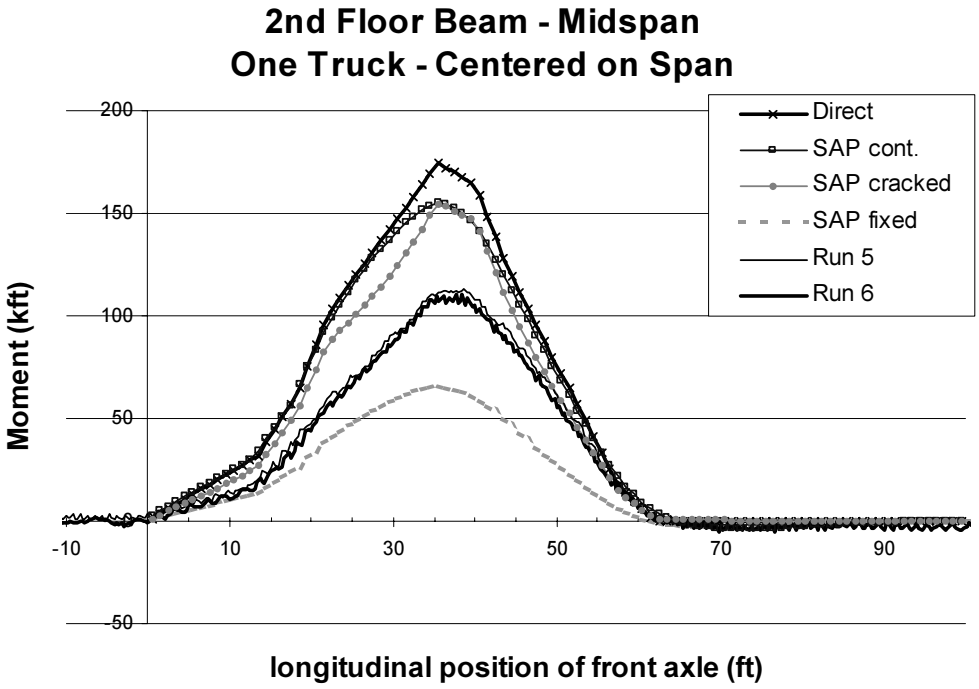
2nd Floor Beam - Midspan
One Truck - Centered on Span
Moment (kft)
200
150
100
50
-50
-10
10
30
50
70
90
Direct
SAP cont.
SAP cracked
SAP fixed
Run 5
Run 6
longitudinal position of front axle (ft)

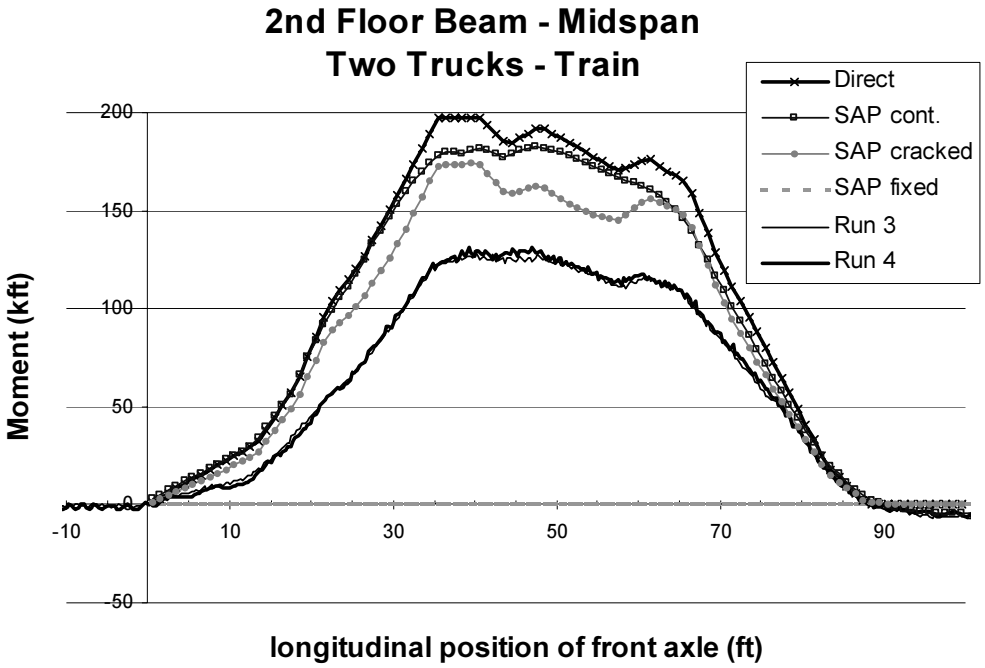
2nd Floor Beam - Midspan
Two Trucks - Train
Direct
SAP cont.
SAP cracked
SAP fixed
Run 3
Run 4
Moment (kft)
200
150
100
50
0
-50
-10
10
30
50
70
90
longitudinal position of front axle (ft)

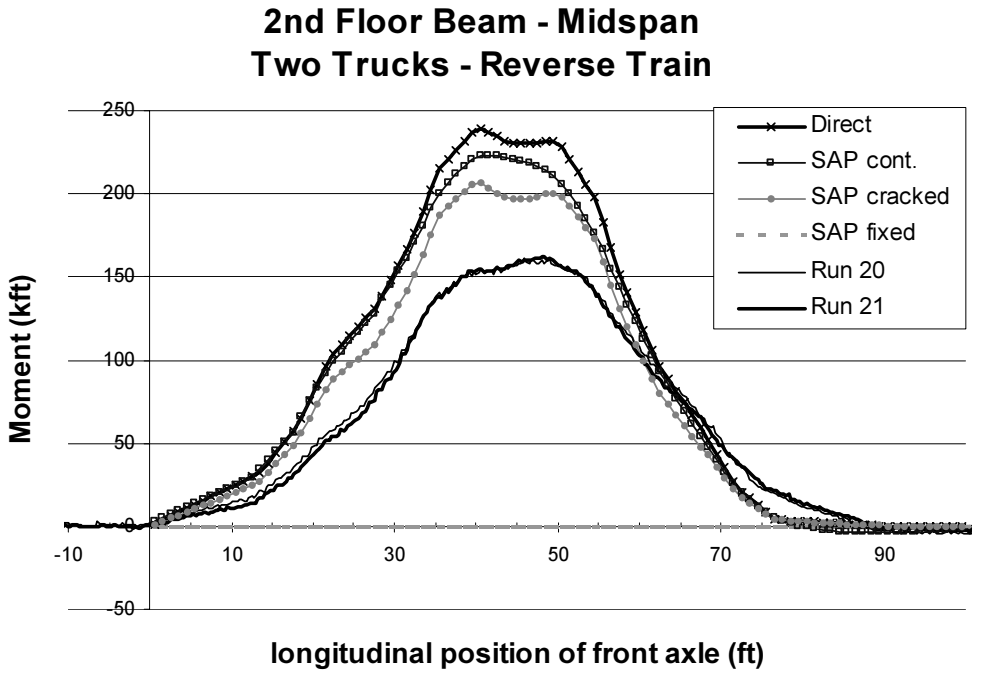
2nd Floor Beam - Midspan
Two Trucks - Reverse Train
Direct
SAP cont.
SAP cracked
SAP fixed
Run 20
Run 21
Moment (kft)
250
200
150
100
50
0
-50
-10
10
30
50
70
90
longitudinal position of front axle (ft)

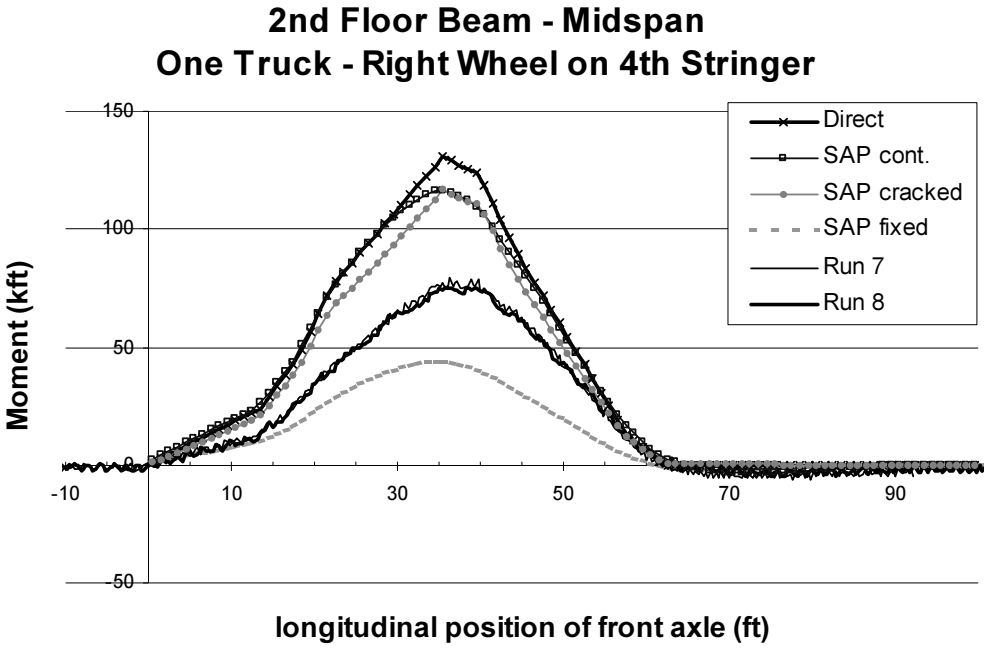
2nd Floor Beam - Midspan
One Truck - Right Wheel on 4th Stringer
Moment (kft)
150
100
50
0
-50
-10
10
30
50
70
90
Direct
SAP cont.
SAP cracked
SAP fixed
Run 7
Run 8
longitudinal position of front axle (ft)

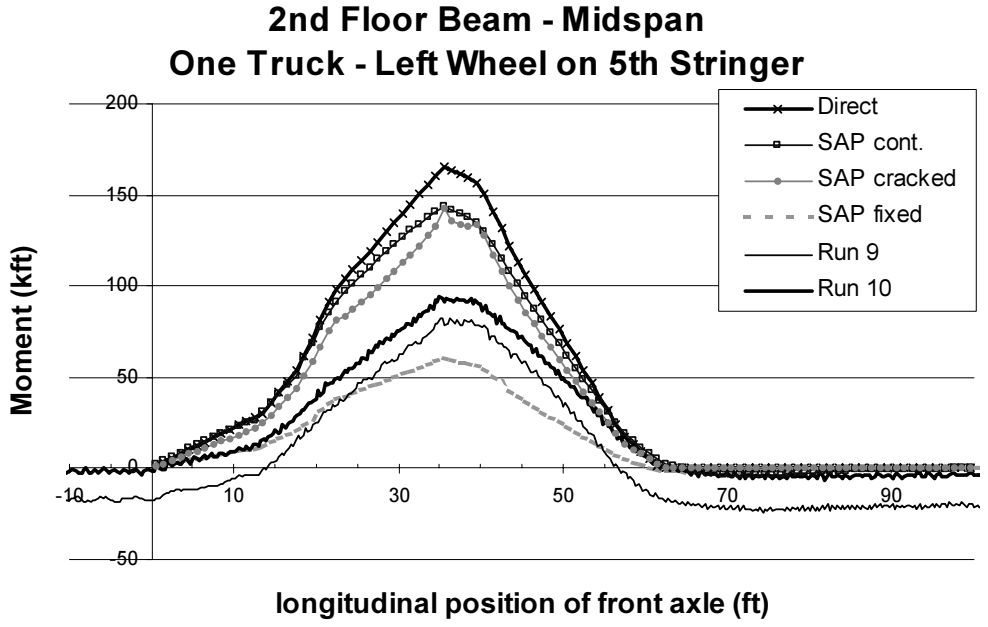
2nd Floor Beam - Midspan
One Truck - Left Wheel on 5th Stringer
Moment (kft)
200
150
100
50
0
-50
-10
10
30
50
70
90
Direct
SAP cont.
SAP cracked
SAP fixed
Run 9
Run 10
longitudinal position of front axle (ft)

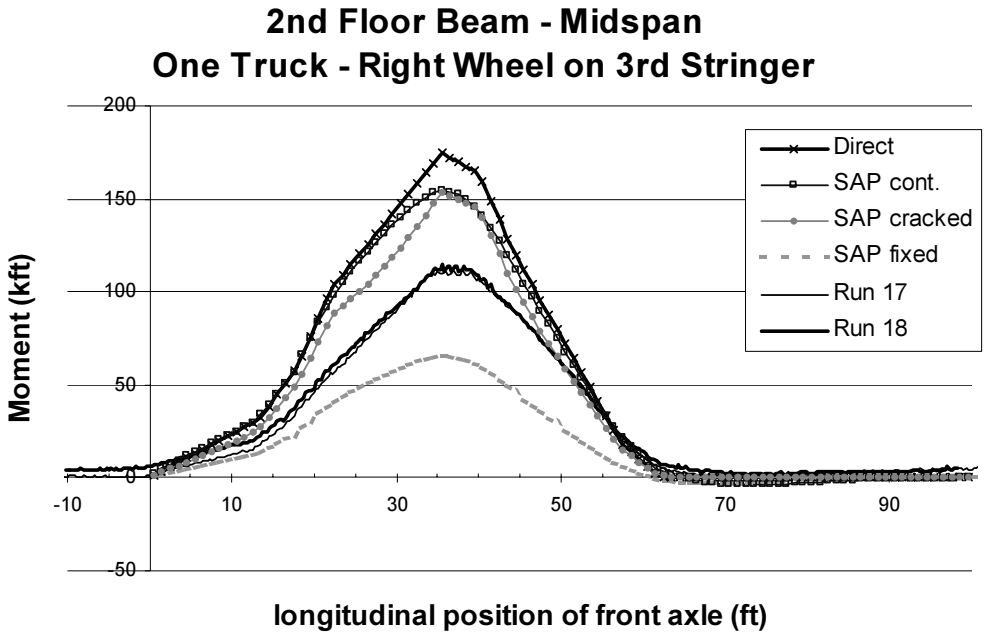
2nd Floor Beam - Midspan
One Truck - Right Wheel on 3rd Stringer
Moment (kft)
200
150
100
50
0
-50
-10
10
30
50
70
90
Direct
SAP cont.
SAP cracked
SAP fixed
Run 17
Run 18
longitudinal position of front axle (ft)

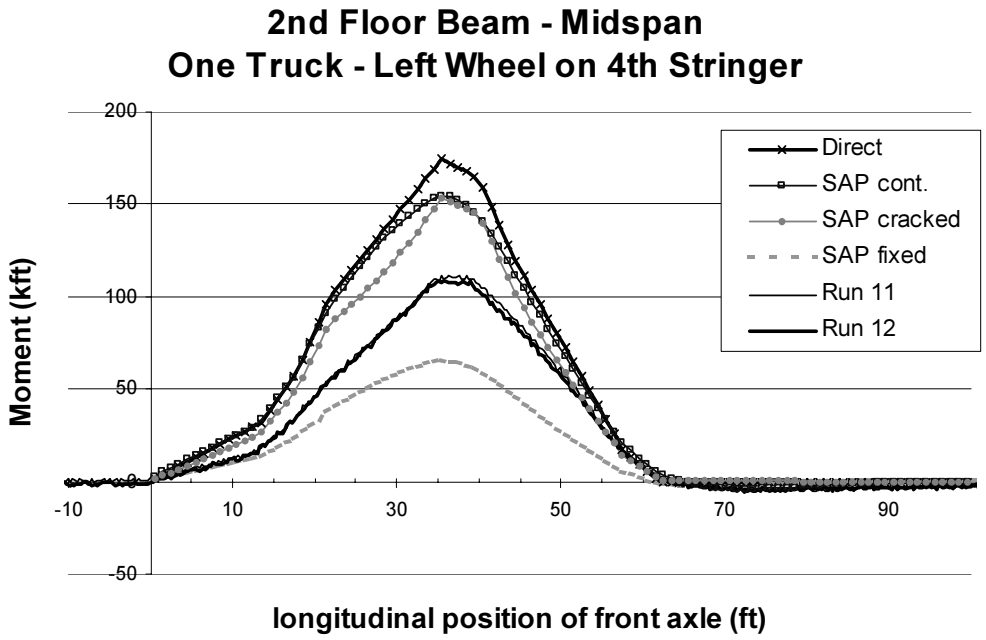
2nd Floor Beam - Midspan
One Truck - Left Wheel on 4th Stringer
Moment (kft)
200
150
100
50
0
-50
-10
10
30
50
70
90
Direct
SAP cont.
SAP cracked
SAP fixed
Run 11
Run 12
longitudinal position of front axle (ft)

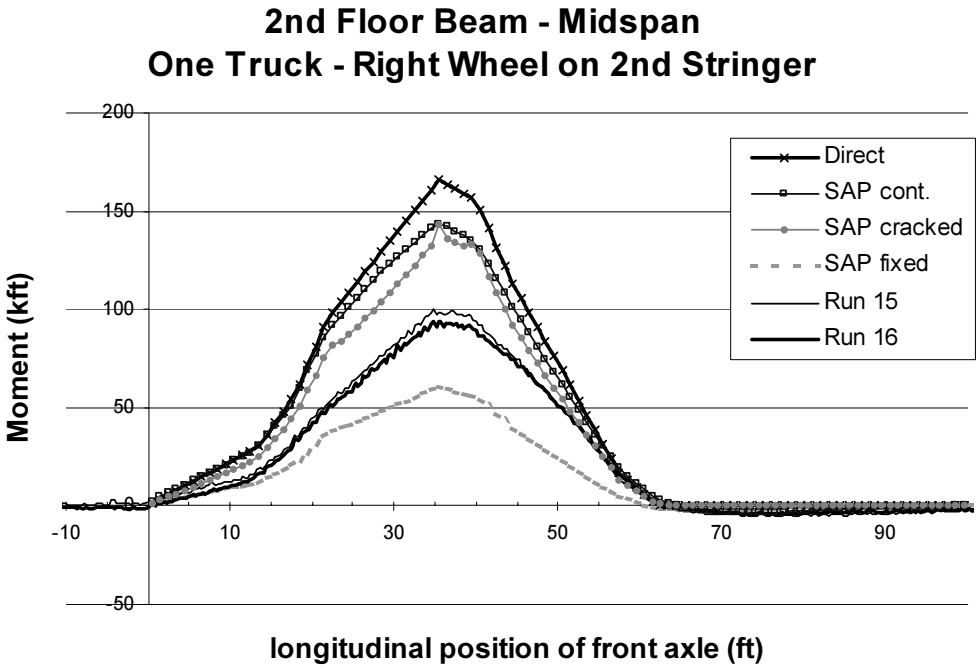
2nd Floor Beam - Midspan
One Truck - Right Wheel on 2nd Stringer
Moment (kft)
200
150
100
50
0
-50
-10
10
30
50
70
90
Direct
SAP cont.
SAP cracked
SAP fixed
Run 15
Run 16
longitudinal position of front axle (ft)

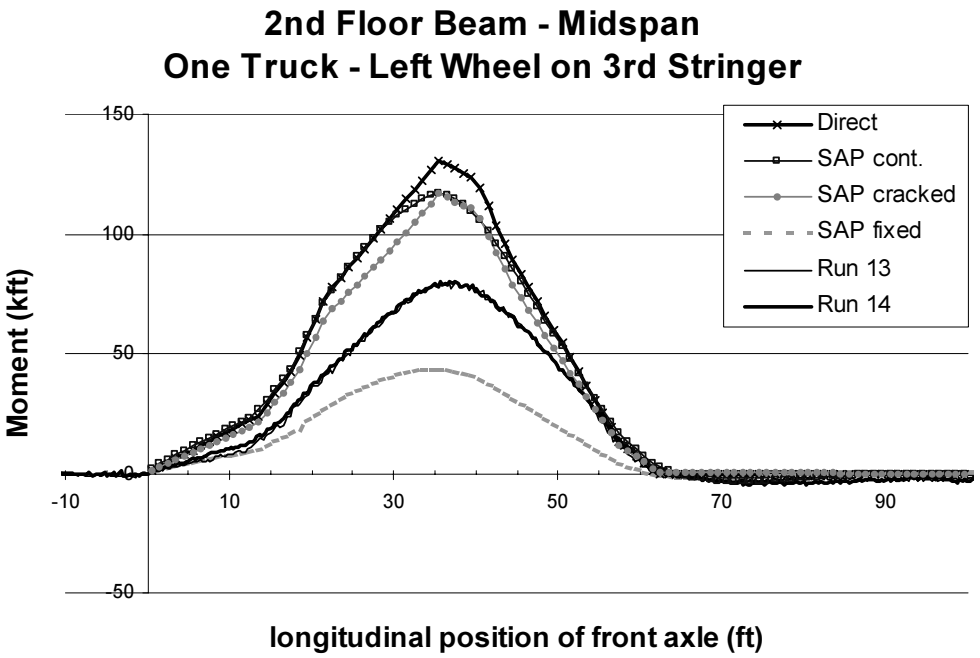
2nd Floor Beam - Midspan
One Truck - Left Wheel on 3rd Stringer
Moment (kft)
150
100
50
0
-50
-10
10
30
50
70
90
Direct
SAP cont.
SAP cracked
SAP fixed
Run 13
Run 14
longitudinal position of front axle (ft)

APPENDIX G

COMPARISON OF MAXIMUM MOMENTS FROM FIRST LLANO TEST

Comparison of Analytical and Experimental Results for 1st Floor Beam Midspan

Truck Information			Experimental Results				SAP cracked		SAP continuous		SAP fixed		direct load
Run (2 truck runs)	description	center (ft)	M_{max} (kft)	Loc. of M_{max} (ft)	direct % of	% of SAP	M_{max} (kft)	% of direct	M_{max} (kft)	% of direct	M_{max} (kft)	% of direct	M_{max} (kft)
1	side by side	0	118.1	18.2	50%	54%	219.0	92%	218.3	92%	81.1	34%	237.8
1b	side by side	0	127.9	17.3	54%	58%	219.0	92%	218.3	92%	81.1	34%	237.8
2	side by side	0	116.1	17.7	49%	53%	219.0	92%	218.3	92%	81.1	34%	237.8
3	train	0	90.9	17.0	57%	63%	145.2	91%	144.7	91%			158.9
4	train	0	92.1	17.1	58%	63%	145.2	91%	144.7	91%			158.9
20	reverse train	0	105.6	30.3	54%	61%	173.8	89%	173.3	89%			195.6
21	reverse train	0	103.9	30.4	53%	60%	173.8	89%	173.3	89%			195.6
avg					54%	59%		91%		91%		34%	
(1 truck runs)													
7	R4	-5.5	60.7	16.8	51%	55%	109.5	92%	109.1	92%	40.6	34%	118.9
8	R4	-5.5	59.4	16.9	50%	54%	109.5	92%	109.1	92%	40.6	34%	118.9
9	L5	-3.5	79.7	16.9	53%	60%	133.5	88%	133.0	88%	50.5	33%	150.9
10	L5	-3.5	73.9	17.1	49%	55%	133.5	88%	133.0	88%	50.5	33%	150.9
17	R3	-1	87.1	17.2	55%	60%	144.5	91%	144.1	91%	55.1	35%	158.9
18	R3	-1	84.9	17.2	53%	59%	144.5	91%	144.1	91%	55.1	35%	158.9
5	center	0	87.6	16.8	55%	60%	145.2	91%	144.7	91%	55.1	35%	158.9
6	center	0	86.2	17.2	54%	59%	145.2	91%	144.7	91%	55.1	35%	158.9
11	L4	1	90.1	17.1	57%	62%	144.5	91%	144.1	91%	55.1	35%	158.9
12	L4	1	88.9	16.9	56%	61%	144.5	91%	144.1	91%	55.1	35%	158.9
15	R2	3.5	80.1	16.9	53%	60%	133.5	88%	133.0	88%	50.5	33%	150.9
16	R2	3.5	76.7	17.1	51%	57%	133.5	88%	133.0	88%	50.5	33%	150.9
13	L3	5.5	65.7	17.1	55%	60%	109.5	92%	109.1	92%	40.6	34%	118.9
14	L3	5.5	62.7	16.9	53%	57%	109.5	92%	109.1	92%	40.6	34%	118.9
avg				17.0	53%	59%		91%		90%		34%	

Comparison of Analytical and Experimental Results for 1st Floor Beam 4.5' from Midspan

Truck Information			Experimental Results				SAP cracked		SAP continuous		SAP fixed		direct load
Run (2 truck runs)	description	center (ft)	M_{max} (kft)	Loc. of M_{max} (ft)	direct % of	% of SAP	M_{max} (kft)	% of direct	M_{max} (kft)	% of direct	M_{max} (kft)	% of direct	M_{max} (kft)
1	side by side	0	102.9	18.2	50%	53%	194.7	95%	197.3	96%	50.9	25%	205.9
1b	side by side	0	110.3	17.3	54%	57%	194.7	95%	197.3	96%	50.9	25%	205.9
2	side by side	0	103.9	17.7	50%	53%	194.7	95%	197.3	96%	50.9	25%	205.9
3	train	0	76.3	17.0	57%	61%	125.4	93%	133.1	99%			134.9
4	train	0	76.0	17.1	56%	61%	125.4	93%	133.1	99%			134.9
20	reverse train	0	89.2	30.3	54%	58%	152.9	92%	160.0	96%			166.0
21	reverse train	0	87.4	30.1	53%	57%	152.9	92%	160.0	96%			166.0
avg					53%	57%		93%		97%		25%	
(1 truck runs)													
7	R4	-5.5	76.5	16.8	60%	64%	119.2	93%	120.2	94%	39.3	31%	128.3
8	R4	-5.5	71.7	16.9	56%	60%	119.2	93%	120.2	94%	39.3	31%	128.3
9	*L5*	*-3.5*	*84.1*	*16.9*	*60%*	*65%*	*129.3*	*93%*	*130.8*	*94%*	*40.9*	*29%*	*139.4*
10	L5	-3.5	80.6	17.4	58%	62%	129.3	93%	130.8	94%	40.9	29%	139.4
17	R3	-1	81.5	17.2	56%	62%	131.3	90%	133.3	92%	40.7	28%	145.3
18	R3	-1	80.8	17.2	56%	61%	131.3	90%	133.3	92%	40.7	28%	145.3
5	center	0	77.8	16.8	58%	62%	124.9	93%	127.0	94%	37.2	28%	134.9
6	center	0	74.8	17.2	55%	60%	124.9	93%	127.0	94%	37.2	28%	134.9
11	L4	1	73.5	17.1	59%	63%	117.2	94%	119.3	96%	32.9	26%	124.5
12	L4	1	69.8	16.9	56%	60%	117.2	94%	119.3	96%	32.9	26%	124.5
15	R2	3.5	53.4	16.9	54%	56%	94.8	96%	96.8	98%	17.4	18%	98.4
16	R2	3.5	46.8	17.1	48%	49%	94.8	96%	96.8	98%	17.4	18%	98.4
13	L3	5.5	36.8	17.1	47%	49%	75.5	97%	77.1	99%	11.5	15%	77.6
14	L3	5.5	36.7	16.9	47%	49%	75.5	97%	77.1	99%	11.5	15%	77.6
avg				17.1	55%	59%		94%		95%		25%	

Comparison of Analytical and Experimental Results for 2nd Floor Beam 4.5' from Midspan

Truck Information			Experimental Results				SAP cracked		SAP continuous		SAP fixed		direct load
Run (2 truck runs)	description	center (ft)	M_{max} (kft)	Loc. of M_{max} (ft)	direct % of	% of SAP	M_{max} (kft)	% of direct	M_{max} (kft)	% of direct	M_{max} (kft)	% of direct	M_{max} (kft)
1	side by side	0	121.0	37.2	53%	60%	203.0	90%	203.4	90%	59.8	26%	226.3
1b	side by side	0	128.8	36.6	57%	63%	203.0	90%	203.4	90%	59.8	26%	226.3
2	side by side	0	119.5	36.9	53%	59%	203.0	90%	203.4	90%	59.8	26%	226.3
3	train	0	91.4	48.6	55%	63%	145.6	87%	154.0	92%			167.4
4	train	0	93.5	48.3	56%	64%	145.6	87%	154.0	92%			167.4
20	reverse train	0	112.6	45.9	55%	65%	173.5	85%	187.7	92%			203.0
21	reverse train	0	116.2	48.4	57%	67%	173.5	85%	187.7	92%			203.0
avg					55%	63%		88%		91%		26%	
(1 truck runs)													
7	R4	-5.5	78.7	35.7	56%	63%	124.3	88%	127.2	90%	46.4	33%	141.0
8	R4	-5.5	76.7	38.6	54%	62%	124.3	88%	127.2	90%	46.4	33%	141.0
9	*L5*	*-3.5*	*87.8*	*36.3*	*57%*	*65%*	*134.5*	*88%*	*137.1*	*89%*	*48.1*	*31%*	*153.2*
10	L5	-3.5	84.1	36.2	55%	63%	134.5	88%	137.1	89%	48.1	31%	153.2
17	R3	-1	82.8	36.0	52%	60%	137.5	86%	139.0	87%	48.4	30%	159.7
18	R3	-1	83.7	35.6	52%	61%	137.5	86%	139.0	87%	48.4	30%	159.7
5	center	0	80.3	35.8	54%	62%	130.0	88%	130.9	88%	43.9	30%	148.3
6	center	0	80.3	36.2	54%	62%	130.0	88%	130.9	88%	43.9	30%	148.3
11	L4	1	74.7	35.4	55%	61%	121.8	89%	121.9	89%	38.7	28%	136.8
12	L4	1	74.9	36.0	55%	61%	121.8	89%	121.9	89%	38.7	28%	136.8
15	R2	3.5	58.4	34.8	54%	59%	98.8	91%	96.9	90%	21.2	20%	108.2
16	R2	3.5	54.1	34.8	50%	55%	98.8	91%	96.9	90%	21.2	20%	108.2
13	L3	5.5	42.4	36.5	50%	54%	78.7	92%	76.3	89%	14.5	17%	85.2
14	L3	5.5	42.4	37.5	50%	54%	78.7	92%	76.3	89%	14.5	17%	85.2
avg				36.1	53%	60%		89%		89%		27%	

APPENDIX H

MOMENT DIAGRAMS OF SECOND FLOOR BEAM IN SECOND LLANO BRIDGE TEST

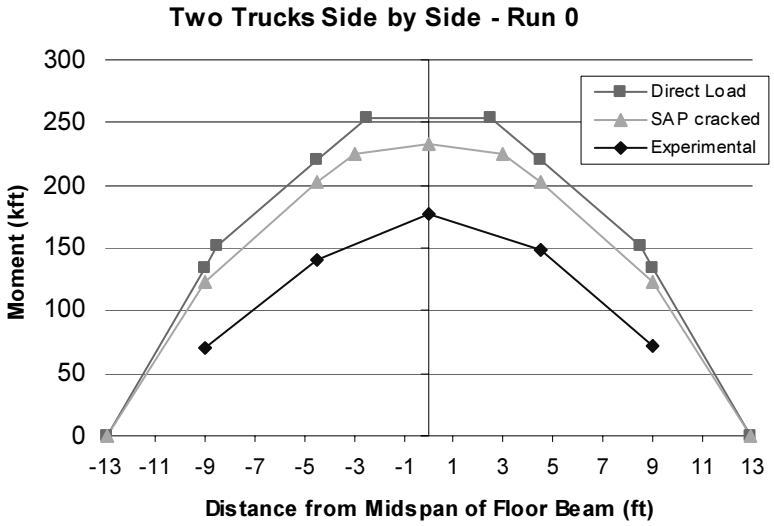

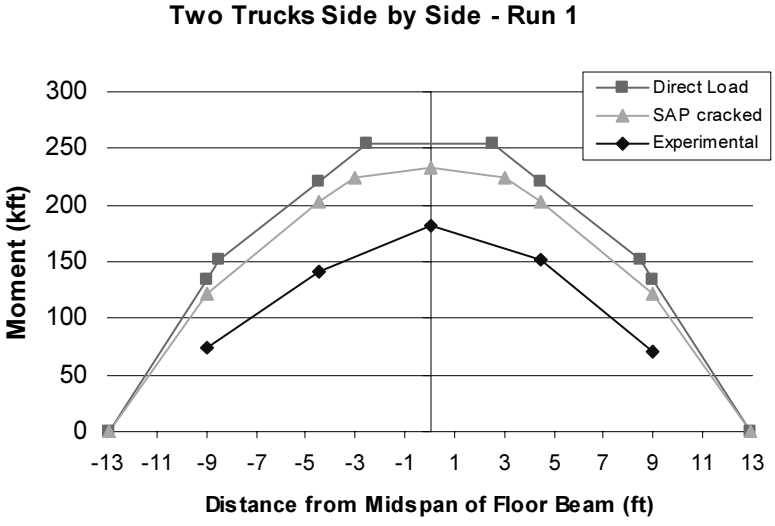

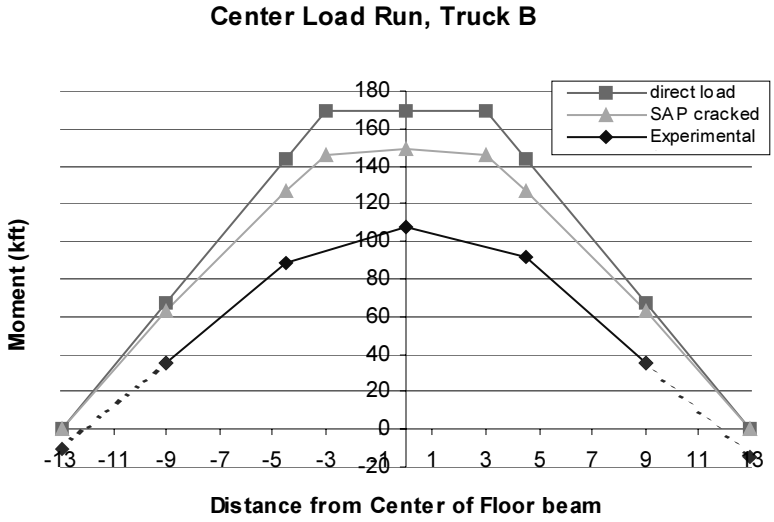
Center Load Run, Truck B
direct load
SAP cracked
Experimental
Moment (kft)
180
160
140
120
100
80
60
40
20
0
-20
-13
-11
-9
-7
-5
-3
-1
1
3
5
7
9
11
13
Distance from Center of Floor beam

REFERENCES

1. Computers and Structures, Inc (CSI), SAP2000 *Integrated Finite Element Analysis and Design of Structures,* Version 6.1, Berkeley, CA, 1997.
2. American Association of State Highway and Transportation Officials (AASHTO), *Manual for Maintenance Inspection of Bridges,* 3rd ed., AASHTO, Washington, D.C., 1978.
3. American Association of State Highway and Transportation Officials (AASHTO), *Manual for Maintenance Inspection of Bridges,* 4th ed., AASHTO, Washington, D.C., 1983.
4. Texas Department of Transportation (TxDOT), *Texas Bridge Load Rating Program,* TxDOT, Austin, TX, 1988.
5. American Association of State Highway and Transportation Officials (AASHTO), *LRFD Bridge Design Specifications: Customary U.S. Units,* 2nd ed., AASHTO, Washington, D.C., 1998.
6. American Association of State Highway and Transportation Officials (AASHTO), *Standard Specifications for Highway Bridges,* 16th ed., AASHTO, Washington, D.C., 1996.